Neogene to Recent tectonic evolution of the Central Mediterranean:

an integrated paleomagnetic approach

Charon E. Duermeijer

Neogene to Recent tectonic evolution of the Central Mediterranean:

an integrated paleomagnetic approach

Charon E. Duermeijer

Neogene to Recent tectonic evolution of the Central Mediterranean:

an integrated paleomagnetic approach

Neogene tot recente tektonische evolutie van het centrale Middellandse Zeegebied:

een geïntegreerde paleomagnetische benadering

(met een samenvatting in het Nederlands)

PROEFSCHRIFT

ter verkrijging van de graad van doctor
aan de Universiteit Utrecht
op gezag van de Rector Magnificus, Prof. Dr. H.O. Voorma
ingevolge het besluit van het College voor Promoties
in het openbaar te verdedigen
op maandag 4 oktober 1999 des middags te 14.30 uur

DOOR

Charon Estelle Duermeijer

geboren 7 december 1970,
te Utrecht

PROMOTOR: Prof. Dr. C.G. Langereis

MEMBERS OF THE DISSERTATION COMMITTEE

Prof. Dr. R. van der Voo
Department of Geological Sciences, University of Michigan
Ann Arbor, U.S.A.

Dr. L. Sagnotti
Instituto Nazionale di Geofisica
Roma, Italy

Prof. Dr. J.E. Meulenkamp
Stratigraphy and Paleontology, Faculty of Earth Sciences
Utrecht University, The Netherlands

Prof. Dr. S.H. White
Structural Geology, Faculty of Earth Sciences
Utrecht University, The Netherlands

Prof. Dr. M.J.R. Wortel
Tectonophysics, Faculty of Earth Sciences
Utrecht University, The Netherlands

αὐτὸ καϑ αὐτὸ μεϑ αὐτοῦ μονοειδὲσ ἀεὶ ὂν

zelf op zichzelf, met zichzelf steeds eenvormig

Plato's symposium

Voor Pim en Loes

Contents

Bibliography

Chapter 1:
Duermeijer, C.E., van Vugt, N., Langereis, C.G., Meulenkamp, J.E. and W.J. Zachariasse. A major late Tortonian rotation phase of the Crotone Basin using AMS as tectonic tilt correction and timing of the opening of the Tyrrhenian Basin, Tectonophysics 287, 233-249, 1998, with permission from Elsevier Science.

Chapter 2:
Duermeijer, C.E. and C.G. Langereis. Astronomical dating of a tectonic rotation on Sicily and consequences for the timing and extent of the Mid-Pliocene deformation phase. Tectonophysics 298, 243-258, 1998, with permission from Elsevier Science.

Chapter 3:
Duermeijer, C.E., Krijgsman, W., C.G. Langereis and J.H. ten Veen. Post-early Messinian counterclockwise rotations on Crete: implications for the late Miocene to Recent kinematics of the southern Hellenic Arc. Tectonophysics 298, 177-189, 1998, with permission from Elsevier Science.

Chapter 4:
Duermeijer, C.E., Krijgsman, W., Langereis, C.G., Meulenkamp, J.E., Triantaphyllou, M.V. and W.J. Zachariasse. A late Pleistocene clockwise rotation phase of Zakynthos (Greece) and implications for the evolution of the western Aegean arc. Earth and Planetary Science Letters, submitted.

Chapter 5:
Duermeijer, C.E., Nyst, M., Meijer, P.Th. and C.G. Langereis. Neogene evolution of the Aegean arc: paleomagnetic and geodetic evidence for a rapid young rotation phase. Earth and Planetary Science Letters, submitted.

Chapter 6:
Duermeijer, C.E. and C.G. Langereis. The late Neogene to Recent geodynamic evolution of the central Mediterranean and the role of the African promontory: a paleomagnetic approach. Tectonics, submitted.

Prologue

Prologue

This thesis reports about an integrated paleomagnetic research concentrating on the central Mediterranean. Aided by different disciplines (bio- and cyclostratigraphy and geodesy) we investigated the tectonic rotation history in Italy and Greece. To fully appreciate the work we did under the burning sun, I will first briefly inform the reader about the history of paleomagnetism, starting around 250 years B.C. Then I will show how we retrieve our data from the rocks and analyse it to obtain useful results. I will also discuss the dating techniques, which give this thesis added value. Last but certainly not least, I will give an overview on the contents of this thesis.

Paleomagnetic history

Long ago, the Greek and Chinese already recognised the attractive forces of lodestone or magnetite (an iron-rich mineral) and named it the "loving stone" (the French still call a magnet "aimant"). Around 250 years B.C., the Chinese produced the oldest known compass, constituting a magnetite spoon rotating on a smooth board and turning in a north-south direction at any place. Only in the twelfth century the compass reached Europe, probably over sea through trading with Arabs. A century later, European philosophers assumed the compass needle derived its directional virtue from the pole star, as this star unlike other stars seemed to be fixed. They believed that the pole star gave magical power to the lodestone, with which the compass needle was rubbed and activated. Around the same time, others suggested that polar lodestone mountains received their power from the pole star to pass it on to the compass needles. In 1269, Petrus Peregrinus wondered why the polar lodestone mountains should be more attractive than other lodestone mountains present all over the world. He discovered the dipole behaviour of a sphere of lodestone and found that comparable poles oppose and opposite poles attract. It was not until 1600 that William Gilbert realised that the Earth itself behaves like a *"magnus magnes ipse"*. Gilbert, 72 years before Newton (saw the falling apple), was the first to attribute a physical property (magnetism) to the Earth. Only centuries later, the most remarkable property of the Earth's magnetic field was discovered: the switching of polarity. In 1906, the French physicist B. Brunhes found a lava flow and an adjacent baked clay in which the magnetisation was exactly opposite to the present field direction. Therefore, Brunhes drew the conclusion that the Earth's field must have reversed. Further observations of lava sequences by Mercanton and Matuyama in the 1920s led to the recognition that some young rocks were magnetised in the same direction of the present-day field and older, underlying rocks revealed an opposite direction. From here, the geomagnetic polarity time scale developed, resulting in an indispensable dating tool in Earth Sciences.

Another important breakthrough in Earth Sciences is the concept of polar wander and continental drift. Observations revealed that paleomagnetic poles from different

continents did not coincide, which must imply that either the paleomagnetic poles change their location (polar wander) or continents move (continental drift). As it turned out, paleomagnetism proved the earlier hypothesis of continental drift (Wegener, 1912). Not until the 60s after normal and reversed polarities (magnetic anomalies) were recognised parallel to the mid-Atlantic ridge, seafloor spreading was found to be a viable mechanism behind continental drift. The theory of plate tectonics was born. These early studies during the 50s were the first (plate)tectonic applications derived from paleomagnetism.

Acquiring data and results

This study forced us to spend every summer over the last four years in Italy and Greece, having to endure Mediterranean food and wine, and sampling along sandy beaches. We visited little over 100 localities and took approximately 3000 cores using a generator, electrical drill and an insect-repellent-pressure tank with cooling water. Whenever possible, we preferred sampling long and continuous stratigraphic sections, but sometimes only sites were taken. To obtain good quality cores, we had to dig (a lot!) to reach fresh, still wet sediments. We decided to sample mostly fine-grained clays, as they appeared to carry the most stable magnetisations. These clays were then wrapped in aluminum foil to keep them wet and (hopefully) unaltered. Then the last challenge before laboratory measurements could start, was to pass customs (without paying overweight) carrying tons of equipment and many small cylindrical rocks in aluminium foil.

In the laboratory, the first analyses always included (non-destructive) measurements of the anisotropy of magnetic susceptibility (AMS). These analyses provide information on the preferred orientation of the induced magnetisation of the paramagnetic (mainly clay), diamagnetic (carbonate) and ferromagnetic minerals. During deposition, the (magnetic) minerals settle down and align their grains according to a sediment transport direction. If the environment is quiet, the grains (typically clays) show random orientations. Grains can also reveal a preferred orientation, after deformation has been active on the sediments. Therefore, if we measure the amount of magnetisation in three directions, we retrieve information on the direction in which most (magnetic) grains are aligned. This tells us the direction of the current or the direction of deformation in the sediments, which appears in many cases visually undeformed. Hence, it allows us to reconstruct part of the tectonic history.

The next step, measuring the direction of the magnetisation in a rock specimen, puts us for many weeks behind a cryogenic magnetometer, with one basic assumption in mind concerning the physical properties of the Earth: we consider it to behave like a bar magnet in the centre of the Earth directed along the rotation axis and we call this a geocentric axial dipole. It implies that averaged over some time (at least 2000 years) the geomagnetic north pole remains at its place: at the geographical North pole. Hence, if we take many samples over a sufficiently long interval, the average pole should be at geographical North within its error. Very often, we find results revealing a systematic deviation from the North pole,

from which we can deduce a paleomagnetic (tectonic or vertical axis) rotation. Subsequently, a tectonic reconstruction can be made, provided we know the age of the rock.

Age and time

The concepts of age and time are crucial for all Earth Scientists if they are to understand geological processes. When we know the duration of a certain process and its absolute age, we are better able to comprehend causes and consequences of the studied processes.

In this thesis, we use available dating techniques to correlate our paleomagnetic results over large geographic areas, which then might inform us about underlying processes. We first used magnetostratigraphy, in which we attribute a polarity (normal and/or reversed) to intervals of the sampled stratigraphic section and correlate the resulting pattern to the geomagnetic polarity time scale (GPTS). This allows us to date the section rather accurately. When a section shows rhythmic variations, we used cyclostratigraphy to obtain a more precise age control, with an accuracy of less than 5000 years. Cyclostratigraphy uses the rhythmic or cyclic variations of sedimentary patterns which can be proven to be related to climate changes. Sometimes, we could not sample long and continuous stratigraphic sections and we only had limited outcrops. Fortunately, many of these outcrops contained age diagnostic fossils of which the evolutionary steps have been astronomically dated. By combining the paleomagnetic results and the cyclo- and biostratigraphy, a strong dating and correlation tool was established to compare specific (tectonic) events over large areas or to detect a tectonic rotation within (tens of) thousands of years.

Summary

The Mediterranean area has been and still is one of the most intensively studied areas of the world. The geodynamics are dominated by the convergence zone between Africa and Eurasia. The history of the area is complicated by micro-plate interactions but can be summarised as the creation and destruction of the Tethys ocean. The Tethys was an eastward widening oceanic gap between the Eurasia and Gondwana continents. Since the Triassic, this ocean has been closing and in Tertiary times the Gondwana continents collided with Eurasia (Van der Voo, 1993).

We are especially interested in solving the evolutionary puzzle of the Aegean and Tyrrhenian area over the last millions of years (Neogene) and whether tectonic/geodynamic processes in these regions are linked. We compare our paleomagnetic results with accurate and precise timing, vertical movements, tomography and geodesy.

Italy

It was in the mid 1970s that paleomagnetic studies (Channell and Tarling, 1975; VandenBerg et al., 1978) detected horizontal movements of Italy. These studies indicated that the Italian peninsula was connected with the African continent from late Early Jurassic to early Tertiary and moved independently from Africa since post early Eocene. Since then, paleomagnetic research concentrated on investigating tectonic events in Italy in more detail and it showed that the Italian peninsula consists of various blocks and thrust sheets, sometimes moving together. Detailed work in southern Italy was done in the thesis of Scheepers (1994a) who detected several rotation phases. His results show that the southern Apennines underwent an anticlockwise rotation during the Pleistocene, whereas the Calabro-Peloritan block underwent a time-equivalent clockwise rotation. Older sediments from Calabria suggested a rotation phase during the late Miocene. On Sicily, a middle Pliocene clockwise rotation phase was found. Furthermore, the Apulian foreland reveals no rotation since the late Pliocene. Scheepers's thesis left some unanswered questions concerning timing of the Miocene rotation in Calabria and of the Pliocene rotation on Sicily, which formed the onset of this thesis.

In **Chapter 1** we study the Miocene rotation phase in connection with the opening of the Tyrrhenian basin and, at the same time, provide a correction tool for deformed sediments.

Scheepers (1994a) detected an anomalously large (80°) anticlockwise rotation in the Miocene sediments in northern Calabria (Crotone basin). To investigate whether this anomalous results is an artefact or a real rotation, we examine the interval in more detail. The interval in which the rotation was found appears to be highly deformed as can be deduced from anisotropy of the magnetic susceptibility (AMS) analyses. After correcting for the deformation, the anticlockwise rotation in that interval is largely reduced (to 13°). To verify the newly established and much smaller anticlockwise rotation, we sampled a time-equivalent section in the same basin. The paleomagnetic results of this section also indicate a small anticlockwise rotation, justifying our deformation correction. Furthermore, data from younger (late Tortonian to early Pleistocene) sediments around Calabria show clockwise rotations, suggesting a Calabrian-wide late Miocene (8.6 - 7.6 Ma) rotation phase. It is known from literature that the Calabro-Peloritan block moved away from the coast of Sardinia in southeastern direction towards the present-day configuration, thereby creating the Tyrrhenian basin. The timing of opening in the Tyrrhenian basin was long disputed. However, the oldest (marine) sediments in the basin, situated next to the Sardinian coast, have an age of ~7.8 Ma. Therefore, we speculate that the opening of the Tyrrhenian basin occurred between 8.6 and 7.8 Ma.

In **Chapter 2**, we discuss a middle Pliocene tectonic rotation phase, which we suggest may result from a Mediterranean wide event. This rotation is astronomically dated at around 3.21 Ma and took place within ca. 80-100 kyr.

The Pliocene sequences combined in the Rossello Composite section along the coast of Sicily in the Caltanisetta basin were used to establish high-resolution chronostratigraphic correlations which have formed the basis of the Pliocene astronomical polarity time scale (Hilgen, 1991a; Lourens et al., 1996). These sequences contain the so-called Trubi and Narbone Formations, which are rhythmically bedded carbonate-rich and carbonate-poor marls. Fossil assemblages indicate a waterdepth of 500-800 m for the Trubi and 100-400 m for the Narbone Formations, implying a rapid shallowing around the Trubi-Narbone boundary astronomically dated at 3.19 Ma. Previous paleomagnetic data from the Rossello Composite revealed a differential rotation (Scheepers and Langereis, 1993) around Kaena times (3.03-3.12 Ma). To estimate the exact timing of this rotation phase, we re-examine the Trubi-Narbone interval. The results show a (10°) clockwise rotation phase at 3.21 Ma which took place within 80,000-100,000 years. The rotation occurs very close to the Trubi-Narbone boundary and therefore coincides with this major change in basin configuration. Even though the rotation can be considered as local, it is most likely the result of a more regional process, because we also notice that the rotation occurs at a time when the opening of the Tyrrhenian basin accelerates. At exactly the same time, we find a major change in climatically induced palaeoceanographic conditions in the eastern Mediterranean. This could imply a regional cause for our middle Pliocene tectonic rotation phase on Sicily, but with Mediterranean-wide implications.

Greece

After the progress we made in Italy by combining our paleomagnetic data with cyclo- and biostratigraphy, we opt for applying the same technique on sediments from the Hellenic arc to see if the current ideas on the evolution of the Greek region can be refined. We also investigate the precise timing of tectonic rotations to see if they are coeval and/or equally rapid in Greece as in Italy. We sampled (mainly marine) sediments located on the Aegean outer-arc islands.

Firstly, we re-examine Messinian and Tortonian sections from Crete. These sections were previously used for magnetostratigraphy (Langereis, 1984; Hilgen et al., 1995; Krijgsman et al., 1994, 1995) and are astronomically dated. The results, discussed in **Chapter 3**, reveal post Messinian anticlockwise rotations for most localities, with the largest rotations found in central Crete. The conclusions from our study are remarkably different from earlier studies by Valente et al. (1982) and Laj et al. (1982) who suggested no rotation of Crete occurred since ~7 Ma, even though results from the same sections in both studies are compatible. We suggest that the paleomagnetic rotations are governed by (local) rotations of sinistral fault-bounded blocks, rather than that Crete rotated as a single block. Furthermore, we consider the anticlockwise rotations to be related to plate interaction, especially transpression along the eastern segment of the overriding plate boundary in eastern Crete.

We continue our examination along the western Aegean arc on the Ionian island of Zakynthos. The sediments on the island range in age between Cretaceous and Pleistocene. Only the Tortonian to Pleistocene sediments reveal good paleomagnetic results, which are described in **Chapter 4**. It is found that the island of Zakynthos underwent a clockwise rotation which agrees well with earlier results of Kissel and Laj (1988). However, we discover that the clockwise rotation took place between 0.77 Ma and Recent. Our results indicate that the western Aegean arc was not formed by a continuous rotation process starting around 5 Ma, as previously postulated by Kissel and Laj (1988). We notice that the tectonic rotation found on Zakynthos is time-equivalent to rapid uplift. This rapid uplift (and simultaneous rotation) is compatible with the hypothesis of slab detachment which can cause lithospheric rebound.

As our approach proves to be successful, we explore the rest of the Aegean outer-arc (**Chapter 5**). Along the western Aegean arc, we visited Epirus, Lefkas, Kefallonia, the Peloponessos and Kythira to investigate whether the young clockwise rotation found on Zakynthos can also be recognised here. In the eastern Aegean arc, we sampled late Neogene sediments from Kassos, Karpathos and Rhodos, as well as Pliocene/ Pleistocene sediments on Crete to constrain the post-early Messinian anticlockwise rotation found on this island. Finally, we examine Plio/Pleistocene sediments on Milos to further constrain the boundary between anticlockwise and clockwise rotating areas.

The paleomagnetic results for the western Aegean arc indicate that a similar young rapid clockwise rotation took place on the Peloponessos. The sediments from the eastern Aegean, in particular from Kassos, Karpathos and Rhodos, show anticlockwise rotations occurring roughly between 2 Ma and Recent. The Plio/Pleistocene sediments from Crete contain no useful paleomagnetic signal and therefore do not constrain the rotation on Crete better that post-early Messinian.

An earlier hypothesis suggested that the current curvature of the Aegean arc was formed in two tectonic phases. The first phase, during the late Miocene, resulted in clockwise rotations in Epirus and counter-clockwise rotations in western Anatolia (Turkey). The second (continuous deformation) phase - during the last 5 Myr - produced only clockwise rotations for the north-western part of Greece. According to this reconstruction, Crete nor the eastern Aegean arc underwent any rotation since ~7 Ma (Laj et al., 1982) and since ~4 Ma, respectively. Our new results imply a different geodynamic evolution for the Aegean arc. First of all, we find no evidence for continuous deformation in the western Aegean starting around 5 Ma. Our results from the western Aegean arc show a young (<0.8 Ma) clockwise rotation. In the eastern Aegean arc, the paleomagnetic results also reveal young anticlockwise (< 2 Ma) rotations. We argue that the current curvature cannot have been established through a continuous rotation process since the opening of the Aegean Sea, as we detected no rotations prior to the Pleistocene. We conclude that the curvature is mainly formed by large-scale translations. As our observed rotations appear to be very young, we examine the current motion of the Aegean by means of geodesy. In general, the geodetic data show similar senses of rotation in the

Aegean; clockwise in the west and anticlockwise rotations in the east. Moreover, our Pleistocene rotation phase occurs when the tectonic regime in the Aegean changed drastically.

Overview

In **Chapter 6** we merge our new results with published paleomagnetic data covering the central Mediterranean. It appears that west of the Apulian platform the Italian peninsula underwent mostly anticlockwise rotations, whereas in the east the Dinarides/Albanides/Hellenides experienced mostly clockwise rotations. The absence of rotation generally expanded over time from the north-east to the south-west, which is in agreement with the model of lateral migration of slab detachment. Furthermore, around 1 Ma large tectonic rotations, a change in stress regime and rapid uplift are found in southern Italy and in north-western Greece, which can likewise be related to slab detachment underneath Calabria and the Peloponessos respectively. This leaves us with the question whether the observations in southern Italy and northwestern Greece are somehow linked through simultaneous slab detachment.

1

A major late Tortonian rotation phase in the Crotone Basin using AMS as tectonic tilt correction and timing of the opening of the Tyrrhenian Basin

Abstract

Paleomagnetic studies of sediments from the Calabro-Peloritan block in southern Italy consequently imply a 15° clockwise rotation for the late Tortonian to middle Pleistocene sedimentary cover; but the results of older sediments are generally less consistent. Earlier paleomagnetic results of Tortonian sites from the Basilicoi section (Crotone basin, northern Calabria) suggested a major counterclockwise rotation of 97° (Scheepers, 1994b). Here, we studied the Basilicoi section in detail and we used anisotropy of the magnetic susceptibility (AMS) to reconstruct the bedding plane needed for tilt correction. This reduced the 97° counterclockwise rotation to a 25° counterclockwise rotation. The Lese section, also in northern Calabria, shows the same counterclockwise rotation in sediments with an age between 10.4 and 8.6 Ma, thus confirming the results from the corrected Basilicoi section. A comparison of the magnetostratigraphy and planktonic foraminiferal biostratigraphy with the magneto-biostratigraphic framework of the Mediterranean late Miocene allows a correlation of the Basilicoi and Lese sections to the GPTS and a timeframe for the rotation. It is concluded that the 25° counterclockwise rotation phase took place between ~7.6 ± 0.1 and 8.6 Ma. We speculate that the timing of this tectonic phase is related to the opening of the Tyrrhenian Sea and the separation of Calabria from Sardinia. We compare our results with those of ODP leg 107 and we suggest an age between 8.6-7.8 Ma for the timing of the opening of the Tyrrhenian Sea.

Introduction

The Neogene evolution of the Central Mediterranean is dominated by the convergence between Africa and Europe. The African/Apulian plate is subducting underneath the European plate with an eastward and westward dipping slab (Wortel and Spakman, 1992). The Calabro-Peloritan block (Fig. 1.1) represents a fragment of the southern European margin and was most likely situated east of Sardinia (Alvarez, 1974) till middle Miocene times. Later, the Calabro-Peloritan block was thrust onto the Apennines to the north and the Sicily-Maghrebides chain to the south during back-arc extension in the Tyrrhenian area, to its present-day configuration at the southernmost part of the Italian Peninsula. This movement of Calabria was a result of a roll-back process, caused by the vertical sinking and detachment of the African/Apulian slab, and the related opening of the Tyrrhenian basin (Malinvero and Ryan, 1986).

Alvarez (1974) was one of the first to consider the location of Calabria with respect to Corsica/Sardinia prior to the opening of the Tyrrhenian basin. He speculated that the timing of opening was between early Langhian and Messinian (15-6 Ma). Clearly, the age of onset of rifting in the Tyrrhenian basin is not firmly dated (Kastens et al., 1987) and there is considerable controversy concerning the precise age of initial subsidence. Some speculate that the onset of rifting in the basin started at ~17 Ma, right after the end of the rotation of the Corsica/Sardinia block (Malinvero and Ryan, 1986), but according to Dercourt et al. (1986) the rifting in the Tyrrhenian basin began approximately at 10 Ma. Dewey et al. (1989) postulates that this rifting took place before 8.9 Ma on the basis of a detailed kinematic study, showing that this extension began prior to a change in Africa's motion. Results from Hsü (1977) and an older drilling campaign (DSDP site 373A, Scandone 1979) indicate that the rifting occurred somewhere between Middle and Late Miocene. Thus, the timing of opening in the Tyrrhenian basin is still highly in debate.

The kinematics of the evolution in the Central Mediterranean can be characterised by rotations and translations of small blocks, which can be detected by paleomagnetic studies. In the Calabro-Peloritan block, such studies showed for the late Tortonian to early Pleistocene sedimentary cover on average a 15° clockwise (CW) rotation. This rotation phase was dated at 0.7 - 0.8 Ma. Several early Tortonian locations, however, display counterclockwise (CCW) rotations, although the data are still scarce and inconsistent (Scheepers, 1994b).

The paleomagnetic results from the Basilicoi section in the Crotone basin suggested a major (80°) counterclockwise rotation for its lower Tortonian and a clockwise (17°) rotation for its late Tortonian/Messinian sediments (Scheepers, 1994b). This implies a major (97°) counterclockwise rotation phase during the middle to late Tortonian. Here, we study the entire (and downward extended) Basilicoi section in detail to determine more exactly when this suggested rotation phase took place. However, we found that the bedding plane in the middle part of the Basilicoi section necessary for tectonic tilt correction could not be measured. Therefore, we used the anisotropy of the magnetic susceptibility (AMS) to reconstruct the bedding plane in the middle part of the section.

Furthermore, we sampled another, continuous section (Lese) in the same basin (Fig. 1.1) to date and confirm this suggested tectonic episode during the Late Miocene in the Crotone Basin.

Sections and sampling

The Calabro-Peloritan block constitutes a complex pile of thrust sheets comprising a Paleozoic basement and a Mesozoic to Miocene cover. It is bounded by two major shearzones - in the north by the Pollino Line and in the south by the Taormina Line - and is intersected by numerous NW-SE-trending oblique transcurrent faults which played a dominant role in the basin configuration. These faults subdivide northern Calabria into
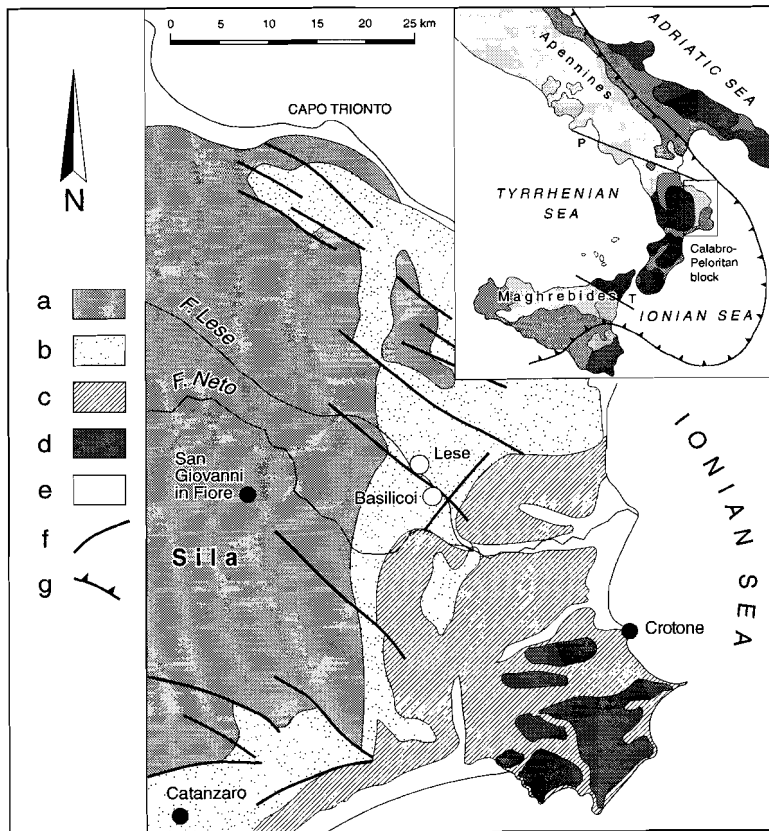

Fig. 1.1 Location of the Basilicoi and Lese sections in Calabria, southern Italy. a = Calabro-Peloritan basement, b = late Miocene sediments, c = Plio-Pleistocene sediments, d = late Pleistocene sediments, e = Holocene, f = faults, g = deformation fault, F = river, P = Pollino line, T = Taormina line.

three segments and account, for instance, for the shape of the Crotone basin, situated in the central segment (Meulenkamp et al., 1986, Van Dijk and Scheepers, 1995). The Lese section and the nearby (~2 km) Basilicoi section are both located in the Crotone basin, on different sides of a NW-SE-trending normal fault (Fig. 1.1) which runs through the Lese River. The late Miocene sections consist of open-marine marls with some sandy intercalations in the lower part. The marl sequences are overlain by Messinian diatomites of the Tripoli Formation. A regressive formation ('Belvedere sands'), extending over the Crotone basin, unconformably overlies these Messinian deposits. In the Lese section, these sands form a duplex structure which suggests NW-SE compression.

In both sections, sampling was aimed at the longest stratigraphic range possible, using an electrical drill and a portable generator. After removing the weathered surface to reach fresh blue-grey clays we took at least two standard-oriented paleomagnetic cores at each level as well as samples for biostratigraphic analyses. In the Lese section, we sampled 81 levels covering approximately 130 m, in the Basilicoi section 103 levels over 97 m. During sampling of the Basilicoi section we observed three sheared clay layers and interpreted these as possible shearzones. The bedding plane could only reliably be determined in the bottom (0-26 m) and top (90-97 m) parts of the section.

Biostratigraphic results

Basilicoi section

The biostratigraphic subdivision of the Basilicoi section can be divided into three major units (based on 110 samples) together with the main faunal characteristics (Fig. 1.5). The lower unit extends from the base up to 46 m and is characterised by abundant *Paragloborotalia mayeri* in the basal part (at 6 m) and frequent small-sized *Neogloboquadrina atlantica* with minor admixtures of *Neogloboquadrina acostaensis* in the remaining interval. All these neogloboquadrinids are dominantly dextrally coiled. In addition, we recorded scattered occurrences of *Globoquadrina dehiscens*, *Globorotalia partimlabiata*, and large-sized *Catapsydrax parvulus*. The middle unit ranges from 47 m up to 75 m and is characterised by dominant *Neogloboquadrina acostaensis*. Coiling is dextral up to 65 m, and shows a rapidly shifting pattern between 65 and 75 m. *Globorotalia partimlabiata* occurs in two samples at 52 m and 53 m, whereas large-sized *Catapsydrax parvulus* is a more regular element. The upper unit is characterised by dominantly sinistral *Neogloboquadrina acostaensis* with last occurrences of *Globorotalia menardii 4* and small-sized *Catapsydrax parvulus* at 91 m and 92 m, respectively. The first occurrence of *Globorotalia menardii 5* is at 95 m, while the first regular occurrence (FRO) level of the *Globorotalia conomiozea* group corresponds with a sample level at 106 m.

The faunal succession in the Basilicoi section (Fig. 1.5) can be correlated to a recently established Mediterranean planktonic foraminiferal biostratigraphy for the late-Middle to Late Miocene. The younger part of this high-resolution biostratigraphy has been published in Krijgsman et al. (1995). Ages of bioevents have been astronomically dated by Hilgen et al. (1995), but in this paper we refer to ages in terms of CK95 (Cande and Kent, 1995; Krijgsman et al., 1995). The older part, which is largely represented by the lower and middle units in the Basilicoi section, can also be tuned to the astronomical solutions (unpublished data). This older part includes the N15/N16 zonal boundary, which we define in the Mediterranean as the level where *Neogloboquadrina acostaensis* starts to outnumber its ancestor *Neogloboquadrina atlantica* (see also Zachariasse and Aubry, 1994). The lower unit in the Basilicoi section, thus, correlates with Zone N15, except for the basal part which belongs to the top part of the *Paragloborotalia mayeri* Zone (=Zone N14). Preservation in the lower unit changes abruptly between 28 m and 29 m with strongly distorted and re-crystallised tests below, and well-preserved ones above that interval. This suggests the presence of a shearplane between these two sample levels, but without being accompanied by a detectable hiatus. The middle unit belongs to the lowermost part of Zone N16. The boundary between the middle and upper unit (between 75 m and 76 m) corresponds to a major hiatus which is probably of tectonic origin since planktonic foraminiferal tests at 75 m (directly below the unconformity) are severely distorted. The sequences of bioevents in the upper unit are characteristic for the late Tortonian to early Messinian with the stage boundary being placed at the level of the first regular occurrence of the *Globorotalia conomiozea* group (see Krijgsman et al., 1995).

Lese section

Biostratigraphic resolution in the Lese section is lower than in the Basilicoi section since we analysed roughly 30% of all samples (Fig. 1.4). The lower part up to about 66 m contains *Neogloboquadrina acostaensis*, large-sized *Catapsydrax parvulus* and scattered occurrences of *Sphaeroidinellopsis* without small-sized *Neogloboquadrina atlantica* and *Globorotalia partimlabiata*. Coiling of *Neogloboquadrina acostaensis* is dextral up to 99 m except for the interval between 52 and 66 m which is characterised by rapid shifts in coiling. Sinistral coiling prevails from 99 m to the top of the section (Fig 4.). The interval up to 66 m seems to correlate with the larger part of the middle biostratigraphic unit in the Basilicoi section, whereas the remainder is not represented in the Basilicoi section because of the presence of a major hiatus. The few occurrences of small-sized *Catapsydrax parvulus* post-dating the LO level of their large-sized representatives at 115 m suggests that the top of the section is older than the frequency shift in *Catapsydrax parvulus* (= bioevent 4 in Krijgsman et al., 1995).

Paleomagnetic results

Rock magnetic properties

We performed some rock magnetic tests to identify the carriers of the remanent magnetisation, including acquisition of an isothermal remanent magnetisation (IRM) and a subsequent demagnetisation of this IRM. The IRM was induced in a pulse magnetiser and measured on a digitised spinner magnetometer based on a Jelinek JR3 driver unit. After each step we measured the low field susceptibility on a KLY-2 kappabridge. Furthermore, thermomagnetic runs were done using a modified horizontal translation Curie-balance making use of a cyclic field (Mullender et al., 1993).
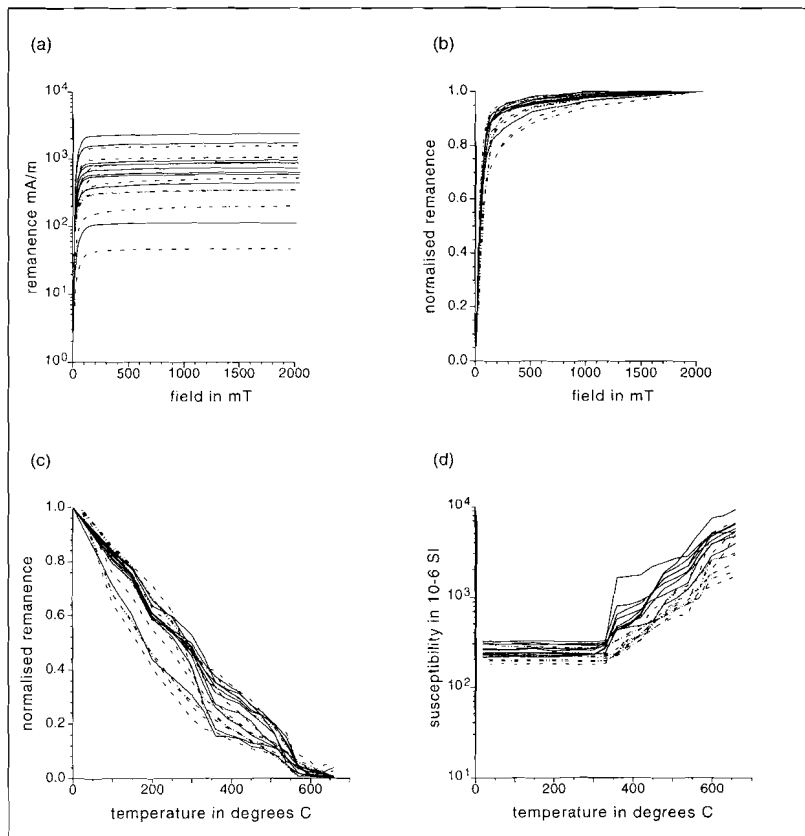

Fig. 1.2 Examples of IRM acquisition: (a) absolute values; (b) normalised values; (c) normalised stepwise thermal demagnetisation of the IRM; (d) low-field susceptibilities during thermal demagnetisation of samples from the Basilicoi (solid line) and of the Lese (dashed line) section.

Both the Lese and the Basilicoi sections reveal the same magnetic carriers. The steep initial rise in the IRM acquisition (Fig 2a and b) indicates magnetite as the dominant magnetic carrier as this low-coercivity mineral saturates around 200 mT. Occasionally, a small amount of high-coercivity minerals are also present. Thermal demagnetisation of the IRM (Fig. 1.2c) generally shows a maximum blocking temperature around 580°C, confirming magnetite as the main carrier. The few maximum unblocking temperatures higher than 600°C are probably caused by slightly maghemized magnetite which may have Curie temperatures of 610 - 645°C (Özdemir, 1990; De Boer and Dekkers, 1996). The sudden decrease in remanence at ~350°C (Fig. 1.2c) found in a few samples may be caused by inversion of submicron maghemite (Dankers, 1978; De Boer and Dekkers, 1996). All samples show an increase in low field susceptibility (Fig. 1.2d) starting at 320° - 350°C which may be the result of oxidation of pyrite (Van Velzen and Zijderveld, 1992). Measurements on the Curie-balance confirmed the information on mineralogy as found by acquisition and subsequent demagnetisation of the IRM. Summarising, it appears that the NRM is mainly carried by magnetite which is slightly maghemized, probably through low-temperature oxidation, i.e. weathering.

Thermal demagnetisation

Thermal demagnetisation was performed using a magnetically shielded, laboratory-built furnace. The natural remanent magnetisation (NRM) was measured on a 2G Enterprises DC SQUID cryogenic magnetometer. At least one specimen per sampling level was analysed using progressive stepwise thermal demagnetisation using temperature increments of 30°C or 50°C, starting from room temperature to the limit of reproducible results.

Demagnetisation diagrams (Zijderveld, 1967) and least-square fitting of lines (Kirschvink, 1980) through selected data points were used to determine the NRM components. The magnetisation vectors were averaged using Fisher (1953) statistics to calculate mean directions per interval.

Apart from a very small and randomly oriented laboratory-induced component removed at 100°C, a secondary component is sometimes present; it is generally removed between 100° and 200°C; it has a present-day direction before bedding tilt correction and is thus of recent origin and caused by weathering. A characteristic remanent magnetisation (ChRM) component is removed at temperatures above 600°C and shows both normal and reversed polarities. Considering the rock magnetic properties, we regard this ChRM to represent the primary magnetic component residing in magnetite or maghemite. Two types of ChRM components are revealed. The first type shows a ChRM component demagnetised at temperatures of 330°- 400°C (Fig. 1.3c and f). Demagnetisation at higher temperatures results either in randomly directed components or in a cluster. These samples have a relatively low NRM intensity (0.01 - 0.90 mA/m). Another group of samples consists of ChRM components with blocking temperatures often higher than 600°

C (Fig. 1.3a, b, d and e). They have relatively high NRM intensities (0.9 - 15.0 mA/m) and their demagnetisation components show a linear decay to the origin.
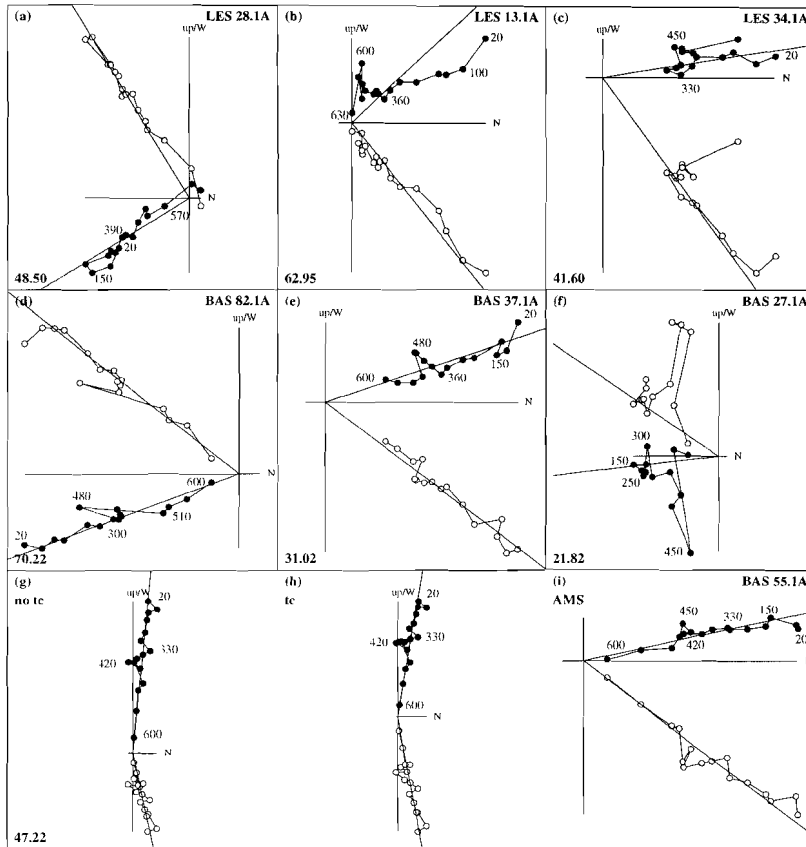

Fig. 1.3 Orthogonal projections of stepwise thermal demagnetisation of selected samples from the (LES) Lese and (BAS) Basilicoi section. Closed (open) circles represent the projection of the ChRM vector endpoint on the horizontal (vertical) plane. Values indicate temperatures in °C; stratigraphic levels are shown in the lower left corners. Sample BAS 55.1A from the middle part of the Basilicoi section is shown without tilt correction (g), and with the measured (h) and AMS tilt correction (i).

The ChRM directions and polarity zones of the Lese section (Fig. 1.4) show that ten polarity intervals are recorded. Using Fisher statistics we find a mean declination (D_m) and mean inclination (I_m) of 349.6° and 45.3°, respectively, for the entire section; this implicates a 10.3° counterclockwise rotation with respect to north (Table 1.1).

The magnetostratigraphic record of the Basilicoi section reveals at least nine polarity zones (Fig. 1.5). After tectonic correction (Table 1.1) we find a CCW rotation (D_m= 167.5°, I_m= -45°) in the lower part of the section, in the uppermost part CW rotations (D_m= 211.7°, I_m= -41.9°). The middle part (40-62 m), however, using the bedding plane from the lower

part of the section reveals a major (79°, D_m= 280.8°, I_m= 36.7°) CCW rotation, the same as found earlier by Scheepers (1994b).
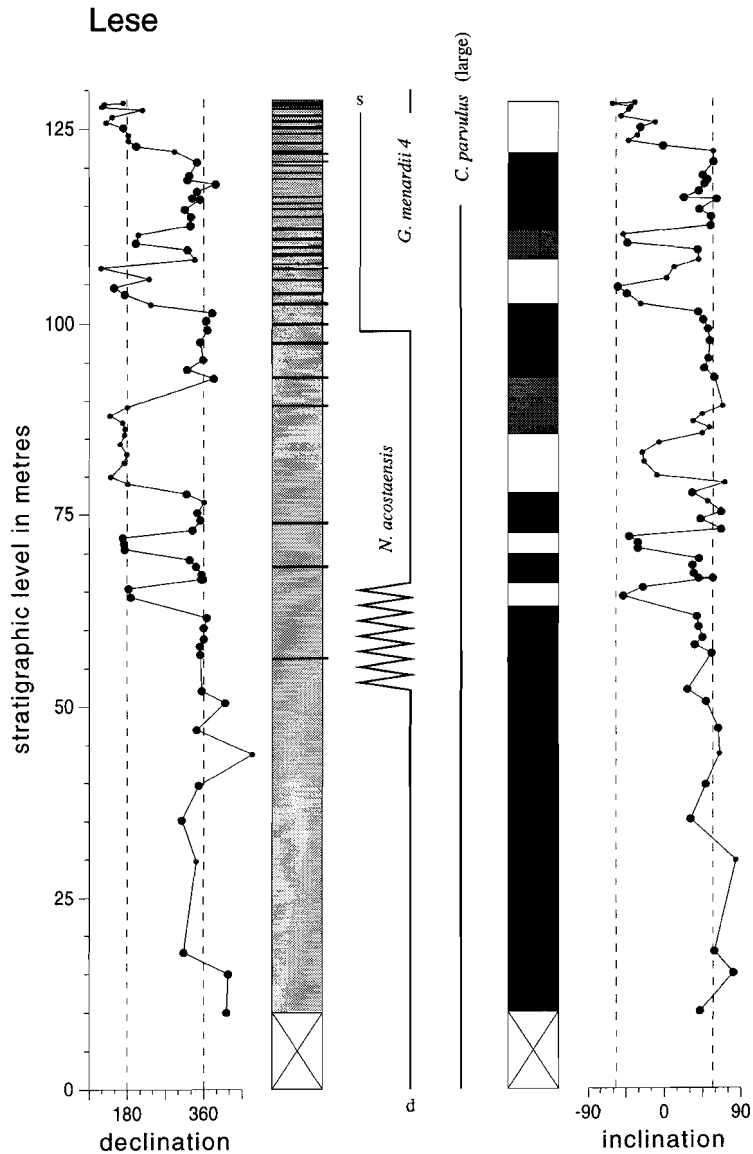
Fig. 1.4 Magnetostratigraphy of the Lese section. Closed circles represent reliable directions, closed small circles represent low intensity samples (see text). In the polarity column, black (white/grey) denotes normal (reversed/unreliable) polarity zones. Crossed area indicates a non-exposed interval. In the lithological column light (dark) grey represents marls (sand layers). Faunal ranges of foraminiferal biostratigraphy and associated bioevents of the Lese section are indicated; s (d) is sinistrally (dextrally) coiled N. acaostaensis.

	Interval (in m)	Strike/dip measured	Decl1/ Incl1	Strike/dip calculated	Decl2/ Incl2	N	k	α_{95}
Basilicoi								
6	75-99	90/3	211.7/-41.9	284.7/55.9	205.1/-12.3	12	2.4	32.3
5	62-75	341/18	3.7/54.3	144.3/21	300/57	10	13.5	11.2
4	40-62	341/18	280.8/36.7	327.6/72		26		
3	32-40	341/18	29.8/33.9	203.2/18	347.2/48	9	21.6	5.1
2	29-32	341/18	143.8/-25.2	357/42.6	-	3		
1	0-29	341/18	167.5/-45	326.3/25.1	171.6/-33.2	25	9.3	11
Lese								
		59/4	349.6/45.3			59	12.1	5.6

TABLE 1.1: Overview of the results from the Basilicoi (different characteristic intervals) and Lese sections. Decl1/Incl1 represents mean directions of the ChRM components with a measured bedding tilt correction, Decl2/Incl2 with an AMS tilt correction. N = number of samples; k= precision parameter and α_{95}= semi-angle of cone of confidence of the 95% level.

Correlation to the GPTS

The magnetic polarity sequences of the Lese and Basilicoi sections (Fig. 1.6) are correlated to the geomagnetic polarity time scale CK95 (Cande and Kent, 1995). Although this time scale is already partly astronomically dated (Hilgen et al., 1995) we refer to CK95 for ages. Mediterranean bioevents have been tied to CK95 (Krijgsman et al., 1995), thus providing constraints on the age of the sections (Fig. 1.6).

The polarity sequence of the Basilicoi section reveals nine polarity zones which can be correlated to the GPTS on the basis of ages of bioevents. Tentative (as work is in progress) ages of about 10.5 Ma for the first regular occurrence (FRO) of *Neogloboquadrina acostaensis* (at 47 m) and about 11 Ma for the last occurrence (LO of *Paragloborotalia mayeri* (at 6 m) agrees well with the correlation of the thick normal polarity interval to C5n.2n of the GPTS. The base of the major hiatus (between 75 m and 76 m) has an estimated age of about 9.9 Ma since it is slightly younger than the base of the interval of the rapidly shifting coiling pattern of *Neogloboquadrina acostaensis* (work in progress). This agrees well with identifying the thin normal zone on top of the thick normal one as C5n.1n. The upper unit (above the hiatus) contains *Globorotalia menardii 4* and small-sized *Catapsydrax parvulus* (last occurrence ages: 7.40 and 7.32 Ma; Krijgsman et al., 1995) without *Sphaeroidinellopsis seminulina* (age of highest regular occurrence (hro): 7.65 Ma; Krijgsman et al., 1995). This indicates a maximum and minimum age of 7.64 and 7.40 Ma respectively for the top of the

hiatus. The interval above the hiatus, thus, ranges in age from 7.64 (7.40) Ma to 7.12 Ma, i.e. age of the FRO of the *Globorotalia conomiozea* group (Krijgsman et al., 1995). According to the integrated high-resolution biostratigraphy a normal subchron is missing between samples containing *Globorotalia menardii 4* and *Globorotalia menardii 5*. Nevertheless, the biostratigraphy gives an age of 7.12 Ma for the top of the Basilicoi section.

Basilicoi

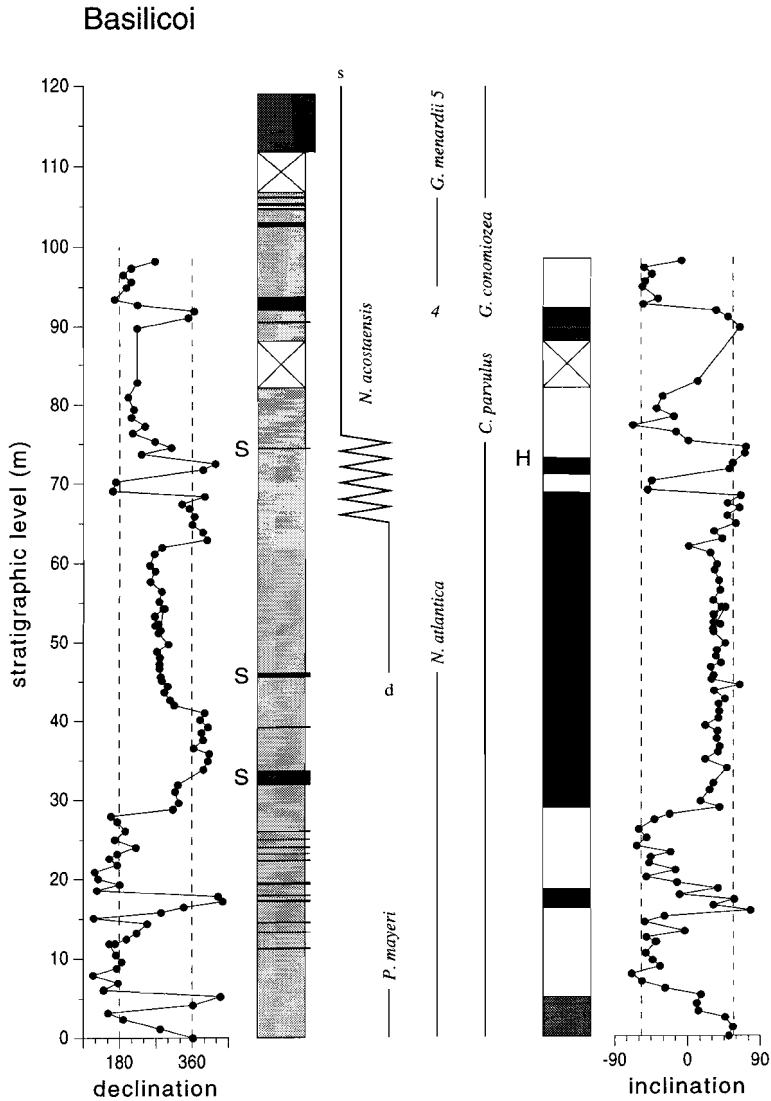*Fig. 1.5 Magnetostratigraphy of the Basilicoi section without any tectonic tilt correction. In the lithological column light grey represents marls and dark grey sand layers. The top of the section (dark grey) is formed by the Messinian diatomites of the Tripoli Formation. S (H) indicates a shearzone (hiatus). Faunal characteristics from foraminiferal biostratigraphy and associated bioevents of the Basilicoi section are indicated.*

The polarity pattern of the Lese section shows ten polarity zones. The uppermost normal polarity zone is chron 4An because the LO of *Catapsydrax parvulus* is within this chron (Krijgsman et al., 1995). The base of the section is (possibly slightly) younger than the first common occurrence (FCO) of *Neogloboquadrina acostaensis* indicating that the oldest normal polarity zone in the Lese section would correlate with the late chron 5n.2n (cf. discussion on Basilicoi section). Since we have no firm evidence for significant hiatuses in the Lese section intervening normal polarity zones (between chron 5n.2n and 4An) can be identified (from bottom to top) as chron 5n.1n, 4Ar.2n and 4Ar.1n.
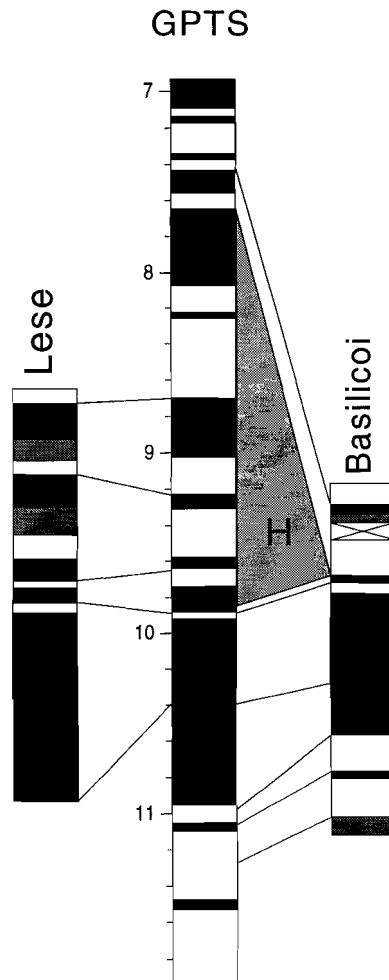

Fig. 1.6 Correlation of the Basilicoi and Lese sections to the GPTS of Cande and Kent (1995). Lines connect corresponding reversal boundaries or events mentioned in text. H (shaded area) represents the hiatus and crossed areas indicate non-exposed intervals. Numbers represent ages in Ma.

Anisotropy of the magnetic susceptibility

Analysis of the anisotropy of the magnetic susceptibility (AMS) is widely used to establish the sedimentary and tectonic history in weakly deformed sediments. Basically, the AMS of a rock is described by a second-order tensor. This tensor can be visualised by an ellipsoid having three principal axes of maximum, intermediate, and minimum susceptibility (k_{max}, k_{int} and k_{min}, respectively). Here, we characterise the total degree of anisotropy by $P = k_{max} / k_{int}$; the magnetic foliation is defined by $F = k_{int} / k_{min}$, while the magnetic lineation is the degree of anisotropy in the magnetic foliation plane and defined by $L = k_{max} / k_{int}$ (see Tarling and Hrouda, 1993). Depositional currents can also account for lineations, but this is unlikely in the fine-grained marine clays of the Basilicoi and Lese sections. In undeformed sediments, the magnetic susceptibility is characterised by an oblate ellipsoid, with the foliation coinciding with the bedding plane. In that case, the magnetic fabric is purely depositional or related to compactional loading; the k_{min} is perpendicular to the bedding plane and the k_{max} and k_{int} are scattered in the foliation or bedding plane itself. If there is deformation acting on a rock, this initially results in clustering of k_{max} in the direction of maximum extension or, equivalently, perpendicular to the maximum compression. The k_{min} is still perpendicular to the bedding plane. An increase of the strain causes the ellipsoid to have a more prolate structure. Finally, progressive strain obliterates the prolate ellipsoid into a 'pencil' structure and the depositional fabric is becoming overprinted by a tectonic fabric (Lee et al., 1990; Tarling and Hrouda, 1993). This pencil cleavage, easily recognised in the field, was not observed in the area.

Susceptibilities ($100 - 350 \times 10^{-6}$ SI) are rather constant throughout the Lese and Basilicoi sections. The uppermost 10 metres of the Basilicoi section, however, have higher mean susceptibilities ($500 - 800 \times 10^{-6}$ SI).

Lese section

The Lese section shows a rather constant lineation (mean L 1%), foliation (mean F 4%) and an AMS ellipsoid with a (sub)vertical k_{min} axis (Fig. 1.7 and 1.8). The k_{max} axes are aligned WNW-ESE, resulting in a lineation indicating a ENE-WSW compression. This compression direction is perpendicular to the 'duplex' compression in the overlying Belvedere sands, which showed NW-SE compression.

The magnetic anisotropy plot (Fig. 1.7) shows that the samples from the Lese section have a distinct oblate - and thus mainly sedimentary - magnetic fabric, with k_{min} -axes perpendicular to the bedding plane.
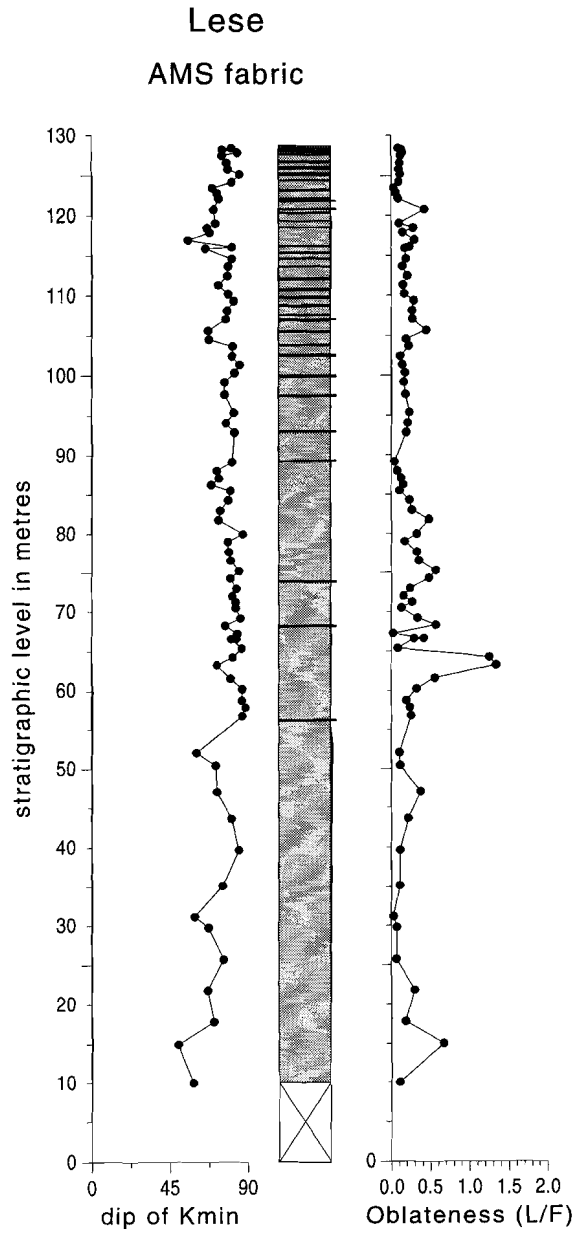
Lese

AMS fabric

Fig. 1.7 The AMS data of the Lese section with the dip of k_{min} and oblateness (L/F), indicating oblate ellipsoids and a sedimentary fabric.

Basilicoi section

In the top (62 -97 m) and bottom (0 - 40 m) part of the Basilicoi section the magnetic lineation (mean L 1%), foliation (mean F 5%) and AMS ellipsoid are relatively constant and similar to those of the Lese section. The AMS data from the top and bottom parts of the Basilicoi section indicate oblate ellipsoids (Fig. 1.9): the foliation coincides with the bedding plane and the k_{min} axes are perpendicular to the bedding. Furthermore, the AMS data display a N-S lineation - equivalent to E-W compression - for the lower part (0-40 m) of the Basilicoi section and a NW-SE lineation (NE-SW compression) for the upper part (62-97 m).

The middle part (42-63 m) of the section is markedly different. A slightly increased lineation (L 3%) and decreased foliation (F 1%), and a (sub)horizontal k_{min} axis is found. This could indicate increased tectonic deformation of the sedimentary fabric. Some 60% of the samples from this middle part show a prolate ellipsoid (Fig. 1.8). The prolate structure defines a well-marked magnetic lineation, while k_{int} and k_{min} form a girdle about k_{max}.
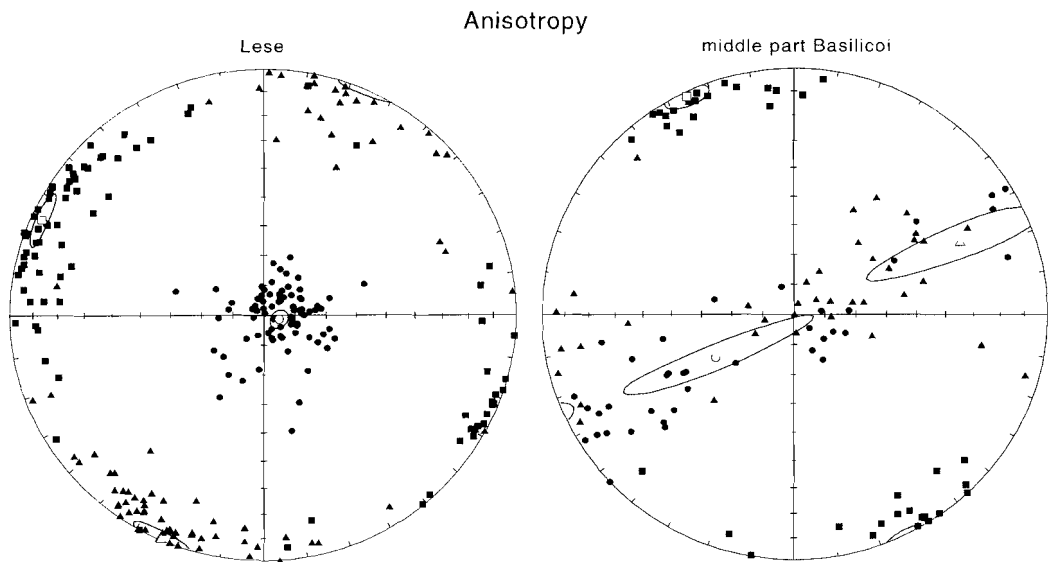
Fig. 1.8 Equal-area projection (without any bedding correction) of the anisotropy from the Lese section and the highly deformed middle part of the Basilicoi section; with k_{min} (circles), k_{max} (squares) and k_{int} (triangles).
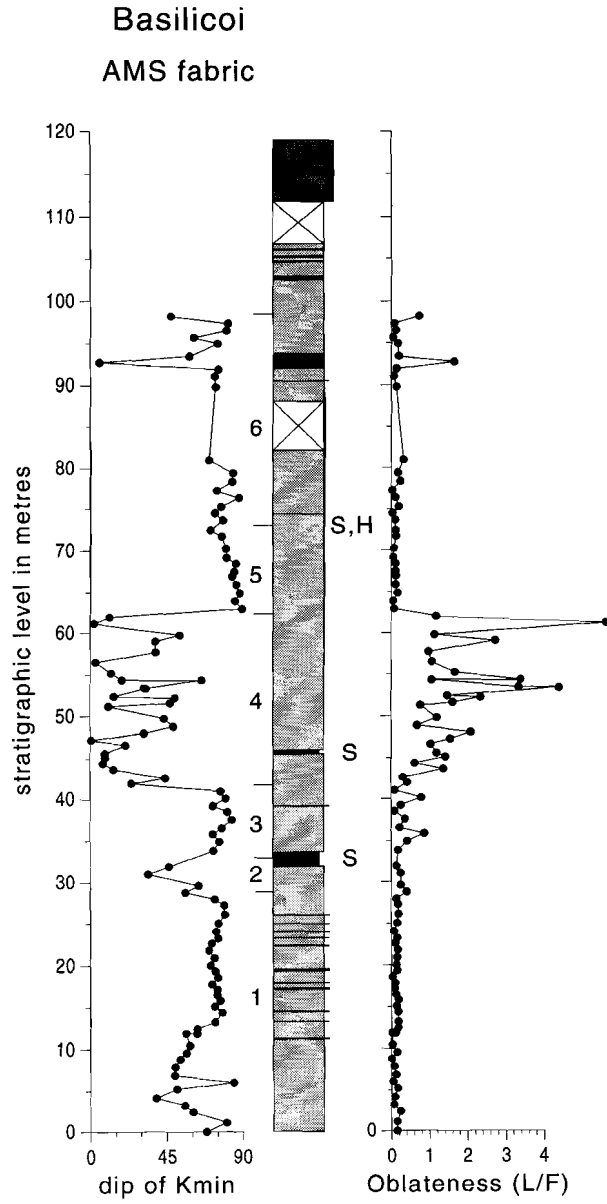
Fig. 1.9 The AMS data of the Basilicoi section with the dip of k_{min} and oblateness (L/F), indicating a strong deformation in the middle part of the section. Numbers refer to the groups that have been discerned (see text). See also caption to Fig. 1.5.

Discussion

Previous results from several sites of the Basilicoi section revealed a major CCW rotation in the middle part of the section and a CW rotation in the upper part (Scheepers, 1994b). For this interval, bedding plane data from the lower part of the section were used for tilt correction. If we use the same correction, our results from the Basilicoi section confirm those of Scheepers (1994b). They show a CCW rotation for the lower part of the section. For the middle part, however, we find the same - anomalously large (79°) - CCW rotation. We do not believe that such a large rotation is realistic, particularly because it occurs in the interval where we find a strongly deviating AMS fabric. Inversely, it is unlikely that the girdled k_{min} are indicative of a tectonic fabric: any large-scale tectonic (compressional) phase would also have deformed at least the underlying part of the sediments. The fact that the upper and lower part of the section show a purely sedimentary fabric, indicates that only local tectonics have caused faulting, leading to a hiatus and the presence of shearzones, and possibly to tilting of parts of the sedimentary sequence, like the middle part of the Basilicoi section. The assumption of local tectonics is confirmed by the absence of an hiatus or shearzones from the nearby Lese section.

To investigate whether this large and anomalous CCW rotation of the middle part was caused by tilting, we have assumed that the sediment has still retained a dominantly sedimentary fabric, although we realise that tilting probably has affected the fabric to some extent, as is suggested by the slight increase of lineation. Therefore, we used the k_{min} axis as a pole to the bedding plane. We discriminate six characteristic intervals (Fig. 1.10) on the basis of the shearzones, the hiatus, and the ChRM and AMS characteristics. The first interval is bounded by the first shearzone, the second small interval is located between the first and second shearzone. The third interval is recognised till around 40 m, where the ChRM directions shows a sudden change in declination and inclination (Fig. 1.5). The next, fourth, interval is characterised by strongly deviating k_{min} axes (Fig. 1.9). The following, fifth interval, starts where the ratio L/F suddenly decreases; it ends at the hiatus. The sixth interval is formed by the top part of the section. This procedure results in a steeply tilted, NE-dipping bedding plane in the middle part which considerably deviates from the bedding plane measured at the base and top of the section. If we correct the samples for the calculated 'AMS bedding plane', the large CCW rotation is strongly reduced; an example is given in Figure 1.3g, h and i.

We then recalculate the direction of the ChRM components using mean values for the corrected bedding planes of each interval. We then find an 8° counterclockwise (D_m = 171.6°; I_m = -33.2°) rotation in the first interval. The second interval only contains 4 samples and statistics do not allow a reliable mean. The corrected ChRM-components in intervals 3 and 4, both located in the deformed middle part of the Basilicoi section, reduce the major (79°) counterclockwise rotation to approximately 13° (D_m=347.2°; I_m=48°) counterclockwise (Fig. 1.11). The fifth interval shows a large CCW rotation of 60° (D_m = 300° and I_m = 57°), which we regard as less reliable because of the presence of two polarity reversals in this small interval and the proximity to the hiatus.

Basilicoi (AMS corrected)
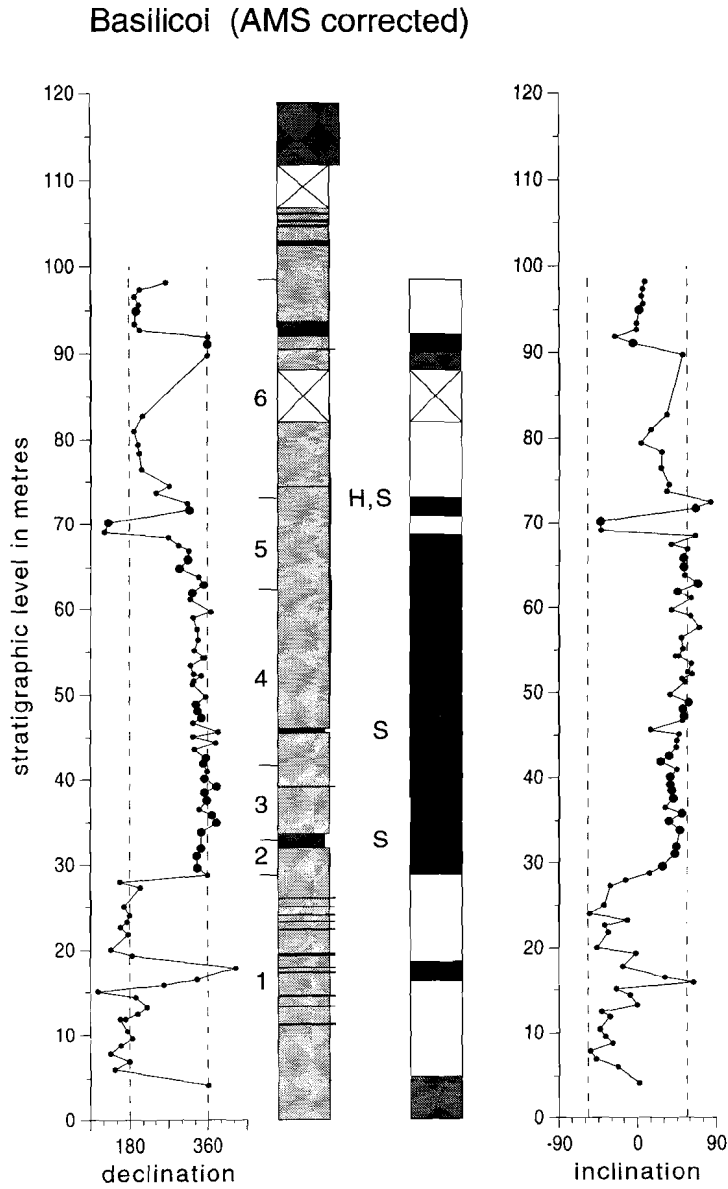
Fig. 1.10 Magnetostratigraphy of the Basilicoi section with an AMS bedding tilt correction. Small closed circles represent low-intensity samples, big closed circles represent reliable directions. In the polarity column, black (white/grey) denotes normal (reversed/questionable) polarity zones. Crossed area indicates a non-exposed interval. In the lithological column light grey represents marls and dark grey sand layers. The top of the section (dark grey) is formed by the Messinian diatomites of the Tripoli Formation. S (H) indicates a shearzone (hiatus). Numbers indicate different characteristic intervals.

To verify the AMS tilt correction, we compared the results with those of the nearby Lese section. This section shows a constant oblate ellipsoid and a sub-vertical k_{min} axis, with on average the same orientation as the measured bedding pole. The ChRM directions of the entire Lese section are consistent, implying a 10° CCW direction (Fig. 1.11). This is in good agreement with the corrected results of the Basilicoi section. This seems to suggest that the AMS-correction is valid.
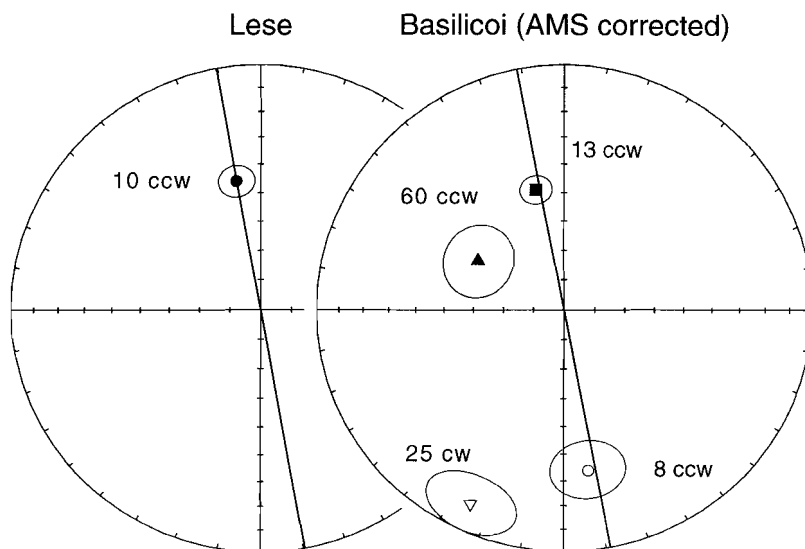
Fig. 1.11 Equal-area projection of the ChRM mean directions of the Lese and the Basilicoi section; circles represent 95% (α95) confidence regions around the mean directions. Open circle refers to the first interval (0-29 m), closed square to the third and fourth interval (32- 62 m), closed triangle to fifth interval (62-75 m) and open triangle to the sixth interval (75- 99 m).

Similar counterclockwise rotations are also found in older (than late Tortonian) rotations elsewhere in Calabria (Montigny et al., 1981; Scheepers, 1994b), although results are often mixed. Perhaps it would be useful to see whether AMS correction gives more consistent results.

The late Tortonian (< 7.5 Ma) sediments in the top of the Basilicoi section (the sixth interval) show a clockwise mean direction (D_m = 205.1°, I_m = -12.3°) after tilt correction by AMS. This fits with the general trend in the area: previous paleomagnetic studies found a 15° clockwise rotation for the late Tortonian to Early Pleistocene sedimentary cover for the Calabro-Peloritan block. This rotation phase was dated between 0.8 and 0.7 Ma (Scheepers, 1994b). The 10° counterclockwise rotation (with respect to north) for the older than late Tortonian sediments and an average 15° clockwise rotation for the late Tortonian to Early Pleistocene sediments result in a 25° counterclockwise rotation phase in the Crotone basin.

With respect to the African paleopoles (Tauxe et al., 1983) this is equivalent to 17° CCW and 11° CW, respectively, resulting in a 28° CCW rotation phase. This counterclockwise rotation must have taken place - at least in the Crotone basin - between ~7.5 Ma and 8.6 Ma. Furthermore, the results from the Basilicoi section are consistent and suggest that no significant rotation of the Crotone basin has taken place between 11.3 and 8.6 Ma.

Our paleomagnetic data imply that a major tectonic rotation phase took place in the Crotone basin between 8.6 and ~7.5 Ma. If we consider the astronomical ages (Hilgen et al., 1995) for the earlier mentioned bioevents, the rotation phase took place between 8.6 and ~7.6 Ma (maximum/minimum age for the hiatus is 7.73 / 7.51 Ma; bioevent 6 and 7, respectively, in Hilgen et al., 1995). Although there is considerable uncertainty concerning the timing of the opening of the Tyrrhenian basin, it seems likely to link this major tectonic event to this rotation phase. This would imply that the opening of the basin may have started between 8.6 - ~7.6 Ma. There is some additional evidence for this: biostratigraphic and magnetostratigraphic results from ODP Leg 107 (Kastens et al., 1987) show that the oldest sediments in the Tyrrhenian basin, east of Sardinia, have an age of approximately 7.8 Ma (Fig. 1.12). The ages of the oldest sediments are increasingly younger towards the Calabro-Peloritan block. We speculate that the opening of the basin started between 8.6-7.8 Ma. Moreover, we know that no significant tectonic rotation for Calabria took place till 0.7 - 0.8 Ma (Scheepers, 1994b). This suggests that the movement of Calabria to its present-day configuration was the result of horizontal translation, without noticeable rotations.
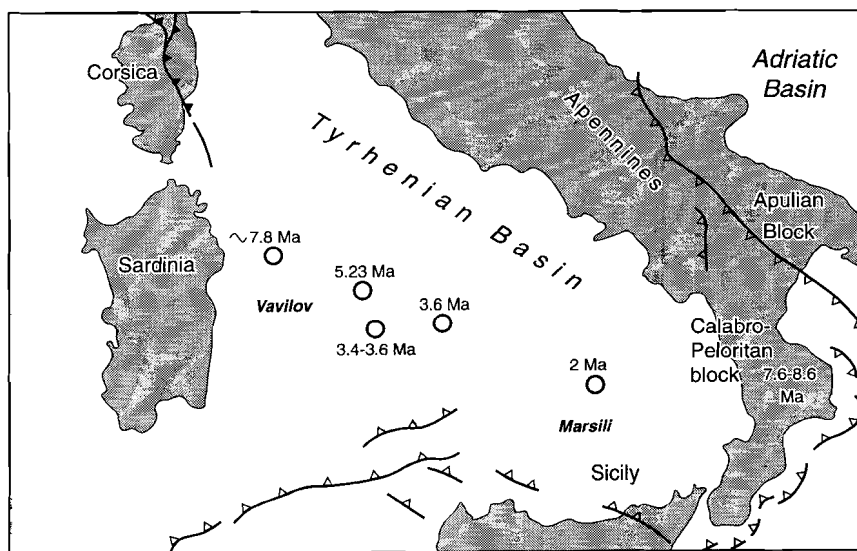
Fig. 1.12 Ages of oldest marine sediments from ODP Leg 107 (Kastens et al., 1987) and timing of the rotation phase in the Crotone area.

Conclusions

Previous results (Scheepers, 1994b) from sites in the Basilicoi section indicated a large anomalous counterclockwise (80°) rotation in the middle part of the section, where no bedding plane could be established. After reducing this major CCW rotation by means of AMS tectonic tilt correction, we find a more consistent 13° counterclockwise rotation in early Tortonian sediments. This rotation is confirmed by data (10° CCW) from the partly time-equivalent and undisturbed Lese section. The late Tortonian part of the Basilicoi section shows a clockwise rotation, in agreement with other late Tortonian to Early Pleistocene sites in Calabria (Scheepers, 1994b). On average these sites indicate a 15° clockwise rotation, which enables us to date a late Tortonian 25° counterclockwise rotation phase for the Crotone basin between ~7.6 and 8.6 Ma. The results from the older part of the Basilicoi section are consistent and indicate that from 11.3 to 8.6 Ma the Crotone basin remained relatively stable. Since the oldest sediments in the Tyrrhenian basin are at least 7.8 Ma, we speculate that the opening of the basin may have occurred between 8.6-7.8 Ma, and has caused major compression resulting in a significant counterclockwise tectonic rotational phase in Calabria.

Acknowledgements

2

Astronomical dating of a tectonic rotation on Sicily and consequences for the timing and extent of a middle Pliocene deformation phase

Abstract

A detailed paleomagnetic study of long and continuous middle Pliocene sections from the Caltanisetta basin on Sicily reveals a differential clockwise rotation occurring around 3.21 Ma. The rotation appears to be a rapid event (80,000-100,000 years) which suggests that the responsible tectonic processes also occur rapidly. Its timing corresponds closely to the transition from the Trubi to the Narbone Formation at 3.19 Ma. This transition marks a major change in sedimentary environment on Sicily and in Calabria, and it is coeval, for instance, with the onset of sapropel formation in the eastern Mediterranean. Apparently it marks a synchronous and central - eastern Mediterranean-wide event. Data from the oldest sediments overlying the Tyrrhenian basement (ODP Leg 107) suggest an acceleration in opening of the Tyrrhenian Sea during the middle Pliocene. We speculate that this acceleration is related to a transpressional event in the Sicilian fold-and-thrust belt and extension which formed troughs in the foreland, the Strait of Sicily. Thrust imbrication accompanying the transpressional event on Sicily induced the middle Pliocene clockwise rotation and resulted in shallowing of the Caltanisetta basin causing the change in sedimentation regime characterised by the Trubi-Narbone transition. Following this middle Pliocene tectonic phase, no rotation took place in the southern Apennines, Calabria and Sicily until the middle Pleistocene (1.0 - 0.7 Ma).

Introduction

During the last decade, detailed studies of the sedimentary cyclicity of Pliocene sequences on Sicily and in Calabria resulted in high-resolution chronostratigraphic correlations (Zijderveld et al., 1986, 1991; Hilgen, 1987). Integrated magnetostratigraphy, biostratigraphy and cyclostratigraphy have provided a reference framework for the Mediterranean Pliocene (i.e. the Rossello Composite section; Langereis and Hilgen, 1991). This framework underlies the astronomical polarity time scale (APTS) for the Pliocene (Hilgen et al., 1991a, b), which is based on the correlation of sedimentary cycles to quasi-periodic variations of precession. Here, we use the most recent APTS of Lourens et al. (1996). The paleomagnetic data set of the Rossello Composite was used by Scheepers and Langereis (1993) to suggest that a differential rotation of 10° occurred 'approximately at Kaena times'. The exact timing of this rotation could not be established since the mean directions of the normal and reversed subchrons of the Rossello Composite were not antipodal. Contrary to the older (Gilbert Chron) part of the Rossello Composite, the samples from the younger (Gauss Chron) part showed no or little normal overprint. Their 'overprint correction', which was successfully applied to the older part, could not be used in the younger part since the sense of the non-antipodality was contrary to what was expected from a secondary, present-day overprint (see Scheepers and Langereis, 1993).

The Pliocene is a period of regional contraction within the Sicilian fold-and-thrust belt (Oldow et al., 1990) and extension in the foreland, the Strait of Sicily (Argnani, 1990). Oldow et al. (1990) have demonstrated that large-scale clockwise block rotations during the late Cenozoic accompany the migration of a thrust front towards the Sicilian foreland. Our objective is firstly to confirm the middle Pliocene tectonic differential rotation found in the Rossello Composite and, secondly, to date it more accurately by using the APTS on sections which show no unexplained non-antipodality and were sampled in much greater detail than the previous magnetostratigraphic sampling. We will investigate further whether this rotation phase was a local phenomenon or caused by a major tectonic event with a regional expression. Therefore, two additional middle Pliocene sections containing the Trubi and Narbone formations, Secca Grande and Punta Secca, were selected. The new results are compared to those of the Rossello Composite. Finally, we link this rotation to the geodynamic processes affecting the Sicilian fold-and-thrust belt, the Strait of Sicily, and the Tyrrhenian basin during the Pliocene.

Sections and sampling

Sicily is composed of five main tectonic units: (1) the Ragusa platform which is part of the Apulian plate; (2) the Gela-Catania foredeep; (3) the Caltanisetta basin; (4) the northern Sicilian fold-and-thrust belt; and (5) the Peloritan units which belong to the Calabro-Peloritan block (Fig. 2.1). The Rossello Composite is located in the Caltanisetta basin and is composed of three cliff sections along the south-west coast of Sicily, i.e. the Eraclea Minoa,

Punta di Maiata and Punta Piccola sections. The Rossello Composite contains the Trubi and Narbone formations. The Lower to middle Pliocene Trubi Formation consists of carbonate-rich, rhythmically bedded grey to white marine marls (Hilgen, 1987). Fossil assemblages indicate that these sediments were deposited at a depth of 500-800 m (Brolsma, 1978). The Trubi Formation is overlain by the Upper Pliocene to Lower Pleistocene Narbone Formation represented by rhythmically bedded, relatively carbonate-poor, marly clay with sapropel layers, deposited at shallower depths of 100-400 m (Brolsma, 1978). Both formations were studied in two additional sections: Punta Secca and Secca Grande (Fig. 2.1). Punta Secca is a cliff section along the southwest coast of Sicily in the Caltanisetta basin, near the village of Siculiana. The section contains a small, well constrained fault, approximately at the Gauss-Matuyama boundary. The Secca Grande section is located between the village of Ribera and the coast. The top of the Secca Grande section is locally formed by an olistostrome. Therefore, it was extended upward at the opposite side of the valley, near the village of Ribera, where no olistostrome is present. During a first field visit the Secca Grande and Punta Secca section were sampled with two levels per sedimentary (precession-related) cycle, corresponding to a resolution of approximately 10,000 years. During a second visit, the Trubi-Narbone boundary interval was sampled in Secca Grande (with a 10 cm spacing) to date accurately any differential rotation. Paleomagnetic coring was carried out following routine procedures, using an electric, water-cooled, drill and a generator as power supply. Care was taken to remove the weathered surface and to drill fresh sediments.
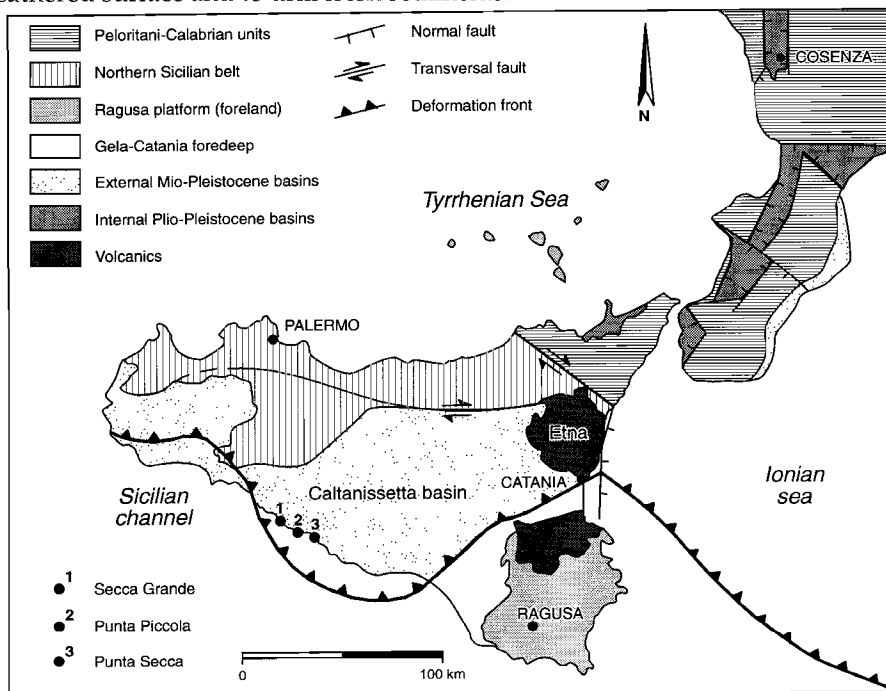
Fig. 2.1 Structural map of Sicily with the sections studied: Secca Grande, Punta Secca and Punta Piccola.

Paleomagnetic results

Rock magnetic properties

Some rock magnetic tests were performed to identify the carriers of the remanent magnetisation. Bulk susceptibilities were measured on a KLY-2 Kappabridge; they were typically 200×10^{-6} SI and are quite constant throughout the Secca Grande and Punta Secca sections. Acquisition of an isothermal remanent magnetisation (IRM) was measured on a digitised spinner magnetometer based on a Jelinek JR3 driver unit. An IRM was induced in three orthogonal directions (Lowrie, 1990) using fields of 30 mT, 200 mT and 2 T in a pulse magnetiser, and subsequently thermally demagnetised. These fields were chosen as most appropriate on the basis of the typical magnetic characteristics of these marine marls (e.g. Van Velzen and Zijderveld, 1990). After each temperature step the low-field susceptibility was measured.
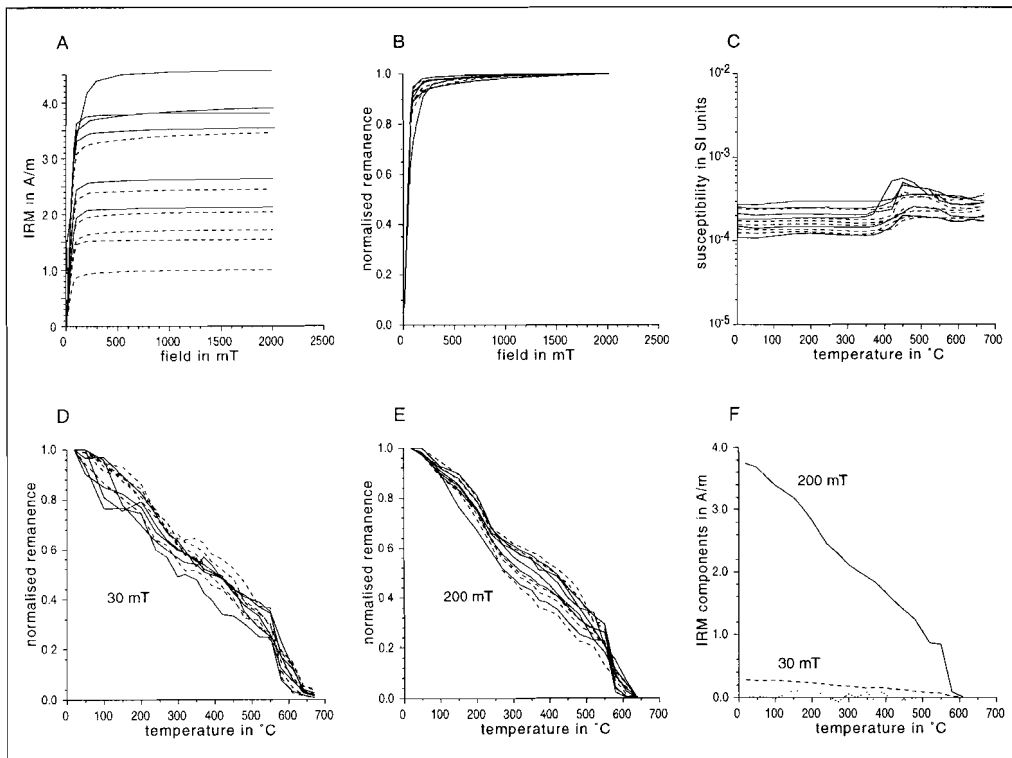
Fig. 2.2 (A and B) Examples of IRM acquisition of samples from the Secca Grande (solid line) and Punta Secca (dashed line) section. (C) The low-field susceptibility measured during stepwise thermal demagnetisation. (D and E) Thermal demagnetisation along the 30 mT and 200 mT axis, respectively. (F) An example of thermal demagnetisation of the 30 mT (dashed line), 200 mT (solid) and 2.0 T (dotted) orthogonal induced IRM components. Note that the remanence mainly resides in the 200 mT axis.

The Secca Grande and Punta Secca sections reveal the same magnetic carriers. The steep initial rise and the acquisition of 90-95% of the saturation IRM (SIRM) at 100 mT (Fig. 2.2a and b) indicates magnetite to be the dominant magnetic carrier. A small percentage (~5%) of the SIRM is acquired at fields higher than 300 mT and indicates that a high-coercivity mineral is also present. All samples show an increase in low-field susceptibility (Fig. 2.2c), just below 400°C caused by oxidation of pyrite which produces magnetite. Thermal demagnetisation of the 3-axis IRM (Fig. 2.2d-f) shows that the remanence is mostly carried along the 200 mT axis. Typically, samples show maximum unblocking temperatures close to 580°C and indicative of magnetite, but often temperatures are above 600°C, indicating the presence of maghemite.

Thermal demagnetisation

Thermal demagnetisation of the natural remanent magnetisation (NRM) was performed using a magnetically shielded, laboratory-built furnace; measurements were done on a 2G Enterprises DC SQUID cryogenic magnetometer. A total of 679 specimens from the Punta Secca and Secca Grande section was demagnetised, using small temperature increments between 30° and 50°C. Demagnetisation diagrams (Zijderveld, 1967) and least-square fitting of lines (Kirschvink, 1980) through selected data points were used to determine the NRM components. The magnetisation vectors were averaged using Fisher (1953) statistics to calculate mean directions per interval/polarity zone.

The demagnetisation behaviour of the sections studied is similar. Representative demagnetisation diagrams show a small randomly oriented laboratory-induced component removed at 100°C (Fig. 2.3). Occasionally, a secondary component caused by weathering and with a present-day field direction before bedding tilt correction is present; it is removed at temperatures between 100° and 250°C. A characteristic remanent magnetisation (ChRM) component is removed at temperatures between 570° and 600°C. It shows both normal and reversed polarities and a linear decay towards the origin. In the Secca Grande section, almost all NRM intensities (30-170 mA/m) of the ChRM-component are one order of magnitude larger than the NRM intensities found in the Punta Secca section. This difference is related to the fact that Secca Grande consists of the Trubi Formation and lower part of the Narbone Formation, with typically high intensities and a stable magnetite-dominated magnetomineralogy (Langereis and Hilgen, 1991), while most of the Punta Secca is much younger and consists of the upper part of the Narbone Formation (shallower marine). Intensities are typically as those found by Zijderveld et al. (1991) in the time- and facies-equivalent Narbone Formation in southern Calabria. The differences in intensities are caused by the different sedimentary environment (see also Van Velzen et al., 1993). Demagnetisation of the NRM above approximately 390°C may result in randomly directed components (Fig. 2.3e,f) which were not used for the calculations.

The ChRM directions and polarity zones of the Secca Grande section (Fig. 2.4) show that five polarity intervals are recorded. In the Punta Secca section (Fig. 2.5) the ChRM

directions reveal seven polarity zones, whereas the Punta Piccola section (Scheepers and Langereis, 1993) contains six zones.
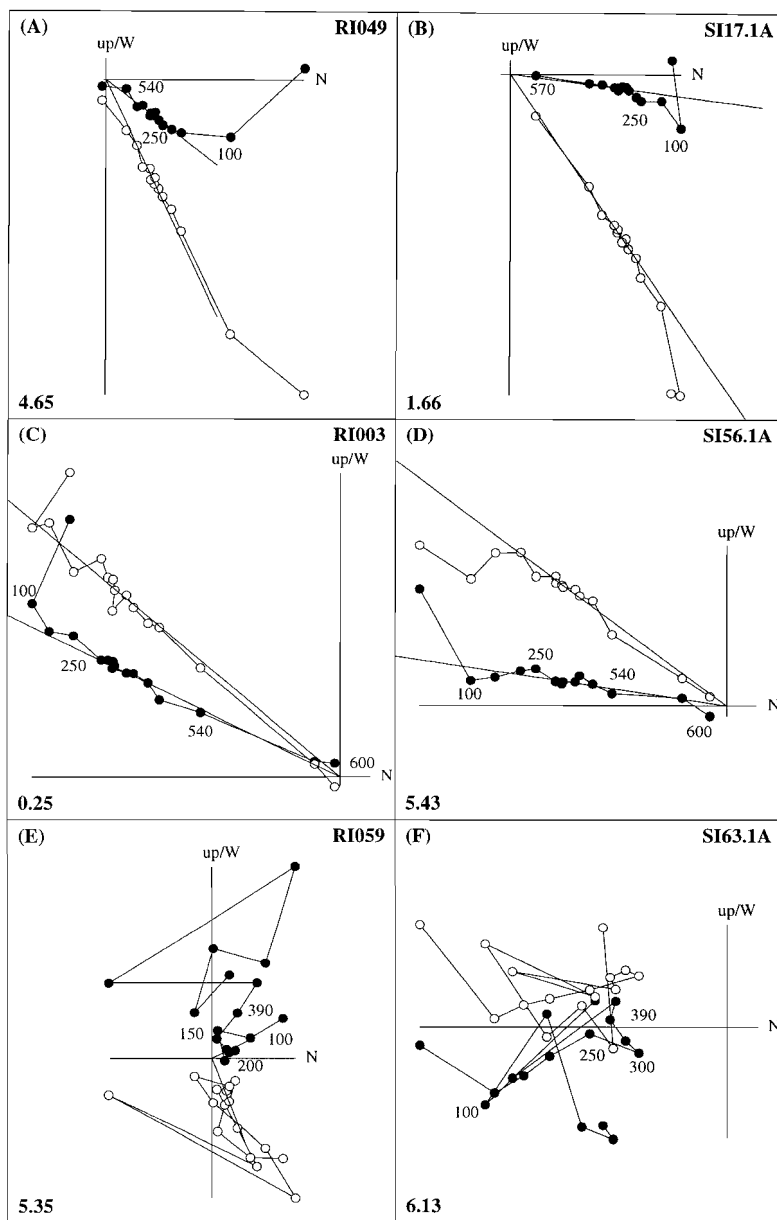

Fig. 2.3 Orthogonal projections of stepwise thermal demagnetisation of selected samples from the Secca Grande (RI) and Punta Secca (SI) section. Closed (open) circles represent the projection of the NRM vector endpoint on the horizontal (vertical) plane. Values indicate temperatures in °C; stratigraphic levels are shown in the lower left corners.

Differential rotations

Scheepers and Langereis (1993) found a differential clockwise rotation of 10° in the Punta Piccola section of the Rossello Composite. Their data revealed an uncertainty in age of the rotation between the Gilbert-Gauss boundary and the youngest normal subchron (C2An.1n) of the Gauss. Although the normal and reversed mean ChRM directions were not antipodal, they suggested approximately Kaena times as the best age estimate. This is slightly younger than the transition from Trubi to Narbone between cycle 95 and 96 at an age of 3.19 Ma in subchron C2An.2n (Langereis and Hilgen, 1991; Lourens et al., 1996). The Punta Piccola section covers the uppermost part of the Gilbert Chron to the lowermost part of the Matuyama Chron. The Secca Grande and Punta Secca sections can be correlated bed-by-bed to the Rossello Composite on the basis of their cyclostratigraphy and magnetostratigraphy. The reversals in the two sections are located in the same cycles as in the Rossello Composite. The lowermost normal polarity zone of the Secca Grande section is subchron C2An.3n, the uppermost zone represents subchron C2An.1n, whereas the reversed zones are the Mammoth and Kaena subchrons (Fig. 2.4). Even though the Punta Secca section contains a small fault approximately at the Gauss-Matuyama boundary, the results confirm that, from bottom to top, the subchrons Mammoth to C1r.2r are present (Fig. 2.5).

The paleomagnetic results from the Secca Grande section indicate a differential clockwise rotation of 10°, from 32° in the Mammoth subchron to on average 22° in the C2An.2n and Kaena subchrons (Figs. 2.6 and 2.7). The mean declinations of C2An.2n and Kaena are exactly antipodal, although the inclinations slightly differ. The upward extension of the Secca Grande section, at the opposite side of the valley, has a significantly larger absolute rotation (Dec = 35° with Inc = 42.9°, N = 39, k = 92.6, α_{95} = 2.4) then the post-Mammoth part of the Secca Grande section (22°). The results of Secca Grande indicate that the differential clockwise rotation must have taken place in a short time considering the change in the average declination over a small interval that encompasses the Mammoth – C2An.2n boundary. The rotation can thus be accurately dated, within an interval of approximately four or five cycles (80,000-100,000 years) around the boundary between the Mammoth and subchron C2An.2n which has an astronomically dated age of 3.21 Ma. The Trubi-Narbone transition, astronomically dated at 3.19 Ma, falls within this rotational interval. These results from Secca Grande agree with the earlier estimate (between 2.58 - 3.60 Ma) of the tectonic rotation in the Rossello Composite.

In the Punta Secca section, a differential rotation could not be substantiated because only a very limited amount of samples could be taken from the Trubi. Furthermore, no differential rotation in the Punta Secca section was found up to the Early Pleistocene, if we exclude the paleomagnetic data near the observed fault (i.e. all data below 40 m; Fig. 2.4). The mean direction is D_{mean}=21.9°, I_{mean}=44.0° (N= 15, k=110.4 and α_{95}=3.7).

Secca Grande
ChRM-directions
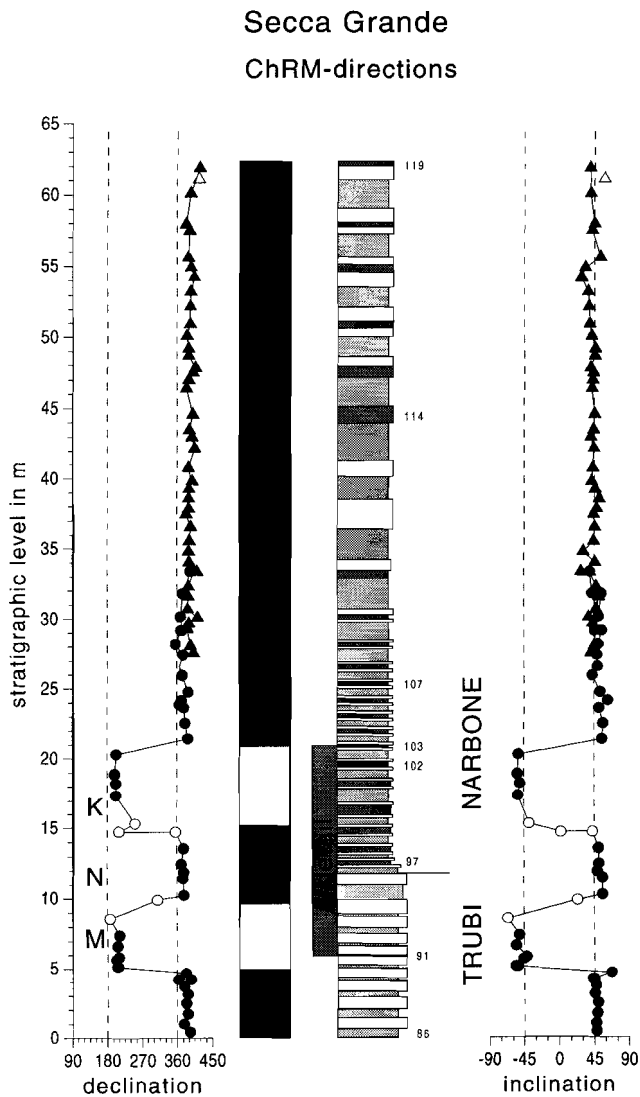
Fig. 2.4 Magnetostratigraphy of the Secca Grande section, including the upward extension (triangles) and detail set (shaded area with 166 samples); K = Kaena, N = normal, C2An.2n; M = Mammoth; see also Figs. 2.6 and 2. 7. Closed circles represent reliable directions, open circles represent low-intensity samples and no linear decay towards the origin (see text). In the polarity column black (white) denotes normal (reversed) polarity zones. In the lithological column grey shading indicates beige marls in the Trubi Formation, whereas in the Narbone Formation dark grey/black represents brown sapropels; white indicates white marls. Numbers represent cycle-numbers of the correlative small-scale cycles in the Rossello Composite section (Langereis and Hilgen, 1991).

Punta Secca
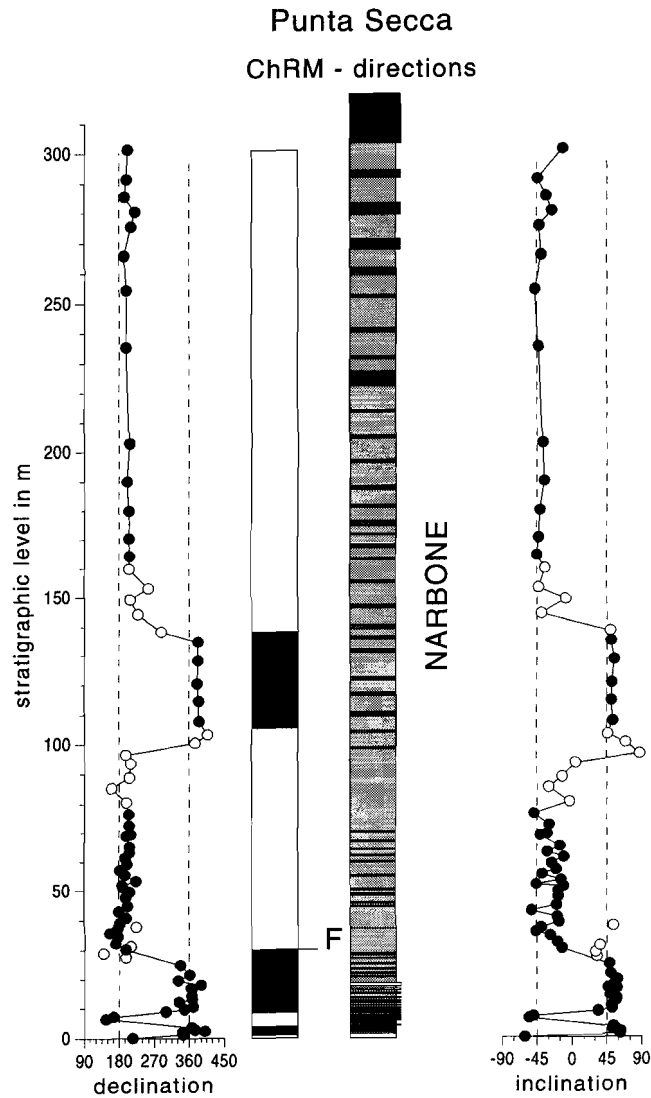
ChRM - directions

Fig. 2.5 Magnetostratigraphy of the Punta Secca section. Closed circles represent reliable directions, open circles represent low-intensity samples and no linear decay towards the origin (see text). In the polarity column black (white) denotes normal (reversed) polarity zones. In the lithological column light (dark) grey represents beige (grey) marls; in the top part of the section, dark grey indicates sand layers. F = a small fault (see text). The lowermost reversed zone represents the Mammoth, the second the Kaena. The uppermost normal zone represents the Olduvai, wherein we find the Plio-Pleistocene boundary.

Secca Grande detail
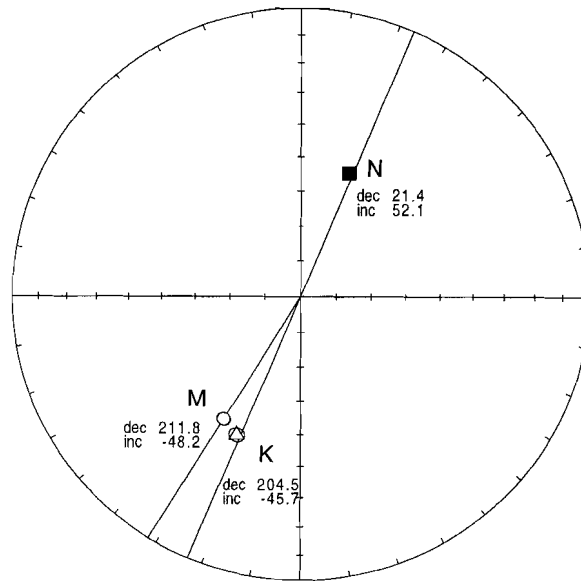
Fig. 2.6 Mean directions of ChRM-components (the Secca Grande detail set) are shown in an equal-area projection, indicating a 9° differential clockwise rotation; K = Kaena (N = 34, k = 140.7 and α_{95} = 2.1); N = normal, C2An.2n (N = 58, k = 161.6 and α_{95} = 1.5) and M = Mammoth (N = 35, k = 166.9 and α_{95} = 1.9) see also Figs. 2.4 and 2.7. Dec (inc) indicates declination (inclination); combined Kaena and normal: declination 22.4°; inclination 49.7°; N = 92, k = 103, α_{95} = 1.5.

Anisotropy of magnetic susceptibility

Analysis of the anisotropy of the magnetic susceptibility (AMS) can be used to establish the sedimentary and tectonic history in weakly deformed sediments (Tarling and Hrouda, 1993). Basically, the AMS of a rock is described by a second-order tensor, visualised as an ellipsoid having three principal axes (k_{max}, k_{int} and k_{min}). In undeformed sediments, the magnetic susceptibility is characterised by an oblate ellipsoid, with foliation coinciding with the bedding plane. Hence, the magnetic fabric is purely depositional or related to compactional loading with the k_{min} axes perpendicular to the bedding plane and the k_{max} and k_{int} axes scattered in the bedding plane itself. In case of small deformation acting on the rock, the k_{max} axes cluster in the direction of maximum extension, or perpendicular to the maximum compression and the k_{min} is still perpendicular to the bedding plane. An increase of strain changes the oblate ellipsoid into a prolate structure. Therefore oblateness (here L-1/F-1; with L/F as lineation/foliation) is used to indicate deformation, and the clustering of the k_{max} axes to indicate the direction of extension (and indirectly the compression-direction).

The AMS fabric in the Secca Grande, Punta Secca and Punta Piccola section has oblate ellipsoids for nearly all samples. The lineation and foliation are rather constant throughout the three sections (Secca Grande: L_{mean} and F_{mean} both 1%; Punta Secca and Punta Piccola both: L_{mean}=0.5%, F_{mean}=2%). The AMS ellipsoid in both the Trubi and the Narbone formations of the Secca Grande and Punta Secca section display k_{max} axes aligning E-W, indicating a N-S compression, and (sub)vertical k_{min} axes (Fig. 2.8). In the Punta Piccola section the k_{max} axes align NE-SW indicating a NW-SE compression. Although the k_{max} directions in Secca Grande (166 samples) seem more dispersed than in Punta Secca (73), there is a clear clustering of the vast majority of the samples, giving small error ellipses and a well defined average lineation direction. In all three sections no noticeable change in compression/extension direction is present around the interval where the differential rotations occur.
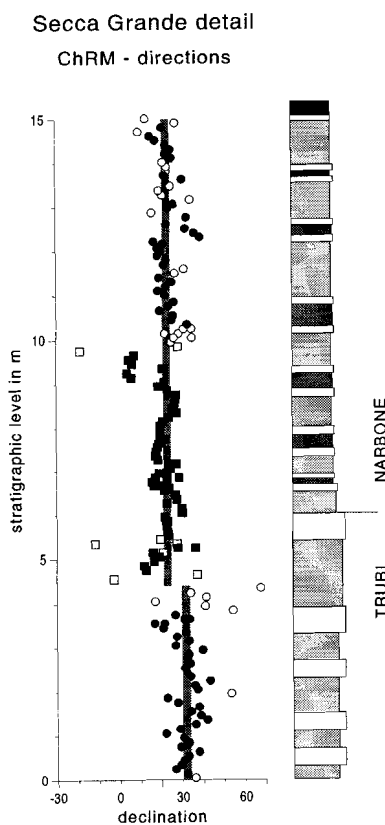
Fig. 2.7 Declinations of the ChRM directions of the Secca Grande detail set (see also Figs. 2.4 and 2.6). Shaded bands are the mean directions with their α_{95} for the Mammoth subchron and the normal + Kaena subchrons, respectively. Open symbols indicate the low-intensity samples; circles are the inverted ChRM directions. Lithological column see caption Fig. 2.4
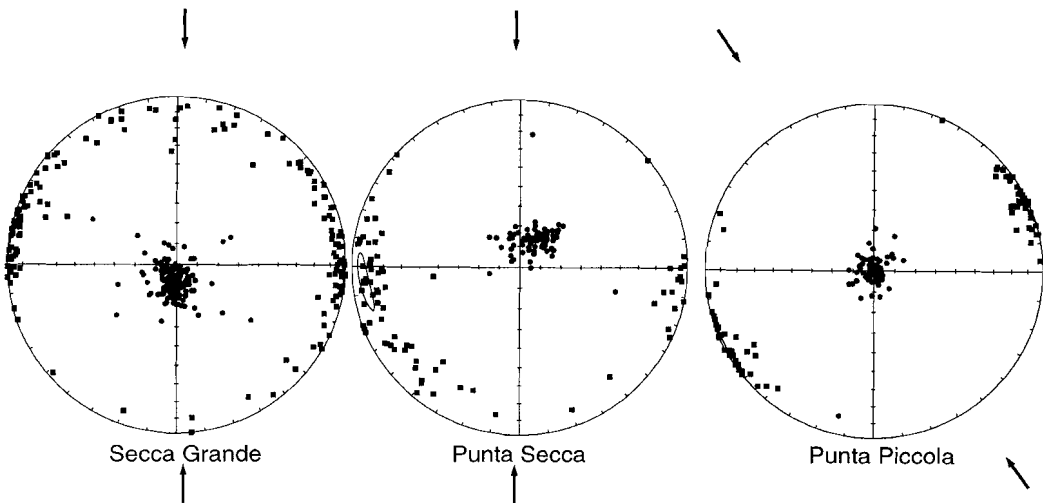
Fig 2.8 The equal-area projections (after bedding correction) show the anisotropy of the sections with k_{min} (circles) and k_{max} (squares). Arrow indicates compression direction.

Discussion

The previous paleomagnetic study by Scheepers and Langereis (1993) indicated a clockwise rotation 'approximately at Kaena times'. The better constrained clockwise rotation around 3.21 (± 0.05) Ma in the Secca Grande section replaces their earlier estimate. Our results imply a middle Pliocene regional event in the Caltanisetta basin where a tectonic rotation coincides with a change towards a more shallow environment. This tectonic phase is not restricted to Sicily; elsewhere in the Mediterranean there is evidence for major changes at the time of the Trubi-Narbone transition. For example, in ODP Leg 160 Sites 967 and 969 in the eastern Mediterranean, the formation of the first sapropels starts directly after the Trubi-Narbone boundary (Kroon et al, 1998), representing a change to periodic anoxic bottom water conditions. The first sapropels at Punta Piccola, Punta Secca and Secca Grande are slightly younger (± 100,000 years) which may be caused by a higher threshold value for sapropel formation in the Caltanisetta basin. The transitions (i.e. both the Trubi – Narbone transition and the first sapropel formation in the eastern Mediterranean) point to a major reorganisation in basin configuration and/or a fundamental change in climatically induced paleoceanographic conditions. Around the same time, a major tectonic event caused an increase in uplift rates and large-scale tilting to the north on Crete (Meulenkamp et al., 1994). In northern Italy, Mary et al. (1993) found a hiatus between the upper part of the Gilbert up to the lower part of the Kaena. Their ChRM directions imply a rotation phase falling within this hiatus; the part below the hiatus shows a considerable counter-clockwise rotation, whereas the younger part has no significant rotation, roughly constraining the age of this differential rotation. These

regional tectonic events, seemingly unrelated, can now be correlated on the basis of an accurate chronology.

The ChRM directions from the long, continuous Punta Secca section indicate no differential rotation until the Early Pleistocene. Also in Calabria and in the southern Apennines (Scheepers et al., 1993; 1994) no evidence of any differential rotation was found, from the middle Pliocene until the early-middle Pleistocene. Scheepers (1994c) suggested that an additional clockwise rotation phase must have occurred between the middle Pliocene and early-middle Pleistocene on Sicily, because he found smaller clockwise rotations in the early-middle Pleistocene (15°) than in the middle Pliocene (25°). This is not conclusive, however, because local tectonics may disturb a recognition of regional versus local tectonics. A good example is the extension of Secca Grande on the opposite side of the valley: ChRM directions show a statistically different absolute rotation, which can only be explained by local tectonics. This demonstrates the importance of establishing a differential rotation within a continuous section rather than from isolated outcrops. Finally, Scheepers (1994c) finds a rotation phase between 1.0 - 0.7 Ma in Sicily, Calabria and the southern Apennines. We conclude that no rotation occurred along the entire Tyrrhenian arc between the middle Pliocene (3.2 Ma) and middle Pleistocene (1.0-0.7 Ma).

Previous paleomagnetic research on the Trubi and Narbone formations (Van Hoof and Langereis, 1991) has shown that delayed NRM acquisition may significantly disturb a record of rapid geomagnetic field changes that occur during a polarity reversal. Since delayed acquisition may cause a reversal to appear older, the timing of the rotation phase may be wrong by one or two precession cycles (20,000 – 40,000 years). The reversals of the Secca Grande and Punta Secca section are located, however, in the same cycles as in the Rossello Composite. There is this no age discrepancy with the APTS which is based on the Rossello Composite and has been corrected for delayed NRM acquisition (Lourens et al., 1996). Thus, the results show a true differential clockwise rotation phase around 3.21 Ma and this age replaces the earlier estimate of Scheepers and Langereis (1993). Furthermore, there is no geographic trend in timing of the differential clockwise rotation phase from Secca Grande to Punta Secca and finally to Punta Piccola.

Geodynamics

A structural study associated with paleomagnetic data (Oldow et al., 1990) indicated that large-scale clockwise rotations of thrust sheets on Sicily occurred during the Late Miocene-Pliocene. This was accompanied by a progressive shift in tectonic transport direction from east to south (Oldow et al., 1990). The timing of thrust imbrication and rotations was closely bracketed. Moreover, detailed seismic and structural studies have revealed a Pliocene transpressional event for the Sicilian fold-and-thrust belt (Catalano et al., 1976; 1996). The Strait of Sicily forms the foreland of Sicily and also reveals evidence of middle Pliocene tectonics (Catalano et al., 1995). This foreland contains half-grabens opened by extension, later filled and structurally inverted because of a change in stress field implying compression along a N-S axis (Catalano et al., 1993). Contractional

structures on Sicily and extensional structures in the Sicilian foreland are coeval (Oldow et al., 1990). Contractional deformation of the Sicilian fold-and-thrust belt (Catalano et al., 1996) and extension in the Strait of Sicily (Argnani, 1990) is linked to extension in the Tyrrhenian Sea. Between 8.6 and 7.8 Ma (Duermeijer et al., 1998a) the Tyrrhenian Sea opened as back-arc basin (Robertson and Grasso, 1995) caused by extension resulting from by SE roll-back of the subducting slab. The oldest marine sediments overlying the basement of the Tyrrhenian Sea (Kastens et al, 1987; Flores at al., 1992; Fig. 2.9) were re-dated using astronomical ages of biostratigraphic markers (from Lourens et al., 1996). The resulting new ages suggest an acceleration in opening of the Tyrrhenian Sea between 3.5 and 2 Ma. Some ODP-cores did not recover basement, and for these wells minimum ages are used (Fig. 2.9). This leads to a simplified model of the geodynamic processes (Fig. 2.10) in which the acceleration caused a wave of contraction throughout Sicily, resulting in southward tectonic transport. In the case of locked continental collision, ridge push can be significantly reduced and extension becomes important in the Sicilian foreland (Argnani, 1990). Compressional systems on Sicily occur because the acceleration in opening of the Tyrrhenian Sea, i.e. the movement of the overriding plate, advances trenchward faster than trench roll-back (see Busby and Ingersoll, 1995). Grasso and Butler (1991) and Butler et al (1995) consider the Caltanisetta basin as a series of basins developed across the frontal part of the thrust belt. Thrusting generated anticlines and synclines which created sediment traps. Therefore, flexural subsidence was of increasing importance during the late Neogene.
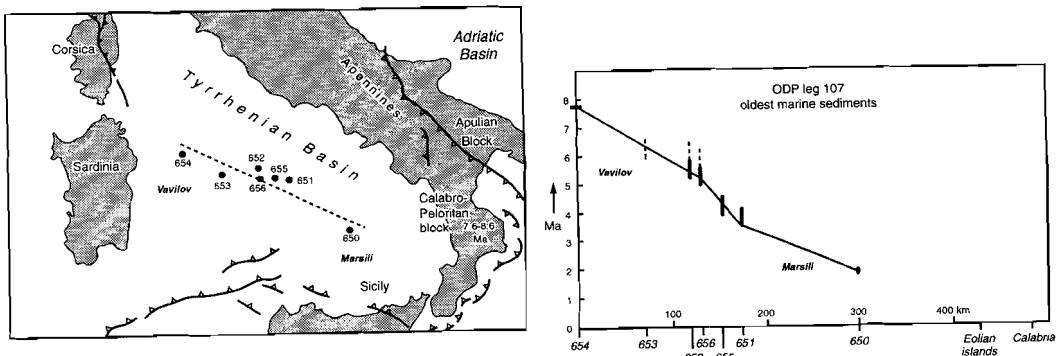
Fig. 2.9 Ages of oldest marine sediments overlying the basement versus distance in km throughout the Tyrrhenian Sea are shown. Location of ODP sites from Leg 107. Note that rapid intervals of opening correspond to the location of the Vavilov and Marsili basin. Sites (ages) are based on re-dating of results from Kastens et al. (1987) and Flores et al. (1992) and are as follows: Site 654 (7.89 Ma), 653* (5.9 Ma), 652* (5.95-5.23 Ma), 656* (5.6-5.02 Ma), 655 (3.98-4.52 Ma), 651 (4.1-3.6 Ma) and 650 (2.0-1.8 Ma); * = no basement recovered, and therefore represents minimum age.

The anisotropy of the magnetic susceptibility (AMS) indicates a N-S compression for the Secca Grande and Punta Secca sections, whereas the AMS data of the Punta Piccola show a NW-SE compression direction. The AMS data are consistent throughout the Trubi and Narbone formations and hence throughout the rotation interval. This implies that the clockwise rotation event is recorded before the AMS ellipsoid was deformed as a consequence of N-S compression. Furthermore, our AMS data and structural studies of Catalano et al. (1993) imply a N-S compression direction for both the Sicilian fold-and-thrust belt and its foreland. Therefore, the AMS data of the Punta Piccola section, implying NW-SE compression, must be regarded as a younger or local overprint.

Because rotations are associated with thrust imbrication (Oldow et al., 1990) and as such with the Pliocene transpressional event, we propose this event to have occurred around 3.21 (± 0.05) Ma. Although most geological processes (e.g. opening of Tyrrhenian Sea, thrusting etc.) are believed to occur gradually, the data presented here indicate that at least some tectonic rotations may occur rather fast. If this rotation is indeed linked to an acceleration in opening of the Tyrrhenian Sea between 3.5 and 2 Ma, this could imply that the change in rate of opening also occurred rather rapidly.
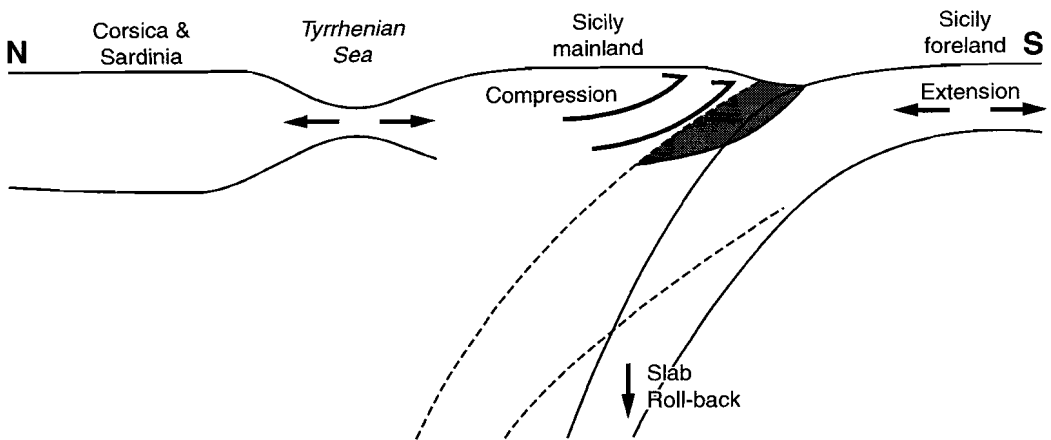
Fig. 2.10 Schematic image of the geodynamic process accounting for compression on Sicily and extension in the foreland as a result of acceleration in opening in the Tyrrhenian Sea.

Conclusions

Paleomagnetic results from three sections along the southwest coast in the Caltanisetta basin, reveal an rapid differential (10°) clockwise rotation phase dated around 3.21 Ma, close to the Trubi-Narbone boundary.

The age of the Pliocene differential clockwise rotation phase found on Sicily can be linked to the transpressional event in the Sicilian fold-and-thrust belt and to the extensional event in the Sicilian foreland. We conclude that both the transpression and extension are related to an acceleration in opening of the Tyrrhenian basin between 3.5 and 2 Ma, this being derived from the oldest (recovered) marine sediments overlying the Tyrrhenian basement. The Trubi-Narbone boundary marks a shallowing in the Caltanisetta basin and, thus, a change in the sedimentary environment of the entire basin caused by this transpressional event. This boundary is probably not the expression of a regional (Sicilian) event, because time-equivalent events are central-eastern Mediterranean-wide, as can be concluded from ODP Leg 160 (eastern Mediterranean). On Crete an increase in uplift and large-scale thrusting is observed and in northern Italy a hiatus and tectonic rotation are documented as additional evidence.

Evidence for phases of non-rotation were identified between the middle Pliocene (3.21 Ma) and middle Pleistocene (1.0-0.7 Ma) throughout the entire Tyrrhenian region (i.e. southern Apennines, Calabria and Sicily).

Acknowledgements

3

Post early Messinian counterclockwise rotations on Crete: implications for Late Miocene to Recent kinematics of the southern Hellenic arc

Abstract

Most geodynamical models for the kinematics of the central Mediterranean recognise that major tectonic rotations must have played an important role during the Neogene. The Hellenic arc is believed to have been subjected to clockwise rotations in the west and counterclockwise rotations in the east, while the southern part (Crete) showed no rotations (Kissel and Laj, 1988). Many qualitative and quantitative models are based on the idea that Crete did not rotate. We present new paleomagnetic data which show that post-early Messinian counterclockwise rotations have occurred on Crete. The amount of counterclockwise rotation generally varies between 10° and 20°, but in central Crete much larger rotations (up to ~40° counterclockwise) were found. Only a few sections did not show any rotation. The anisotropy of magnetic susceptibility (AMS) shows lineations, which are consistently WNW-ESE throughout Crete, indicating post-rotational WNW-ESE extension or NNE-SSE compression. The observed counterclockwise rotations are consistent with the results of tectonic modelling by Ten Veen and Meijer (1998). The latter study compares the late-Middle Miocene to Recent kinematics with modelled intra-plate stresses for various possible distributions of plate boundary forces. Observations reveal that motion along left-lateral and right-lateral faults occurred during the Pliocene. The model analysis shows these motions to be consistent with transform resistance along the eastern segment of the overriding margin. The counterclockwise block rotations observed by us are probably a consequence of displacements along the left-lateral and right-lateral faults and could reflect a similar tectonic regime that involved transform resistance.

Introduction

The origin and evolution of the Hellenic arc (Fig. 3.1) system is primarily controlled by the effects of continent-continent collision due to relative motion of the African and European plates. In the subsequently developing land-locked configuration of the Mediterranean basin, southward roll-back of the trench system induced arc migration which ultimately shaped the present-day geometry of the arc system (Wortel and Spakman, 1992). Seismic tomography has shown that the African plate subducts to a depth of 200 km at the longitude of Crete (Spakman et al., 1988). Slab pull on the subducted plate caused a southward retreat (roll-back) of the subduction zone, generating extension in the Aegean Sea and the movement of Crete to the south (Le Pichon, 1982; Meulenkamp et al., 1988). Important changes in the paleogeography during the late Serravallian and early Tortonian times (Miocene) can be attributed to the initiation of the slab roll-back process. Migration of the trench system to the south-west, estimated at 12-11 Ma, gave rise to an extensional regime in the back-arc domain, which led to general subsidence (Angelier et al., 1982).
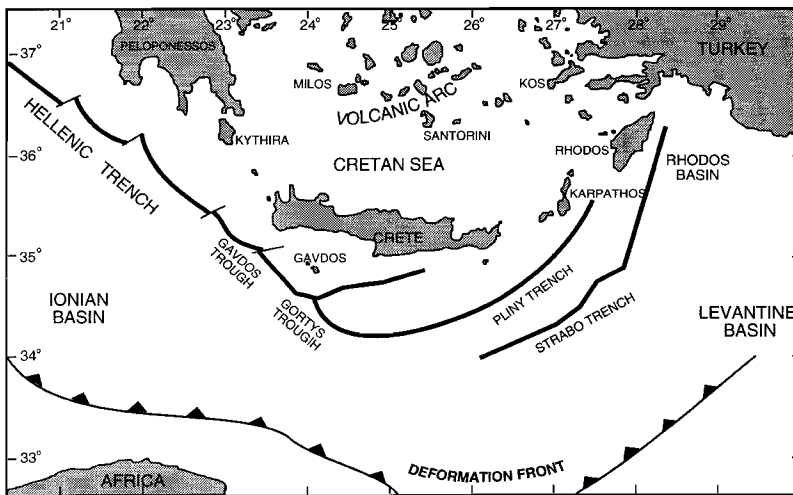
Fig. 3.1 Major structural features of the Aegean region.

The extension in the Aegean region occurred shortly after a crustal thickening episode, which culminated in the Late Eocene (Blake et al., 1981; Bonneau and Kienast, 1982). Crustal thickening, by imbrication of thrust slices, was active in the Eocene in the central Aegean Cycladic region (Bonneau, 1982), after which extension was active in the Early Miocene. At that time crustal thickening was probably still active in the most external zones (Crete) until some time during the (late) Middle Miocene. The present-day morphology results from large-scale normal faulting cross-cutting the Hellenide nappe pile during the late Neogene and Quaternary (Angelier et al., 1982). Crete appears,

following intensive post-orogenic block-faulting as a mosaic of horsts and grabens. The Late Miocene to Recent evolution of the Aegean region is thus dominated by extensional tectonics, although compressional events are also thought to have occurred (Meulenkamp et al., 1988). Existing kinematic models (Le Pichon and Angelier, 1981; Angelier et al., 1982; Taymaz et al, 1991; Westaway, 1991) which attempt to account for the geodynamic development of the Aegean imply that major tectonic rotations must have played an important role during the late Cenozoic evolution of the Hellenic arc.

On the basis of numerous paleomagnetic studies, Kissel and Laj (1988) concluded that the Aegean arc had an almost rectilinear E-W-trending geometry during the Early Miocene. They further suggested that the current curvature of this region was acquired in two major phases. The first phase, during the Middle Miocene, resulted in clockwise rotations in the west (Epirus) and counter-clockwise rotations in western Anatolia (Turkey). The second phase, during the last 5 million years, produced only clockwise rotations for the northwestern part of Greece. According to this reconstruction, Crete did not undergo any rotation since ~7 Ma (Laj et al., 1982) because paleomagnetic directions from Tortonian sediments on Crete were found to be closely aligned along a N-S direction (Valente et al., 1982).

Recently, Meijer and Wortel (1996; 1997) used a numerical model to analyse quantitatively the horizontal patterns of stress and deformation of the Aegean region during the Pliocene to Recent. Subsequently, Ten Veen and Meijer (1998) applied a similar analysis to the Late Miocene to Recent deformation of Crete. Fault kinematics are based on geological observations, such as lineaments, observed kinematic indicators and relative burial histories and are compared with modelled horizontal stress patterns. These techniques contribute to the understanding of forces that control the state of stress and associated deformation of the overriding continental margin. The Pliocene stress field on Crete, as inferred from kinematic indicators, is consistent with counterclockwise rotation of fault blocks (Ten Veen and Meijer, 1998).

Several cyclo-, bio- and magnetostratigraphic studies on Crete, in addition to earlier studies (Langereis, 1984), establish an integrated stratigraphic time-frame for the late-Middle to Late Miocene time-interval in the Mediterranean. The resulting high-resolution stratigraphic framework (Krijgsman et al., 1994; 1995) has enabled the extension of the astronomical polarity time-scale into the Late Miocene (Hilgen et al., 1995). Here, we use these paleomagnetic results and apply them to rotational studies, with the added benefit of an accurate timing of possible tectonic rotations. In addition, we have measured the anisotropy of the magnetic susceptibility (AMS) of all new sections, and we used the data of Langereis (1984) for the older sections.

The studied marine sections are located throughout Crete (Figs. 3.4 and 3.5) and cover part of the Tortonian and Messinian time-span (between 9.7 and 6.7 Ma). For detailed information on the location of the sections, the lithology and accurate age determination of the sediments, we refer to earlier studies (Langereis, 1984; Krijgsman et al., 1994; 1995). The sections are divided into three groups: (1) the Potamida, Skouloudiana, Vasilopoulo, Kotsiana and Apostoli sections on western Crete and the Metochia section on the island of
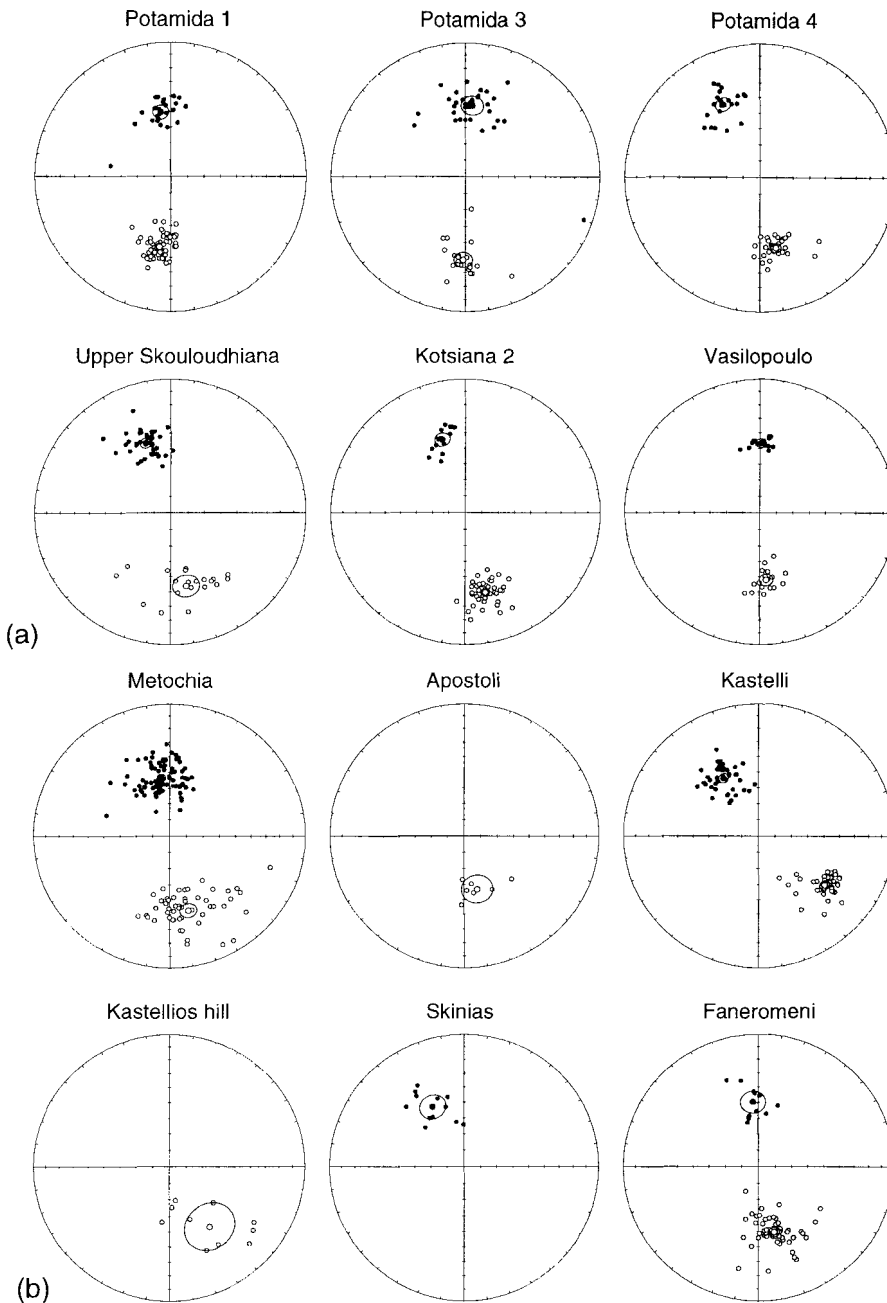
Fig. 3.2 Equal-area projections of characteristic remanent magnetisation (ChRM) results. Closed (open) circles represent downward (upward) projections. The circles give α_{95} for the different site means. (a) Western Crete, previously measured by Langereis (1984). (b) Central and eastern Crete, previously measured by Krijgsman et al. (1994, 1995).

Gavdos (south of Crete); (2) the sections of Kastelli, Kastellios Hill and Skinias on central Crete; and (3) the Makrilia and Faneromeni sections on eastern Crete. The Koufonisi section is located on the Island of Koufonisi (Figs. 3.4 and 3.5). In central Crete, the sections cover the largest time-interval; Skinias contains the oldest sediments of 9.7 Ma and Kastelli the youngest with an age of 6.7 Ma. In western and eastern Crete, the sections cover an interval from approximately 7.9 to 6.7 Ma.

Paleomagnetic results

Characteristic Remanent Magnetisation (ChRM) directions

Details of the natural remanent magnetisation (NRM) characteristics can be found in previous studies of Langereis (1984) and Krijgsman et al. (1994; 1995). For this study, we only used the thermal demagnetisation results from samples with relatively high NRM intensities (1-20 mA/m) and showing a linear decay towards the origin, providing the most reliable characteristic remanent magnetisation (ChRM) components. In total, 688 specimens from 12 continuously sampled sections were used (Table 3.1). In several sections, the results did not meet our reliability criteria. These data are omitted from Table 3.1 and were not used in this study. Specimens with relatively low intensities, with alterations at high temperatures (> 400°C), with a large present-day overprint, and which are close to a polarity reversal were also excluded. Generally, a reasonable to very good precision parameter (k) was found and the mean direction per section shows a small cone of confidence at the 95% level (α_{95}), with the exception of the Kastellios Hill section (Table 3.1).

The ChRM results reveal counterclockwise rotations for most of the sections studied (Figs. 3.2 and 3.4), revealing a pattern of counterclockwise rotations on Crete. The amount of rotation, however, differs from 27°-42° counterclockwise on central Crete, to ~12° on eastern Crete (Table 3.1). The sections on western Crete also show small counterclockwise rotations between 14° and 19°, although two sections (Vasilopoulo, Potamida 1/3) did not reveal any significant rotations. A comparison of the paleomagnetic directions with those expected from the pole for Eurasia (Besse and Courtillot, 1991) during the Late Miocene (the African pole of the same epoch is not significantly different), indicates that declination rotations (R in Table 3.1; Butler, 1992) are counterclockwise and vary between 8° and 25° in western and eastern Crete (except for Potamida 1 and 3), whereas in central Crete rotations amount to 33-48° (Table 3.1). The inclination data of the sections studied generally have values between 40° and 50° compared to a geocentric axial dipole field value of ~55°, representing an inclination error of 10-15° which is characteristic for such sediments (marine marls, clays). The inclination flattening (F in Table 3.1; Butler, 1992), compared to a Eurasian pole, is typically less than the inclination error.
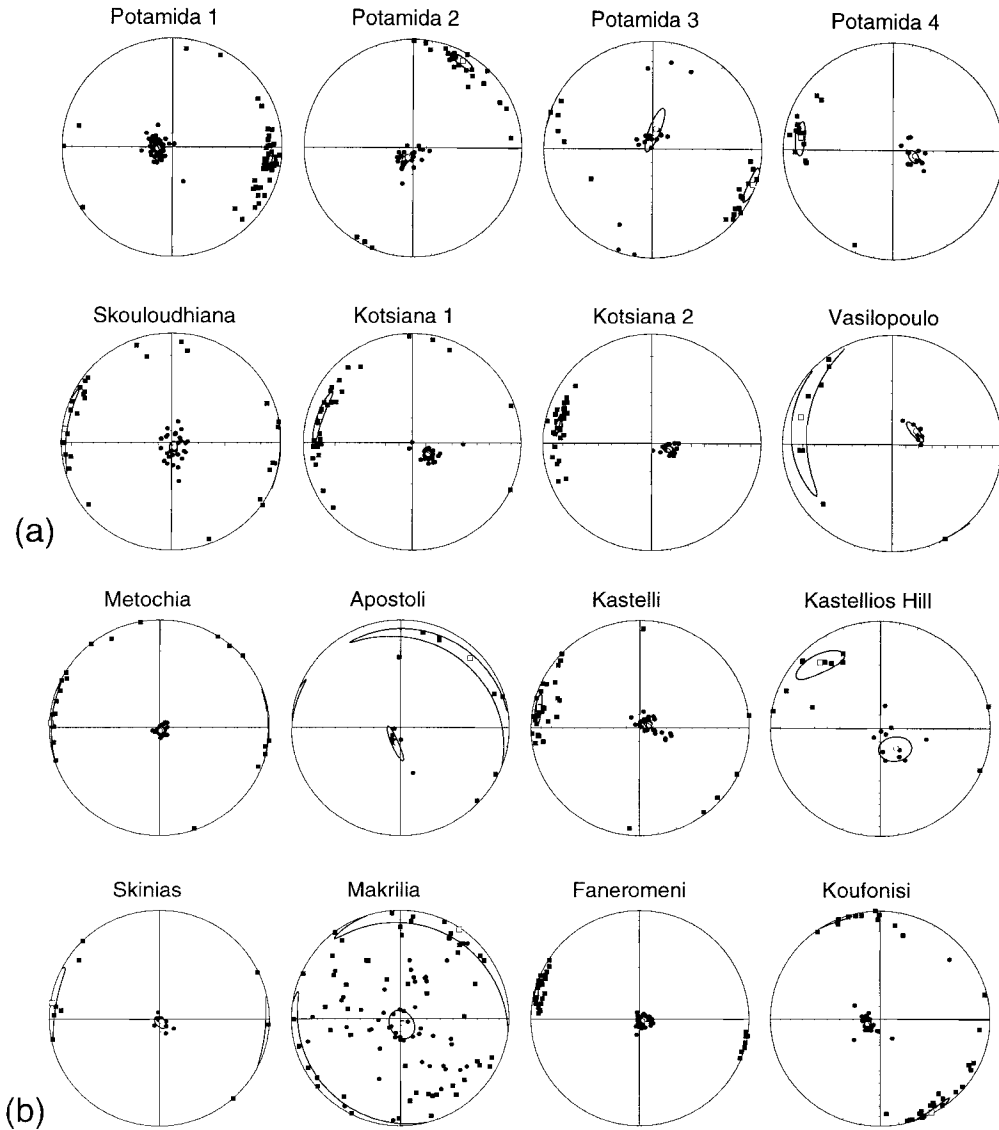
Fig. 3.3 Equal-area projections (bedding-tilt corrected) of k_{max} (squares) and k_{min} (circles) of the ellipsoid of the AMS for individual samples, with the calculation of mean ellipsoid for each site. (a) Western Crete. (b) Central and eastern Crete.

Anisotropy of the Magnetic Susceptibility

The anisotropy of the magnetic susceptibility (AMS) in (weakly) deformed and unmetamorphosed rocks can be used to provide information on the sedimentary and tectonic history of a rock. There is often a relationship between the AMS of rock samples

and the regional stress field of the area (Tarling and Hrouda, 1993). In undeformed sediments, the magnetic susceptibility is characterised by oblate ellipsoids, with a foliation coinciding with the bedding plane (i.e. the minimum axes of AMS, k_{min}, perpendicular to the bedding plane) and a random orientation of the lineation denoted by the maximum axes of AMS, k_{max}. If there is deformation acting on a rock, this initially results in a lineation, i.e. clustering of k_{max} in the direction of maximum extension or, equivalently, perpendicular to maximum compression. The k_{min} is still perpendicular to the bedding plane. An increase of the strain may cause the ellipsoid to have a more prolate structure, but this stage is never reached in the sections on Crete.

Section:						NRM-Analysis				
	n	Decl	Incl	*k*	α_{95}	rot	R	DR	F	DF
*West-Crete**										
Potamida 1	97	4.8	47.4	54.6	2.0	4.8 c	0.9	3.1	3.4	2.5
Potamida 2										
Potamida 3	57	3.9	42.9	20.1	4.3	3.9 c	1.8	5.1	7.9	3.9
Potamida 4	55	341.2	43.2	48.4	2.8	18.8 cc	-24.5	3.7	7.6	3
Skouloudiana	60	343.3	43.5	33	3.2	16.7 cc	-22.4	4.1	7.3	3.2
Kotsiana 1										
Kotsiana 2	62	345.2	38.8	73.1	2.1	14.8 cc	-20.5	3	12	2.6
Vasilopoulo	33	357.5	47.2	102.3	2.5	2.5 cc	-8.2	3.6	3.6	2.8
Apostoli	7	346.3	55.9	44.9	9.1	13.7 cc	-19.4	13.3	-5.1	7.6
Gavdos										
Metochia	144	349.6	48.9	23.7	2.5	10.4 cc	-16.1	3.7	1.9	2.8
Central-Crete										
Kastelli	83	317.6	43.9	33.7	2.7	42.4 cc	-48.1	3.6	6.9	2.9
Kastellios Hill	10	326.3	45.3	11.6	14.8	33.7 cc	-39.4	17.1	5.5	12
Skinias	12	332.6	47.9	33.5	7.6	27.4 cc	-33.1	9.3	2.9	6.4
East-Crete										
Makrilia										
Faneromeni	68	347.9	48.7	37.4	2.9	12.1 cc	-17.8	4.1	2.1	3
Koufonisi										

TABLE 3.1 Results from NRM analysis from the different sections on Crete; corrected for bedding tilt. All sections are of the same age (late Tortonian/early Messinian). n = number of specimens; Decl, Incl = site mean ChRM declination and inclination; k = Fisher's precision parameter; α_{95} = 95% cone of confidence; rot = sense of rotation, (c)c = (counter)clockwise with a 0° reference direction; R/F = vertical axis rotation/flattening of inclination (R = positive when clockwise rotation and F = positive when "flatter" than expected inclination) and DR/DF as confidence limits (Butler, 1992) with Eurasian Miocene reference pole (Besse and Courtillot, 1991); * marks data previously published by Langereis (1984).

The anisotropy of the magnetic susceptibility was measured on a Kappabridge KLY-2 or KLY-3. Many of the AMS measurements from western Crete were previously done by Langereis (1984), and an additional 198 specimens were measured (total of 413 specimens) by us. All sections show oblate ellipsoids, the k_{min} axes being generally close to (but often significantly different from) the pole of the bedding plane, and the k_{max} axes are mostly WNW-ESE aligned (Figs. 3.3 and 3.5, Table 3.2). Error ellipses of the susceptibility axes are according to Jelinek (1978) and are given for k_{max} in Table 3.2. The majority of the lineations imply WNW-ESE extension or, equivalently, NNE-SSW compression, except in the case of the Vasilopoulo, Makrilia and Apostoli sections which show considerable dispersion and near-random lineations (Fig. 3.3 and Table 3.2).

Section:	AMS-Analysis (kmax directions)					
	n	Az	dip	dAz	ddip	L
*West-Crete**						
Potamida 1	50	97.6	11.1	5.6	1.8	1.0074
Potamida 2	25	29.2	9.4	8.4	3.6	1.0084
Potamida 3	19	109.9	3.3	10.1	4.0	1.0196
Potamida 4	14	277.0	15.8	10.3	4.2	1.0108
Skouloudiana	28	277.6	1.8	23.6	3.0	1.0085
Kotsiana 1	31	286.3	12.7	16.8	3.0	1.0031
Kotsiana 2	32	282.3	13.1	6.5	1.5	1.0065
Vasilopoulo	8	287.0	13.4	49.1	7.3	1.0029
Apostoli	8	44.7	11.4	73.7	5.4	1.0013
Gavdos						
Metochia	22	271.9	0.4	23.1	1.7	1.0090
Central-Crete						
Kastelli	36	280.5	5.9	8.4	3.0	1.0045
Kastellios Hill	11	317.4	18.9	17.2	8.0	1.0108
Skinias	10	278.3	1	20.9	4.7	1.0037
East-Crete						
Makrilia	52	33.2	3.2	72.3	9.0	1.0006
Faneromeni	34	284.1	2.7	3.5	1.8	1.0073
Koufonisi	33	152.2	0.9	13.1	2.3	1.0025

*TABLE 3.2 Results from AMS analysis from the different sections on Crete; corrected for bedding tilt. All sections are of the same age (late Tortonian/early Messinian). n = number of specimens; Az, Dip = mean azimuth and dip of k_{max} axes; dAz, ddip = errors on mean k_{max} axes; L = magnetic lineation (k_{max}/k_{int}); * marks data previously published by Langereis (1984).*

Discussion and conclusions

Earlier, Valente et al. (1982) studied Late Miocene and Pliocene marine sediments on Crete. Their conclusion was that Crete did not undergo any significant rotation since Tortonian times. Kissel and Laj (1988) used this paleomagnetic result to suggest that Crete as a whole has been decoupled from the western part of the Hellenic arc. This was based on the clockwise rotations found in the northwestern part of the Hellenic arc (Epirus, Ionian Islands and Peloponnesos) and a non-rotated southeastern section (Crete). Their ideas were supported by geological observations of Lyberis et al. (1982) and Angelier et al. (1982) and led to a paleomagnetic reconstruction with an originally almost rectilinear E-W trending Hellenic arc. Since these publications, a stable non-rotated position of Crete was used as a boundary condition in many kinematic studies of the Aegean region (Le Pichon and Angelier, 1981; Angelier et al., 1982; Taymaz et al, 1991; Westaway, 1991).
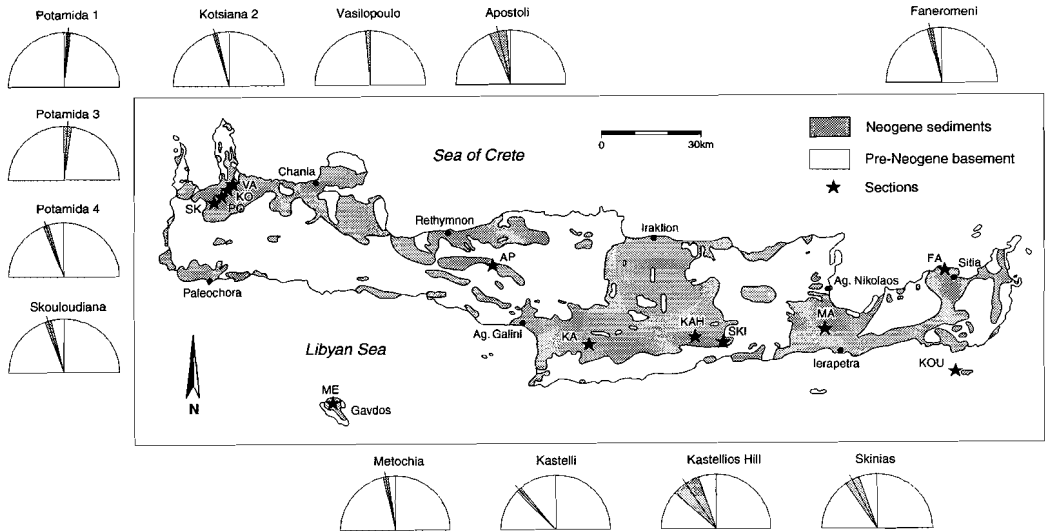
Fig. 3.4 Distribution of ChRM data on Crete; shaded segment represent α_{95} with solid line as mean declination per section. PO = Potamida; SK = Skouloudiana; KO = Kotsiana; VA = Vasilopoulo; ME = Metochia; AP = Apostoli; KA = Kastelli; KAH = Kastellios Hill; SKI = Skinias; MA = Makrilia; FA = Faneromeni; KOU = Koufonisi.

Our paleomagnetic results from the late Tortonian to early Messinian sections, however, clearly show that predominantly counterclockwise rotations have occurred on Crete (Fig. 3.4) some time after the early Messinian. The largest counterclockwise rotations were found in central Crete. Considering the time-span of some of these sections it also follows that no differential rotations occurred during the interval 9.7-6.7 Ma. In western Crete, two groups of rotations are shown (~ 20° counterclockwise and ~ 0° rotation), which cannot be explained by different ages of the sediments. Because all sections were initially sampled for magnetostratigraphic purposes, care was taken to sample sections as

long and continuous as possible, and to avoid sections which are disturbed by internal faults. Furthermore, the proven suitability of our sections for magnetostratigraphic correlation (see Langereis, 1984; Krijgsman et al., 1994, 1995) indicate that the magnetisation components are of primary origin. In addition, the sections show a positive reversal test (Langereis, 1984), which indicates that any secondary overprint has been successfully removed. There is one exception which concerns a subchron (zone D+; in Langereis, 1984) of very short duration (Krijgsman et al., 1994) and of which the directions may have been subject to delayed acquisition (Van Hoof and Langereis, 1991). All other subchrons, however, share a common true mean direction according to the test of McFadden and Lowes (1981).

Although we also observed three sections without any rotation, our predominantly counterclockwise results are not compatible with the conclusion derived by Valente et al. (1982) that Crete has not undergone any significant rotation with respect to Europe or Africa since middle Tortonian time. Valente et al. (1982) based their conclusion on the mean direction for all their Miocene sites being 356.5°. However, it appears that 5 of their 14 sites also show counterclockwise results (up to 22.5°). This is not amazing considering the fact that at least several sites are sampled from the same outcrops as our sections. Additional paleomagnetic data of central Crete (Kastellios Hill) by Sen et al. (1986) also revealed counterclockwise results (14°), although to a lesser extent than our average result (34°) for the same section. However, no confidence limits are given for their section. A large error in our mean direction (a counterclockwise rotation of 34 ± 15°) which is based on fewer samples, reflects the presence of some results with anomalously low inclinations (Fig. 3.2). Thus, the results of the two studies do not necessarily disagree.

Our results, in addition to those of Valente et al. (1982) and Sen et al. (1986), show that in some cases no rotations but mainly counterclockwise rotations have taken place. This suggests that paleomagnetic rotations are governed by (local) rotations of fault-bounded blocks, rather than Crete rotating as a single block. We note, however, that there is little evidence for clockwise rotations, and this helps constrain the overall tectonic regime.

Morris and Anderson (1996) have suggested a domain with clockwise rotations extending from northern Greece as far south as Mykonos. The southern boundary of this domain must lie between Mykonos which shows clockwise rotations and Naxos showing counterclockwise rotations (Morris and Anderson, 1996), and possibly south of Milos, where counterclockwise rotations were also found (Kondopoulo et al., 1990). Although the Cretan paleomagnetic results do not indicate that Crete has rotated counterclockwise as a single block, at least the sense of the rotations is in good agreement with the more regional Aegean tectonic regime.

Numerical modelling was performed to calculate the intra-plate stress fields for various distributions of forces (Meijer and Wortel, 1996, 1997) and the results were compared with the observed deformation. Recently, this modelling was done for the entire Aegean region, but with emphasis on the deformation in the Cretan segment of the arc (Ten Veen and Meijer, 1998). Comparison of the stress patterns modelled with those inferred from tectonostratigraphic analyses derived from observed fault directions and

their episodes of activity shows that from 11 till 5 Ma arc-normal pull was the dominant force generating radial tension. For the period from ~5 Ma onwards, there is evidence for the activity of a sinistral strike-slip fault system. The model analysis shows this to be consistent with the presence of transform resistance in the eastern Aegean trenches (Fig. 3.6). This sinistral fault system will account for counterclockwise rotations of different fault bounded blocks. The amount of counterclockwise rotation will depend on the size of the rotating block. We note that the largest counterclockwise rotations are found in central Crete which corresponds to an area bounded by the largest and most active strike-slip (sinistral) faults (Ten Veen, 1998). The results of Ten Veen and Meijer (1998) are, thus, in good agreement with our new paleomagnetic rotational results.
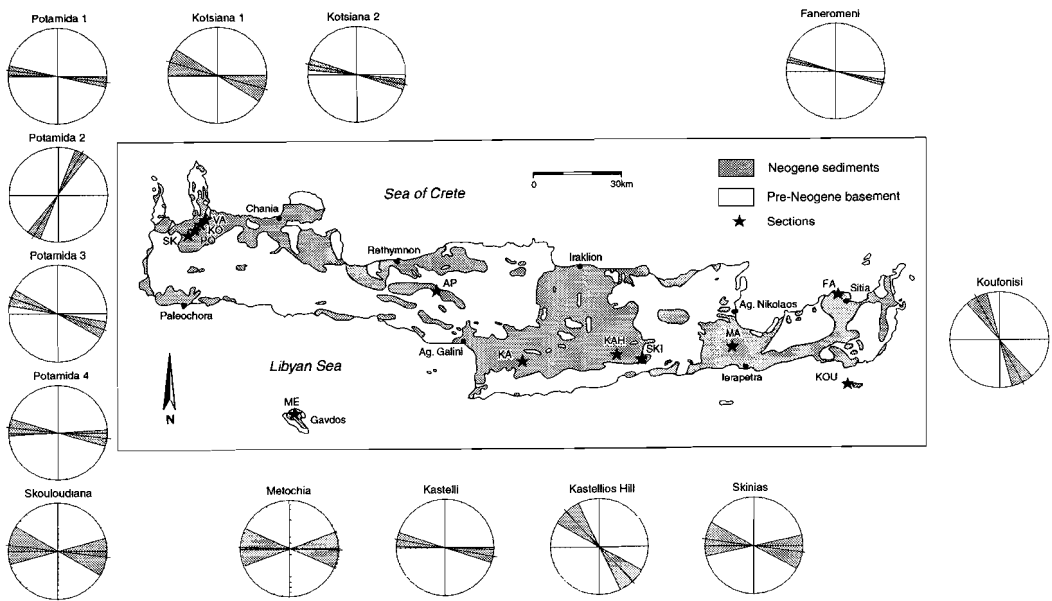
Fig. 3.5 Distribution of AMS data on Crete; shaded segment represents error on mean k_{max} axes (dAz) with solid line as mean lineation direction per section. PO = Potamida; SK = Skouloudiana; KO = Kotsiana; ME = Metochia; KA = Kastelli; KAH = Kastellios Hill; SKI = Skinias; FA = Faneromeni; KOU = Koufonisi. The near-random lineation results of the Vasilopoulo, Apostoli and Makrilia sections were omitted.

Our AMS analyses (Figs. 3.5 and 3.6) indicate a WNW-ESE extension or NNE-SSW compression direction which is roughly parallel to the extension-compression direction of the Pliocene to Recent, as shown by their stress ellipsoids (Fig. 3.6c and d). Correction of the observed lineations for the counterclockwise rotations results in a less consistent pattern of lineations. This indicates that the lineations are younger than the post-early Messinian rotations on Crete. A similar relation is observed by Scheepers and Langereis (1994a), who suggested, based on paleomagnetic data from southern Italy, that the end-
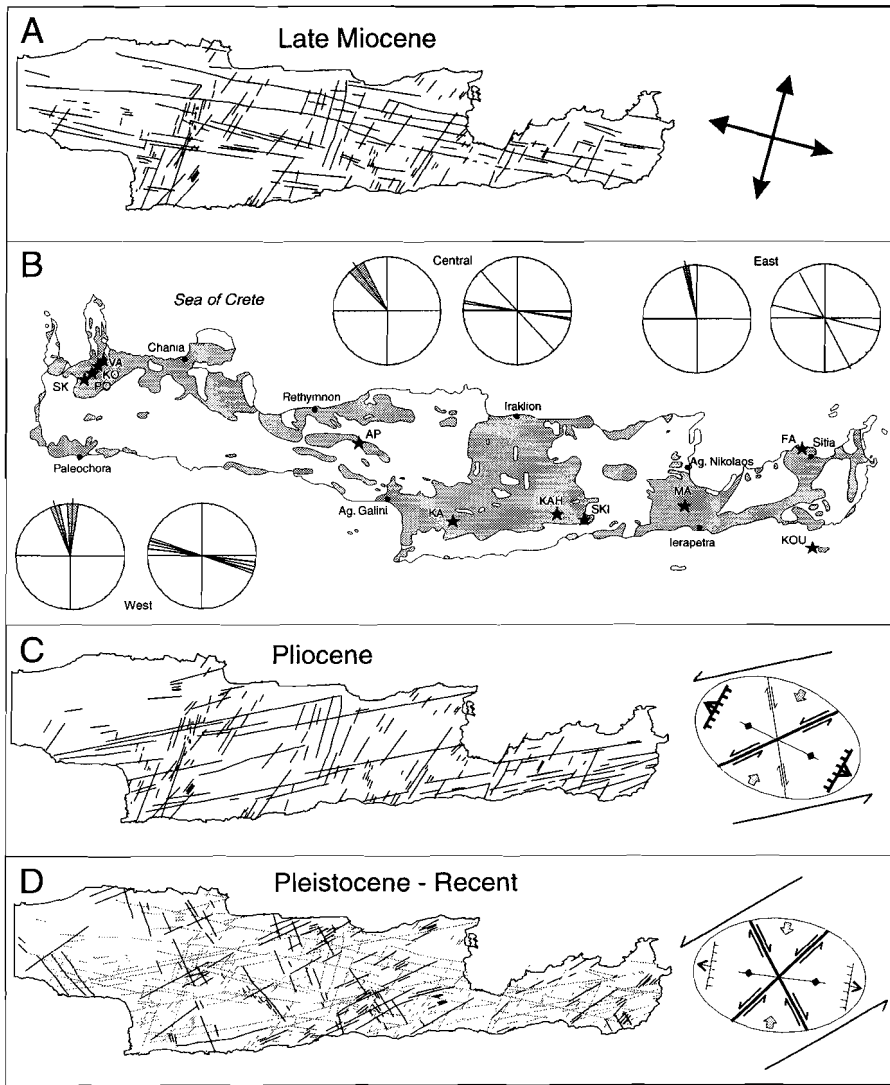
Fig. 3.6 Tectono-stratigraphic episodes of central and eastern Crete. Structures obtained from Landsat satellite imagery and field observations. Black lines indicate active structures and dashed lines represent reactivated faults. Fault activity is based on differential vertical motions of Cretan fault blocks as determined from geohistory analysis (burial history) applied to the stratigraphic cover of the blocks. The stress field is inferred from few observed kinematic indicators and the kinematics as inferred from stratigraphical and sedimentological data, allowing an impression of the state of stress during a certain episode. The orientation of the stress ellipses explain the deformation along the highlighted (bold) fault directions. (A) Late Miocene. (B) Overview of the tectonic rotations and AMS data of Crete, derived from paleomagnetic research, per area. Shaded area represents α_{95} with solid line as mean tectonic rotation. In the AMS plot the solid line denotes the mean lineation direction. (C) Pliocene. (D) Pleistocene to Recent.

phase of tectonic rotations corresponds (during compression) to blocking of the system, followed by the alignment of the lineation.

We conclude that during the change from radial extension in the late Miocene to a sinistral fault system in the Pliocene (Fig. 3.6), (local) block rotations occurred in response to the changing tectonic configuration. The NNE-SSW compressional or WNW-ESE extensional direction caused the lineations observed in our AMS results. These were induced after post-early Messinian counterclockwise rotations on Crete. Our scenario is in good agreement with the comparison of modelled stress patterns and observed fault patterns (Ten Veen and Meijer, 1998). The observed counterclockwise rotations may be explained by arc-normal pull on an increasing curvature of the arc through time, aided by an additional east-west tension caused by transform resistance in the overriding plate, initiated at approximately 5 Ma.

Acknowledgements

4

A late Pleistocene clockwise rotation phase of Zakynthos (Greece) and implications for the evolution of the western Aegean arc

Abstract

Palaeomagnetic measurements have been carried out on Eocene to Pleistocene sediments on the Ionian Island of Zakynthos, NW Greece. Magnetostratigraphic constraints, biostratigraphic analyses of planktonic foraminifera and calcareous nannofossils provide a reliable time frame for these deposits. The results show that no significant rotation occurred between 8.11 and 0.77 Ma, but that Zakynthos must have undergone a 21.6° ± 7.4° clockwise rotation between 0.77 Ma and Recent. Thus, our data indicates a rapid rotational event, in contrast to continuous rotation since 5 Ma as previously postulated (Laj et al., 1982). We speculate this late Pleistocene tectonic rotation phase to be linked to rapid uplift in the Greek region which results from rebound processes caused by (African) slab detachment underneath the Ionian islands.

Introduction

The main part of Greece belongs to the Hellenides, an approximately NW-SE running orogenic belt which forms the connection between the mountain chains of the Dinarides (northern Albania and former Yugoslavia) in the west and the Taurides (Turkey) in the east. The Hellenides are divided into a number of sedimentary facies belts or isopic zones (Aubouin et al., 1976) from internal (east) to external (west): Vardar, Pelagonian, Pindos, Gavrovo-Tripolitsa, Ionian and Pre-Apulian zone. These zones are separated by major NW-SE striking thrusts on the Greek mainland and on the Ionian Islands. The geological evolution of the Hellenides is dominated by divergence and convergence of the African and Eurasian plates (Aubouin et al., 1976) and related processes like subduction, roll back followed by extension in the Aegean back-arc, and possibly an additional westward Anatolian push. During Mesozoic times, troughs and platforms developed between the foreland, Adria (the African promontory), and the internal oceanic part of the Neotethys. Subsequently, the oceanic part closed and the different isopic zones were emplaced as well-defined thrust sheets. The timing and locus of emplacement migrated progressively towards the foreland (Smith and Moores, 1974). The (outer) western-most thrust zone, the Ionian thrust, was probably active during the early Pliocene (Sorel, 1976).

The current southern and western boundaries of the deforming Aegean region are formed by the subduction (Hellenic trench system) of the African slab underneath Eurasia, with Adria separating Greece from Italy. Tomography has shown that subduction occurred at both sides of Adria (Spakman, 1990). The seismic velocity structure reveals detachment of the (African) slab from the surface in northern Greece (Spakman, 1990) and beneath the Calabrian arc in southern Italy (Spakman, 1986). According to Wortel and Spakman (1992) the detachment of the slab started in the north and migrated southwards in time, causing temporal and spatial variations in the slab pull. Where the slab is just detached, a basin (deflection downward) can develop, succeeded by a period of rebound processes in which the area will be uplifted. Although other authors have used tomography data to propose a continuous slab in southern Italy and Greece (Selvaggi and Chiarabba, 1995; Mele, 1998) there is a growing number of studies, e.g. on migration of depocentres along the Apennines (Van der Meulen et al., 1998), that are consistent with the process of migration of slab detachment.

Over the last decades, palaeomagnetic studies have aided in the understanding of the Neogene geodynamic evolution of the Aegean arc (Fig. 4.1). Kissel and Laj (Kissel and Laj, 1988) concluded that the curvature of the Aegean arc has been acquired by deformation during two major tectonic phases, an older one during the middle Miocene and a younger one during the Plio-Pleistocene. They suggested, on the basis of palaeomagnetic results from the Ionian islands of Zakynthos, Kefallonia and Corfu, that the western part of the Aegean arc underwent a continuous clockwise rotation during the younger phase, from approximately 5 Ma to Recent, with an average rate of 5°/Myr (Laj et al., 1982). The area of clockwise rotations extends further north, including the external Albanides and ends at the Scutari-Pec transverse zone (Kissel and Speranza, 1995; Speranza et al., 1995). More to

the centre of the Aegean region, on the Cycladic island of Mykonos (Morris and Anderson, 1996), Tinos (Avigad et al., 1998), Evia and Skyros (Kissel et al., 1986), comparable clockwise rotations are found. In western Turkey, forming the eastern part of the arc, anticlockwise rotations up to 45° were identified during the middle Miocene (Valente et al., 1982). Based on palaeomagnetic data from Crete and Rhodes (Laj et al., 1982; Valente et al., 1982), it was suggested that the central and eastern part of the Aegean arc did not rotate since Tortonian respectively Pliocene times. The area of non-rotation (at least since 15 Ma) extends to the east including the Antalya region in southern Turkey (Kissel and Poisson, 1986). Many geophysical modelling studies concerning the Aegean arc have used constraints derived from these palaeomagnetic data (Angelier et al., 1982; Mercier et al., 1987; Taymaz et al., 1991). However, recent results from Crete indicate predominantly post early Messinian anticlockwise (*ac*) rotations, in agreement with a tectonostratigraphic analysis (Duermeijer et al., 1998b). These *ac* rotations are governed by rotations of fault-bounded blocks. Evidence for anticlockwise rotations in the central Aegean was also found on Naxos since the middle Miocene (Morris and Anderson, 1996) and on Milos since the Plio-Pleistocene (Kondopoulou and Pavlides, 1990), constraining the overall sense of rotation in the central part of the Hellenic arc.
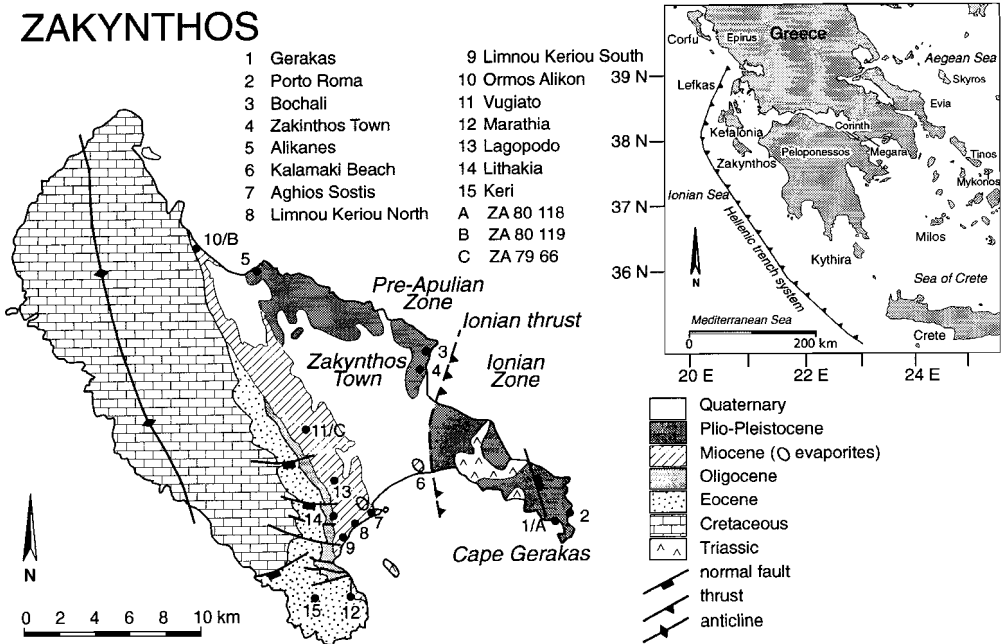
Fig. 4.1 Location of Zakynthos in the Aegean region. Numbers denote the sampled sections/sites (geological map after Underhill, 1989). A, B and C represent sites sampled by Laj et al. (1982). The inlay represents the geographical/geological map and the islands discussed in the text.

Recently, accurate astronomical (polarity) time scales including a significantly improved biostratigraphic resolution (Hilgen et al., 1995; Krijgsman et al., 1995; Lourens et al., 1996) have allowed to constrain more precisely rotation phases in the central Mediterranean. In contrast to continuous deformation, e.g. as proposed for the western Aegean area, there is increasing evidence for short periods of rapid, pulsed tectonic rotations. For instance, in southern Italy, palaeomagnetic data indicate a large 25° anticlockwise tectonic rotation phase in Calabria that has taken place somewhere between 8.6 and 7.8 Ma (Duermeijer et al., 1998a). During the Pliocene, a 10° clockwise rotation event occurred on Sicily around 3.21 Ma within some 80-100 kyr (Duermeijer and Langereis, 1998), while a Pleistocene rotation phase has been documented in Calabria (15° clockwise) and the southern Apennines (23° anticlockwise) which must have taken place between 0.8 and 0.7 Ma (Sagnotti, 1992; Scheepers, 1994a). For this reason, we decided to examine in detail the timing and duration of tectonic rotations in the western Aegean area. We first selected the island of Zakynthos (Fig. 4.1) because it contains the most complete sedimentary record of the Ionian islands, with rocks ranging in age from Cretaceous to Pleistocene. The new dating techniques enable to accurately confine the age of the sediments and to determine more precise constraints on rotation phases, and thus on the geodynamics of the Aegean area.

Sections and sampling

The island of Zakynthos belongs partly to the Ionian and partly to the Pre-Apulian zone (Fig. 4.1); the latter zone comprises the eastern slope of the African promontory. These two zones are separated by the Ionian thrust, which runs east of Zakynthos town (Underhill, 1989) and was emplaced in the early Pliocene according to Sorel (1976).

The sediments on Zakynthos range in age from Cretaceous to Pleistocene and occur in approximately parallel, linear zones running NW-SE (Fig. 4.1). A mountain belt, formed by Cretaceous limestones, dominates the western part of the island, the pre-Apulian zone. To the east, we encounter rhythmically bedded Eocene deposits, followed by Oligocene olistostromes embedded in Miocene (Aquitanian to Serravallian) pelagic limestones. Scattered outcrops of Tortonian age mainly consist of alternations of marls and sapropels. The southern part of Zakynthos encompasses a long and continuous Messinian section of marls and sandy turbidites, which at the top abruptly pass into evaporites related to the Messinian salinity crisis. These evaporites are overlain by Pliocene "Trubi"-like marls, representing the basal Zanclean flooding of the Mediterranean. Younger Pliocene sediments are found along the northeast coast of the island and at the base of the "Citadel section" near Zakynthos town. This section has previously been subjected to detailed studies as it contains the Plio-Pleistocene boundary (Bizon and Muller, 1977; Triantaphyllou, 1996). The Pliocene part consists of alternating clays and silt/sandstones with some sapropelitic intercalations in the lower part; the sand content is increasing

towards the top. The Pleistocene part (Citadel-Bochali sequence) consists of an alternation of open marine turbidites, which in turn are overlain by calcarenites.

The southeastern peninsula of Zakynthos is believed to belong to the Ionian zone and is predominantly formed by Triassic evaporites and Plio/Pleistocene sediments (Underhill, 1989). This part is separated from the Apulian zone by an area of intense deformation. Diapirism of Triassic evaporites, large scale faulting and thrusting resulted in scattered and highly deformed outcrops of sediments in the western part of this peninsula. The SE-part of the Ionian zone at Cape Gerakas contains well-exposed sections of Pliocene/Pleistocene marls, although signs of deformation (steeply dipping layers, folding and normal faulting) caused by late Pliocene to Quaternary diapiric intrusion, are observed (Underhill, 1988). These marls, immediately adjacent to the diapirs in SE Zakynthos, are steeply dipping and overturned (Underhill, 1988, field observations), and are overlain by an undeformed series of Pleistocene marls alternating with calcareous sandstones/calcarenites (Dermitzakis et al., 1979), resembling the Citadel-Bochali sequence. A detailed stratigraphic study also revealed the Plio-Pleistocene boundary in this area (Triantaphyllou et al., 1997).

For our study, 15 sites and sections have been selected all over Zakynthos with ages ranging from Eocene to Pleistocene. Most sections/sites consist of undeformed sediments with (slightly) inclined strata. However, two sites, Messinian marls and evaporites at Kalamaki Beach and the Plio/Pleistocene marls at Cape Gerakas were sampled despite their signs of deformation (folding, faulting and anomalously steep strata). We have also sampled the three sites on Zakynthos (Fig. 4.1) used by Laj et al. (1982). In total, 609 cores were sampled and drilled with an electrical drill and generator. Preferentially, continuous sections were sampled - with 3 cores per level - formed by outcrops of more than 10 metres stratigraphic thickness. This allows magnetostratigraphy to be used as an age constraint in addition to the detailed biostratigraphy. Individual outcrops were sampled with 8 to 14 cores per site. Mostly, fine-grained sediments (clays, marls) were sampled with a low sedimentation rate (typically 5 cm/kyr) and over a sufficiently large interval, thus averaging out, to a large extent, secular variation. In addition, early post-depositional processes typically smooth out the finer-scale variations of the geomagnetic field (Van Hoof et al., 1993).

Ages of sections are mainly obtained by recording foraminiferal and calcareous nannofossil species (caption to Fig. 4.2) of which last (common) occurrences (L(C)O) and first (common) occurrences (F(C)O) have been dated. Foraminifers have been analysed in washed residues of > 125 micron; for calcareous nannofossils we have used smearslides. The sections/sites including the age diagnostic species are shown in Figure 4.2 and described in the Appendix together with their Mediterranean chronostratigraphy and numerical ages (Hilgen et al., 1995; Lourens et al., 1996; Langereis et al., 1997). Most sections have additional magnetostratigraphic constraints (Appendix).
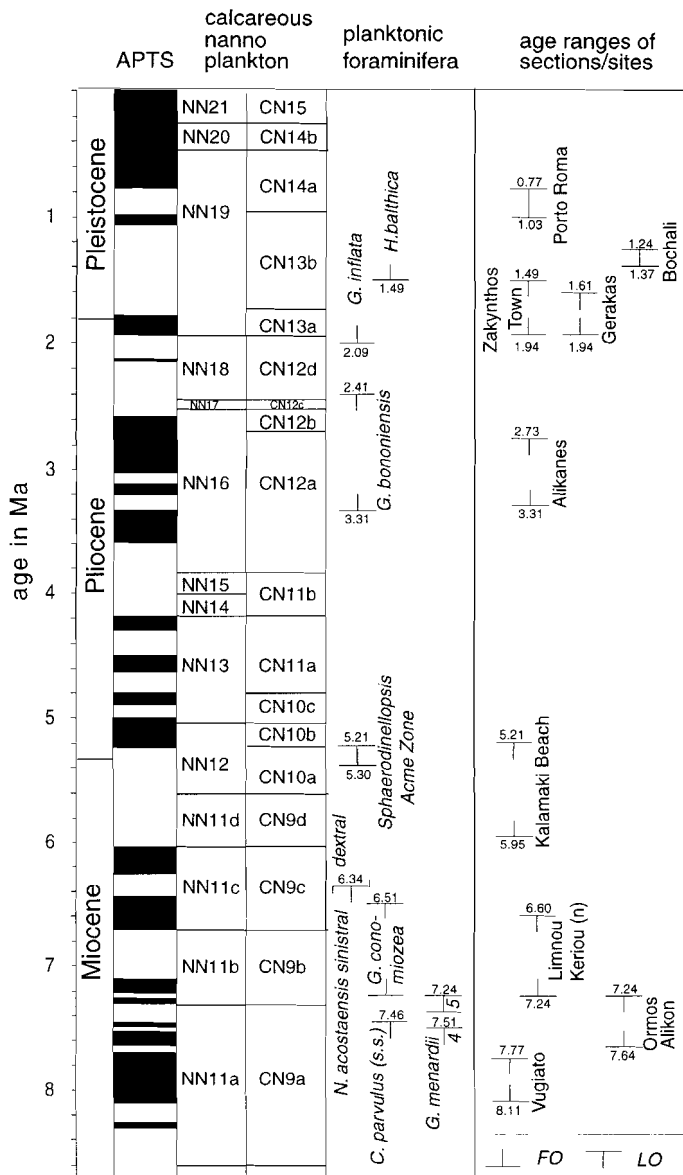
Fig. 4.2 Astronomical polarity time scale (APTS) of Lourens et al. (1996) for the Pliocene and Hilgen et al. (1995) and Krijgsman et al. (1999) for the Miocene with calcareous nannoplankton zones (Berggren et al., 1995a and 1995b) and planktonic foraminifera (Hilgen et al., 1995; Krijgsman et al., 1995; Lourens et al., 1996; Lourens et al., 1998) biochronology. FO (LO) indicates first (last) occurrences and s.s. small sized. The sections/sites from Zakynthos are correlated on the basis of magnetostratigraphy, planktonic foraminifera, calcareous nanno plankton and polarities. For details, see Appendix

Palaeomagnetic results

Analysis of the natural remanent magnetisation (NRM) and isothermal remanent magnetisation (IRM)

The natural remanent magnetisation (NRM) was measured on a 2G Enterprise DC SQUID cryogenic magnetometer using progressive stepwise thermal demagnetisation with temperature increments of 30 or 50 °C, from room-temperature to the limit of reproducible results. The demagnetisation results (Figs. 4.3, 4.4) show that often a small viscous and laboratory induced component is removed at 100 °C, while occasionally a relatively small secondary present-day field component exists which is typically removed at ~200 °C. As a rule, steps below ~200 °C are never used to determine characteristic components because of possible overlap of blocking temperature spectra (e.g. Fig. 4.3b).

Miocene
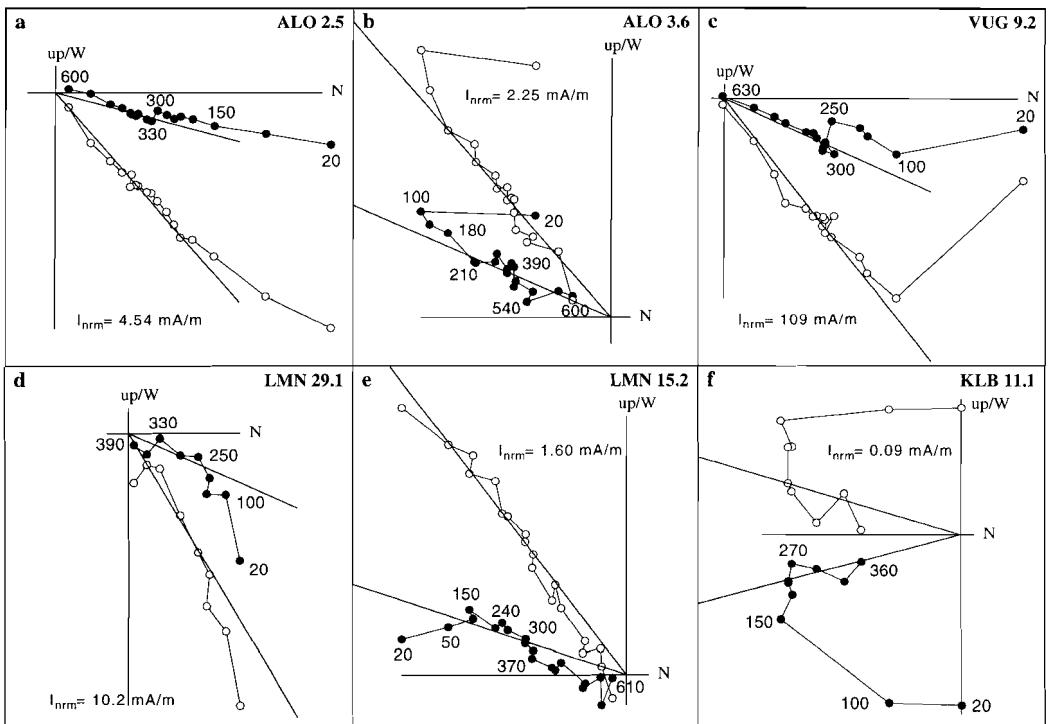
Fig. 4.3 Orthogonal projections of stepwise thermal demagnetisation diagrams (corrected for bedding tilt) from Miocene sediments on Zakynthos. Closed (open) circles represent the projection of the NRM vector endpoint on the horizontal (vertical) plane. Values denote demagnetisation steps in °C. Codes can be found in Table 4.1; line represents the interpreted result. The initial NRM intensities (I_nrm) are given.

Pliocene-Pleistocene
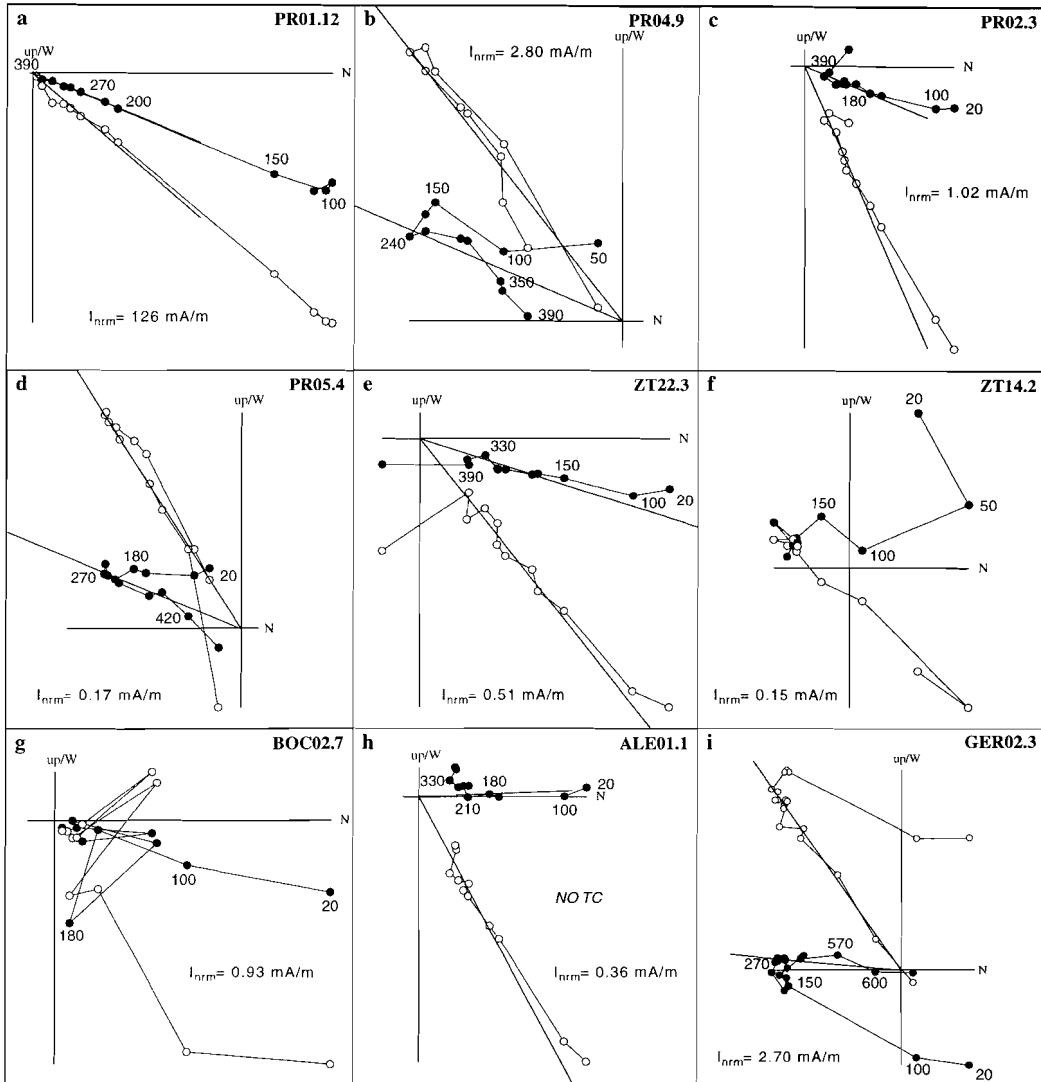
Fig. 4.4 Orthogonal projections of stepwise demagnetisation diagrams (corrected for bedding tilt) from Plio/Pleistocene sediments on Zakynthos. See also caption to Fig. 4.2; no tc (h) means without tectonic tilt correction.

Demagnetisation at higher temperatures reveals two types of demagnetisation behaviour related to intensities and different maximum unblocking temperatures. In general, samples with a relatively low NRM intensity have a characteristic remanent magnetisation (ChRM) which is completely removed at 360-400 °C (Fig. 4.3d,f and 4.4a-e,h). Demagnetisation at temperatures higher than 360-390 °C results in randomly directed magnetisations because of alteration (oxidation) of iron sulphides (typically pyrite), which

is commonly observed in this type of marls and clays. In high NRM intensity samples the ChRM is usually only completely removed at 580-620 °C (Fig. 4.3a-c,e and 4.4i), but also here disturbing magnetisations may occur at temperatures above 360-390 °C, depending on the presence of iron sulphides. Since this may cause an apparent decay of the ChRM passing the origin (e.g. Fig. 4.3e), we have in such cases conservatively used only the data points below ~390 °C. Samples with a large present-day overprint (Fig. 4.4f) or unstable samples (Fig. 4.4g) were not used. As the outcrops are monoclinal, the fold-test could not be performed. The reversal-test was negative or indeterminate as commonly observed in these types of sediments (Langereis et al., 1992). Although Scheepers and Langereis (1993) devised a method to correct the non-antipodality between normal and reversed polarity, it appears that simply averaging normal and reversed directions yields essentially the same result.
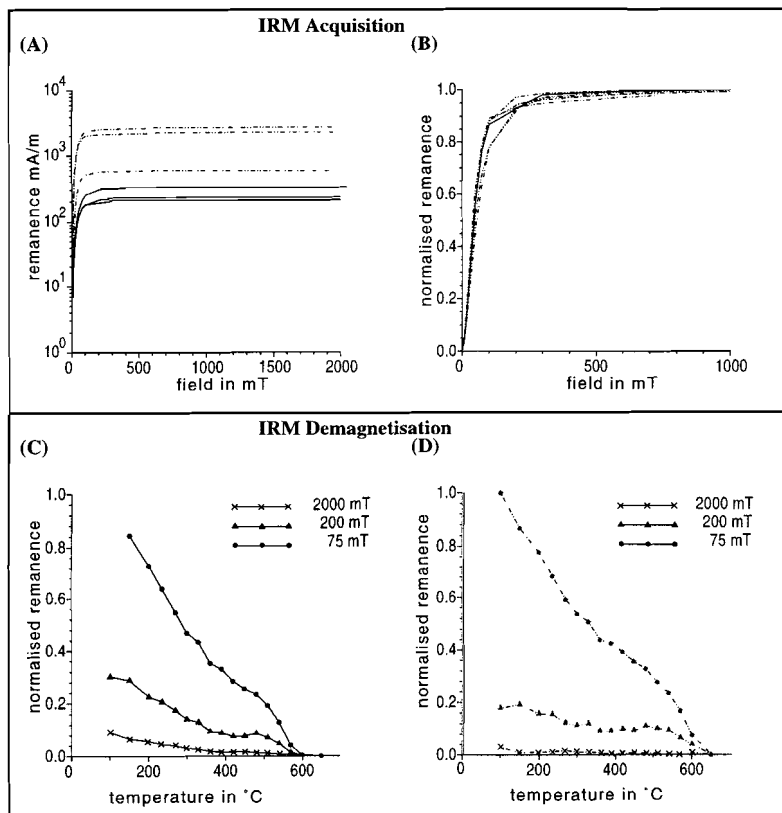
Fig. 4.5 Examples of absolute (A) and normalised (B) IRM acquisition of samples from Zakynthos. Solid (dotted) lines represent relatively low (high) intensity samples. Stepwise thermal demagnetisation of the normalised three component IRM of a low (C) and high (D) intensity sample indicates magnetite respectively maghemite as the main carriers of the ChRM.

We performed some rock magnetic tests to identify the dominant carriers of the remanence, including acquisition of a three component (Lowrie, 1990) isothermal remanent magnetisation (IRM) and subsequent demagnetisation of this IRM. The IRM was induced in a pulse magnetiser and was measured on a digitised spinner magnetometer based on a Jelinek JR3 driver unit. The IRM was induced in three orthogonal directions using fields of 75 mT, 200 mT and 2 T. All samples, both normal and reversed, are characterised by the dominance of a low coercivity mineral (Fig. 4.5a and b) and the magnetisation is carried by magnetic minerals with coercivities below 200 mT, mostly below 75 mT (Fig. 4.5c,d). The relatively low intensity samples (0.2-0.8 mA/m) show a maximum blocking temperature around 570 °C, indicating the presence of magnetite, but iron sulphides are likely present as well as can be seen from the inflexion at ~350 °C (Fig. 4.5c,d). The ChRM in these low intensity samples was removed at 360-400 °C; the ChRM at higher temperatures could not be measured. The relatively high intensity samples (3-55 mA/m) have a maximum blocking temperature between 600 and 650 °C, suggesting (partly) oxidised magnetite as the dominant carrier of the NRM (Fig. 4.5d).

For each section or site, average ChRM-directions were calculated using Fisher statistics (Fig. 4.6; Table 4.1). The distribution of the ChRM directions on Zakynthos can be seen in Fig. 4.7; the errors are calculated using $\alpha_{95}/\cos(I)$.
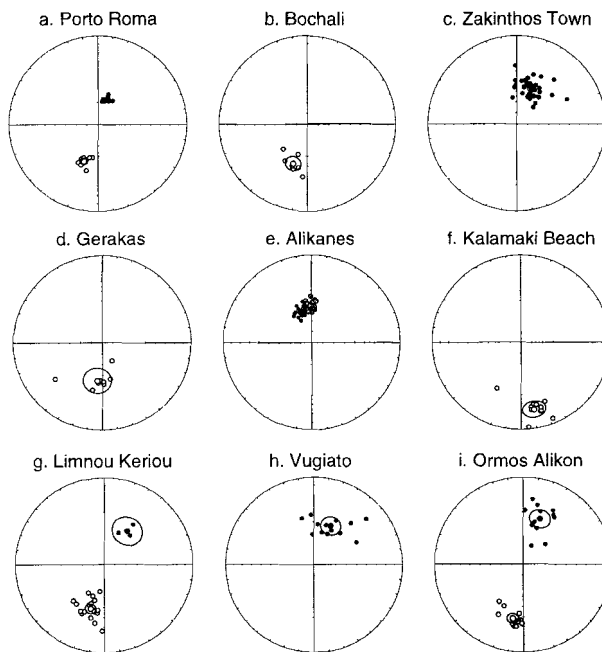
Fig. 4.6 Equal area projections of the ChRM from Mio/Plio and Pleistocene sections on Zakynthos, corrected for bedding planes. Closed (open) circles represent downward (upward) projections. Ellipses denote α_{95}. The grey circles (Alikanes) indicate the ChRM results before bedding plane correction and are indistinguishable from the present day field direction.

NRM-Analysis											
Site/Section	CODE	N	D_{notc} (°)	I_{notc} (°)	k	α_{95} (°)	D_{tc} (°)	I_{tc} (°)	k	α_{95} (°)	rot (°)	$\alpha_{95}/\cos(I)$ (°)	Age (Ma)

Site/Section	CODE	N	D_{notc} (°)	I_{notc} (°)	k	α_{95} (°)	D_{tc} (°)	I_{tc} (°)	k	α_{95} (°)	rot (°)	$\alpha_{95}/\cos(I)$ (°)	Age (Ma)
Porto Roma[1]	PR	20	12.1	62.0	136	2.8	20.0	59.2	98.4	3.3	20 c	6.4	1.03-0.77
Bochali[1]	BOC	8	193.5	-58.2	65.3	6.9	199.5	-50.2	65.3	6.9	20 c	10.8	1.37-1.24
Zakynthos Town[1]	ZT	41	21.8	63.8	43.2	3.4	22.3	54.5	43.6	3.4	22 c	5.9	1.94-1.44
Gerakas	GER	8	137.2	-55.2	12.9	16.0	187.9	-54.1	20.9	12.4	8 c	21.2	1.94-1.61
ZA 80 118*	A	10	-	-	-	-	184.0	-57.0	84.5	4.8	4 c	8.8	1.8-1.61
Alikanes	ALE	18	358.7	55.0	225	2.3	341.5	58.9	204	2.4	-	4.0[#]	3.31-2.73
Kalamaki Beach	KLB	11	143.2	-19.3	27.3	8.9	169.2	-22.6	27.3	8.9	11 ac	9.6	5.95-5.21
Aghios Sostis	SOS	9	-	-	-	-	-	-	-	-	-	-	Messinian
Limnou Keriou (N)[2]	LMN	23	176.4	-58.2	44.9	4.6	199.2	-47.4	47.7	4.4	19 c	6.5	7.24-6.60
Linmou Keriou (S)	LMS	4	-	-	-	-	-	-	-	-	-	-	Tortonian
Ormos Alikon[2]	ALO	25	170.6	-58	30.1	5.4	195.1	-40.5	34.1	5.0	15 c	6.6	7.64-7.24
ZA 80 119*	B	7	-	-	-	-	206.8	-39.8	248.0	3.5	27 c	4.6	7.64-7.24
Vugiato[2]	VUG	14	350.3	70.2	22.3	8.6	23.9	50.3	20.9	8.9	24 c	13.9	8.11-7.70
ZA 79 66*	C	15	-	-	-	-	25.3	44.9	76.6	4.1	25 c	5.8	8.11-7.70
Marathia	MA	8	-	-	-	-	-	-	-	-	-	-	Serravalian
Lagopodo	LAG	20	-	-	-	-	-	-	-	-	-	-	early M-Miocene
Lithakia	LIT	7	-	-	-	-	-	-	-	-	-	-	early M-Miocene
Keri	KE	7	-	-	-	-	-	-	-	-	-	-	Eocene
Mean													
Pleistocene.[1]		3	-	-	-	-	20.6	54.6	312	7.0	20 c	12.1	0.77-1.94
Miocene[2]		3	-	-	-	-	19.1	46.1	190	9.0	19 c	13.0	6.60-8.11
all*[12]		8	-	-	-	-	21.6	48.4	128.0	4.9	22 c	7.4	8.11-0.77
* Laj et al., 1982													redated

TABLE 4.1 Results from NRM analysis from the different sections on Zakynthos; corrected and uncorrected for bedding tilt, ages are indicated. N = number of specimens; D, I = site mean ChRM declination and inclination; k = Fisher's precision parameter; α_{95} = 95% cone of confidence; rot = sense of rotation, (a)c = (anti)clockwise with a 0° reference direction; $\alpha_{95}/\cos(I)$ = error (see figure 4.6); # = error of notc Alikanes data.

Discussion

Our palaeomagnetic investigations of all sampled late Neogene sections on Zakynthos, in both the Pre-Apulian and Ionian zones, show no significant differences in rotation. Since the ages of the sediments range from Tortonian (8.11 Ma) to Pleistocene (1.03-0.77 Ma), it must be concluded that no differential rotations took place between 8.11 Ma and 0.77 Ma. Thus, the overall 22° clockwise rotation (Table 4.1) must have occurred since 0.77 Ma.

Three sites, however, show anomalous results. The sediments at Cape Gerakas only show a small clockwise rotation, in contrast to the results from the rest of the island (Table 4.1). The (late) Messinian evaporites at Kalamaki Beach reveal anticlockwise rotations. A

possible cause for these anomalous results is that both sections are located in the vicinity of an intense zone of deformation. Kalamaki Beach is adjacent to the Ionian thrust, while the marls from Gerakas are steeply dipping and overturned caused by late Pliocene to Quaternary diapirism (Underhill, 1988). Furthermore, the Alikanes section is evidently overprinted because it yields a present-day field direction before tilt correction (Fig. 4.6e). Therefore, the results from Cape Gerakas, Kalamaki Beach and Alikanes have been disregarded.

Our new results have considerable implications for the geodynamic evolution of the western Aegean arc. A previous tectonic reconstruction for the north-western part of Greece was made by Kissel and Laj (1988), based on combined palaeomagnetic data from the Ionian islands of Zakynthos, Kefallonia and Corfu. They suggested that all three islands were subjected to a continuous rotation starting at 5 Ma, with an average rate of 5 °/Myr. This scenario was predominantly based on (9) results from Corfu, whereas fewer results were obtained from Zakynthos (3) and from Kefallonia (4). Kissel and Laj (1988) thus considered the Ionian islands as a structural unity, and they argued that this is supported by structural data from Mercier et al. (1976).

We sampled the Laj et al. (1982) sites from Zakynthos and re-dated them. It appears that our ages of these sites are significantly younger. The reason for this difference cannot be determined because no age diagnostic fossils are given in Laj et al. (1982). Our larger number of sample localities and accurate age constraints clearly reveal a different tectonic evolution at least for the island of Zakynthos. A continuous rotation during the last 5 Myr seems no longer tenable, since our new palaeomagnetic data indicate that a significant clockwise rotation of ~22° occurred between 0.77 Ma and Recent, while no rotational motions occurred between at least 8.11 and 0.77 Ma (Fig. 4.8). A different geodynamic history for Zakynthos need not be surprising, because Zakynthos (and Kefallonia) are separated from Corfu by the important Kefallonia Fault Zone. Moreover, Corfu does not overlie the Hellenic subduction zone, in contrast to Zakynthos and Kefallonia. It may thus have experienced a tectonic evolution quite different from that of Zakynthos. Although the rotation phase might have been influenced by local tectonics, considerable evidence is present suggesting a more regional cause, as outlined below.

The tomographic studies of Spakman (1990) have shown that the African slab (Adria) is subducting in the west underneath Italy, and in the east underneath Greece. These studies have also shown that the African slab is detached both underneath Calabria in southern Italy and beneath the southern Peloponessos in Greece (Spakman et al., 1988). After slab detachment, rebound processes can cause rapid uplift in the internal zones caused by stretching of the shallow remainder of the slab (Buiter et al., 1998). This scenario is used by Sorel et al. (1988) to explain the Pleistocene uplift of the Ionian islands, and which consequently would date the detachment in the Ionian region at that period (Spakman, 1990). As detachment proceeds, the gravitational pull of the detached part of the slab is transferred to the undetached part. This leads to an increase in the effective slab pull exerted by the undetached slab. A more pronounced outward migration of the trench,
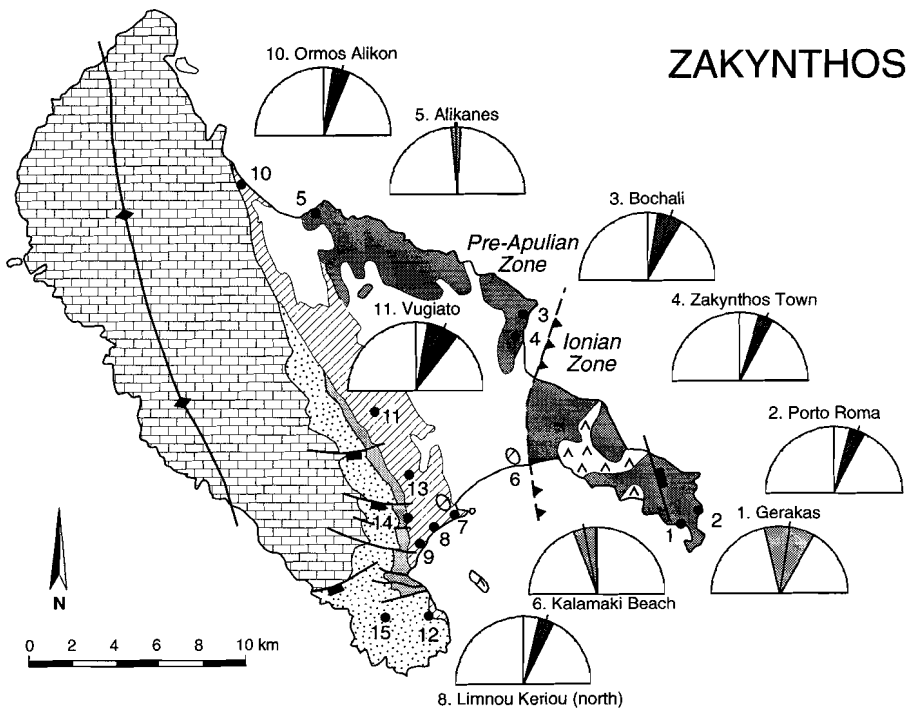
Fig. 4.7 Locality mean ChRM declinations on Zakynthos; shaded segment represents the statistical error $\alpha_{95}/cos(I)$ (Table 4.1). See also caption to Fig. 4.1.

relative to the situation where only the roll-back process is active, is expected above the undetached slab (Buiter et al., 1998) and therefore resulting in rotations.

Another scenario, concerning crustal flow, was put forward by recent work of Westaway (1996), based on former coast line studies. He observes that much of the relief of southern Greece has developed during the last million years. In his view, crustal thickening has accompanied the surface uplift and has been caused by flow of lower continental material from beneath other regions, such as the Gulf of Corinth. The added topography will then exert a force on its surroundings to the south-west, which will act to move the Hellenic arc outward, leading to (clockwise) rotation in its immediate vicinity (Westaway, *personal communication*, 1999).

Furthermore, detailed studies of present-day and past stress fields in the Aegean (Angelier et al., 1982) revealed a temporal change in the orientation of tensional stress - from NE-SW to NNW-SSE in the northern Aegean region - during the late Pleistocene (post-Calabrian and pre-Milazzian) (Mercier, 1976), i.e. roughly between 0.8 and 0.3 Ma. Numerical modelling of stress patterns by Meijer and Wortel (1996) indicated that this change in orientation is likely caused by lateral migration of slab detachment (Wortel and Spakman, 1992) on the eastern side of Adria. Our clockwise rotation phase on Zakynthos
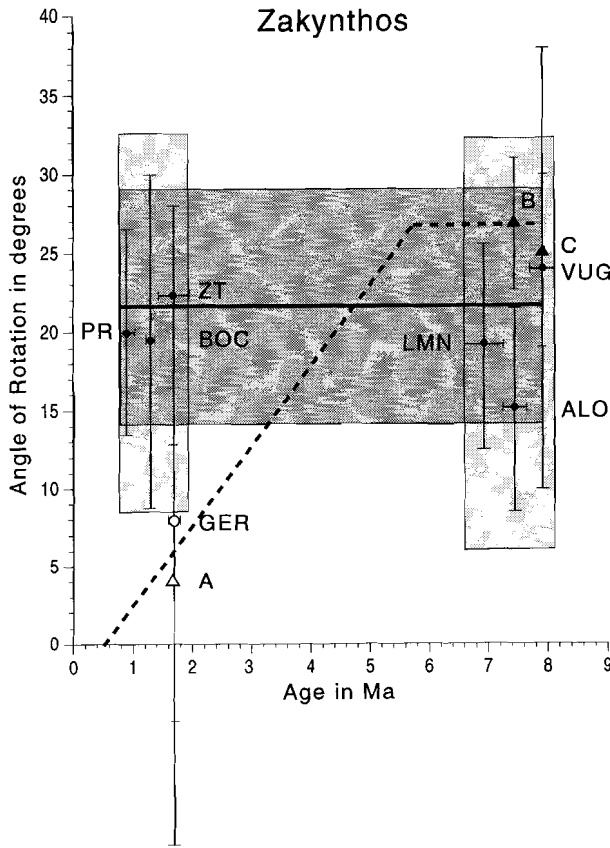
Fig. 4.8 Locality mean ChRM declination versus age on Zakynthos; codes are according to Table 4.1. Closed symbols indicate reliable results, open symbols are disregarded (see text for discussion). Circles are derived from this study, triangles from Laj et al. (1982). Vertical bars indicate error ($\alpha_{95}/cos(I)$), horizontal bars denote age range. Light shaded rectangles give $\alpha_{95}/cos(I)$ of Miocene and Pleistocene localities. The thick line and the dark shaded rectangle shows the mean rotation and the error $\alpha_{95}/cos(I)$. Dotted thick line is the interpretation of Laj et al. (1982) for the Ionian islands, indicating 5°/Myr starting around 5 Ma.

occurred after 0.77 Ma, corresponding to this change in stress regime. Hence, we prefer a scenario in which slab detachment and the subsequent rebound causes uplift and a change in stress regime, which in turn causes rotations. The rapid Pleistocene uplift observed by Westaway (1996) is easily reconciled in this scenario.

The Pleistocene rotational phase on Zakynthos appears to have been rapid since it must have taken place sometime during the last 0.77 Myr. A similar young and rapid Pleistocene tectonic rotation phase was found in southern Italy. In Calabria, the Calabro-Peloritan block underwent a 15° clockwise rotation between 0.8 and 0.7 Ma (Scheepers, 1994a), whereas the southern Apennines experienced a time-equivalent 23° anticlockwise

rotation (Sagnotti, 1992; Scheepers, 1994a). Concurrently (0.9-0.7 Ma), uplift in Calabria (southern Italy) occurred which Westaway (1993) related to slab detachment. Thus it appears that on both sides of the Adriatic platform a similar process of slab detachment, rebound, uplift and tectonic rotations occurred.

Conclusions

Our palaeomagnetic data show that during the last 8 Myr, the geodynamic evolution of the Ionian island of Zakynthos is marked by no significant rotational movements during Tortonian (8.11 Ma) to Pleistocene (0.77 Ma) times. A well-defined and rapid tectonic event occurs younger than 0.77 Ma causing a 22° clockwise rotation of the island. The early Pliocene emplacement of the Ionian thrust did not result in any differential rotations of the island.

We link the clockwise rotation of Zakynthos to late Pleistocene uplift in (mainland) Greece (Westaway, 1996), related to rebound processes resulting from (African) slab detachment underneath the Ionian islands (Wortel and Spakman, 1992; Meijer and Wortel, 1996). A similar process of slab detachment, rebound, uplift, and subsequent rotations is also found in southern Italy. This implies that rotations may ultimately be linked to slab detachment.

Acknowledgements

Appendix

Limnou Keriou South

Age:	early Tortonian
Geographical Coordinates:	37°41'N/20°50'E
Lithology:	5 metres marly clays with 4 intercalated sappropels
Cores:	1 site/4 levels/12 cores in the marly clays
Fossil Content:	*Neogloboquadrina acostaensis*, small-sized *Catapsydrax parvulus* without keeled globorotaliids, *Discoaster calcaris* and *Discoaster hamatus*
Magnetostratigraphy:	undetermined

Marathia

Age:	Serravalian
Geographical Coordinates:	37°40'N/20°51'E
Lithology:	~30 metres blue marls
Cores:	4 sites/32 cores in marls
Fossil Content:	*H. walbersdorfensis* and *H. orientalis*
Magnetostratigraphy:	undetermined

Lithakia

Age:	late early to early middle Miocene
Geographical Coordinates:	37°42'N/20°49'E
Lithology:	blue laminated limestones
Cores:	3 sites/26 cores
Fossil Content:	*H. ampliaperta* and *H. heteromorphus* (pre-*Orbulina* age)
Magnetostratigraphy:	undetermined

Lagopodo

Age:	late early to early middle Miocene
Geographical Coordinates:	37°44'N/20°47'E
Lithology:	scattered outcrops of laminated limestones/marls
Cores:	5 sites/39 cores in marls
Fossil Content:	*H. ampliaperta* and *H. heteromorphus* (pre-*Orbulina* age)
Magnetostratigraphy:	undetermined

Vugiato (=ZA 79 66)

Age:	8.11-7.77 Ma
Geographical Coordinates:	37°46'N/20°46'E
Lithology:	25 metres clays with 16 intercalated sappropels
Cores:	15 levels/38 samples in clays
Fossil Content:	*D. pentaradiatus, H. stalis*, left coiled *N. acostaensis*, small-sized *C. parvulus* and *G. menardii* 4
Magnetostratigraphy:	normal

Ormos Alikon (=ZA 80 119)

Age:	7.64 - 7.24 Ma
Geographical Coordinates:	37°52'N/20°44'E
Lithology:	60 metres clay and sappropel alternations
Fossil Content:	*Globorotalia menardii* 4, small-sized *C. parvulus* (in the lower part) and *G. menardii* 5 (in the upper part) and *M. convallis, D. brouweri , D. pentaradiatus, and H. brouweri.*
Magnetostratigraphy:	normal (first 17 metres), reversed (next 30 meters), normal (13 metres)

Limnou Keriou North

Age:	7.24 - 6.60 Ma
Geographical Coordinates:	37°42'N/20°51'E
Lithology:	~300 metres blue clays and sand alternations
Cores:	1 site/31 levels/97 cores in blue clays
Fossil Content:	sinistral *N. acostaensis, G. conomiozea* group and *R. rotaria*
Magnetostratigraphy:	250 metres reversed, followed by 50 metres normal

Kalamaki Beach

Age:	5.95-5.21 Ma
Geographical Coordinates:	37°44'N/20°53'E
Lithology:	125 metres evaporites alternating with clays, followed by 10 metres marls/sappropel
Cores:	5 levels/15 cores in clays between evaporites and 35 cores in marls/sappropels
Fossil Content:	*Reticulofenestra rotaria* in evaporitic part and high relative abundances of *Sphaeroidinellopsis* and dextral *N. acostaensis* in the Trubi part (*Sphaerodinellopsis* Acme Zone).
Magnetostratigraphy:	evaporitic part and base of marls (first 3.5 m) is reversed, top marls normal

Alikanes

Age:	3.31-2.73 Ma
Geographical Coordinates:	37°51'N/20°47'E
Lithology:	10 metres blue clays and sand alternations
Cores:	2 sites/20 cores in clays
Fossil Content:	*N. acostaensis, G. ruber, G. bononiensis* and *Discoaster tamalis*
Magnetostratigraphy:	overprinted

Zakynthos Town

Age:	1.94-1.49 Ma
Geographical Coordinates:	37°47'N/20°54'E
Lithology:	200m metres clay, sappropel alternations with occasional sand layers
Cores:	22 levels/64 cores mostly in clays (top of section was not reached)
Fossil Content:	*Discoaster triradiatus, G. inflata* and no *H. balthica*
Magnetostratigraphy:	normal (first 50 metres) followed by reversed

Gerakas (=ZA 80 118)

Age:	1.94-1.61 Ma
Geographical Coordinates:	37°42'N/20°58'E
Lithology:	~60 metres of laminated clays and sandy alternations
Cores:	8 levels/28 cores
Fossil Content:	Absence of *H. balthica* and *G. inflata* in the basal, presence of *Sphaeroidinella* and of *D. asymmetricus* (reworked)
Magnetostratigraphy:	normal (first metre) followed by reversed

Bochali

Age:	1.37-1.24 Ma
Geographical Coordinates:	37°48'N/20°54'E
Lithology:	scattered outcrops of sandy clay and sand alternations
Cores:	4 sites/43 cores in clays
Fossil Content:	large-sized *Gephyrocapsa, G. inflata, H. balthica* and 100% right coiled neogloboquadrinids.
Magnetostratigraphy:	reversed

Porto Roma

Age:	1.03-0.77 Ma
Geographical Coordinates:	37°42'N/20°59'E
Lithology:	outcrops of blue clays in between calcarenites along the coast
Cores:	11 levels/54 cores
Fossil Content:	The presence of *P. lacunosa, G. inflata* and *H. balthica* together with less than 15% - 20% left coiled neogloboquadrinids (in the middle/upper part of the section).
Magnetostratigraphy:	normal (first 10 metres), reversed (next 5 metres) followed by a calcarenite and 10 metres of reversed clay, again calcarenite with 10 metres normal clay

5

Neogene evolution of the Aegean arc: paleomagnetic and geodetic evidence for a rapid young rotation phase

Abstract

New paleomagnetic data of the entire Aegean outer-arc are presented. The results indicate a young (< 0.8 Ma) and rapid clockwise rotation phase in the western Aegean arc, covering Zakynthos and the Peloponessos. The eastern Aegean arc, incorporating at least Kassos, Karpathos and Rhodos, experienced Pleistocene (presumably < 2 Ma) anticlockwise rotations. We conclude that, prior to the Pleistocene, the Aegean arc was dominantly being formed by translations, rather than by rotations about nearby poles. The anisotropy of the magnetic susceptibility (AMS) data reveals arc-parallel extension in the south and south-eastern Aegean arc and arc-normal compression in the north-west, in agreement with structural and geodetic observations. We compare the paleomagnetic results with the present-day pattern of rotation as computed from the geodetic velocity field. The overall distribution is in agreement with the paleomagnetic data. The inferred time of onset of the Pleistocene rotations coincides with the start of uplift and a change in the pattern of extension, around 0.8 Ma. We evaluate mechanisms proposed to control the Aegean deformation in the light of our new findings.

Introduction

Many paleomagnetic studies have contributed to the reconstruction of the Neogene evolution of the Aegean area (Laj et al., 1982; Kissel and Laj, 1988; Morris and Anderson, 1996; Avigad et al., 1998; Duermeijer et al., 1998b; 1999a). Kissel and Laj (1988) have postulated an evolution for the Aegean arc during the Cenozoic in which the starting configuration was almost rectilinear (E-W) between the Paleocene and the late Burdigalian. During the middle Miocene, the western (Epirus, NW Greece) and eastern Aegean arc (Bey-Daglari, SW Turkey) started to rotate clockwise, respectively anticlockwise. A second supposedly continuous phase of rotation was thought to have occurred only in the western Aegean arc (Ionian islands) during the last 5 Myr.

Since the early nineties, new dating techniques have emerged. The astronomical polarity time scale and its related high accuracy biostratigraphy (ages of bio-events of planktonic foraminifera and nannofossils) provide the possibility to correlate sections/sites over a large geographic area and to accurately constrain the timing of tectonic events. Aided by these new techniques, we decided to explore the outer Aegean arc which contains mostly Neogene sediments. This non-volcanic arc comprises from west to east: Epirus, the Ionian islands (Corfu, Lefkas, Kefallonia, Zakynthos), the Peloponessos, Kythira, Crete, Kassos, Karpathos and Rhodos (Fig. 5.1, 5.3). In addition, we studied sediments from the central Aegean island of Milos. The present paper describes the synthesis of all our paleomagnetic data derived from the Aegean. We postulate a new tectonic evolution of the Aegean area and compare our results to geodynamic models that have been proposed for the region. Furthermore, we will evaluate geodetic data from the western Aegean arc in the context of the new tectonic evolution.

Geology and sampling

Central/South Eastern Aegean arc

We sampled 38 localities (691 cores) of sedimentary rocks in the central/eastern Aegean arc on Rhodes, Karpathos, Kassos, central-Crete and Milos (Fig. 5.1). The ages of the sediments in the eastern Aegean are not very well constrained as most sediments lack an age diagnostic biostratigraphy. The eastern arc is characterised by topographic highs in the centre of Rhodes, Karpathos, Kassos and Crete, consisting mostly of Jurassic to Eocene limestones. On Rhodes, a small ophiolitic and flysh unit of Oligocene age can be found on top of these limestones, surrounded by Neogene (Miocene to Pleistocene) sediments. These sediments are mostly of continental, fluvio-lacustrine origin, but some shallow marine to beach deposits are present. The Neogene sediments on Karpathos are restricted to three small basins in the south of the island. In SW and SE Karpathos, Plio/Pleistocene

beach deposits are found, while Pliocene shallow marine clays occur in the south, near the airport. The small island of Kassos consists mainly of high peaks of strongly deformed limestones. The only two roads on the island lead to two small areas with limestone in the SE and marls and clays in the W, both of Miocene age. On Crete, close to Heraklion, the Messinian to late Pliocene succession is characterised by Messinian limestones overlain by marl-breccias with some intercalations of Pliocene "Trubi-like" sediments (Jonkers, 1984). On top of the marl-breccias, Trubi-like sediments with sapropels are deposited, followed by shallow marine sandy yellow marls and white diatomites. The complete succession can be found at the village of Prassas (PRA in Fig. 5.1). The Pleistocene is absent in the northern Iraklion basin, but sandy shallow marine clays and red conglomerates of Pleistocene age outcrop in the southern part. We have chosen the central part of Crete as this area contains most of the Plio/Pleistocene sediments on the island and the largest (up to 40°) post early Messinian anticlockwise rotations were detected (Duermeijer et al., 1998b). The volcanic island of Milos is located more to the internal part of the Aegean arc. This inner-arc island contains Pelagonian basement formed by volcanic rocks of various ages overlain by white tuffites and yellow marls of Plio-Pleistocene age. In the NW of Milos, a marine section containing a rhythmically alternation of early Pliocene silty clays and sapropels was sampled.

Western Aegean arc

In the western Aegean arc we took 52 sites/sections (1912 cores) from Mio-Plio-Pleistocene sediments on Lefkas, Kefallonia, Zakynthos, the Peloponessos and Kythira (Fig 5.1). The western Aegean is characterised by NNW-SSE trending sedimentary units (Aubouin et al., 1976) called isopic zones and named from west to east Pre-Apulian, Ionian, Gavrovo-Tripolitsa, Pindos, (Sub)Pelagonian and Vardar. Each unit contains Mesozoic carbonates at its base and is separated from the juxtaposed unit by a major Tertiary thrust. In general, the age of deformation, the degree of metamorphism and tectonism and the age of the oldest rocks exposed within each isopic zone all decrease from east to west (Underhill, 1988). Our sites/sections are mainly from the Pre-Apulian, Ionian and Pindos zones.

The Ionian Island of Lefkas consists of Jurassic to Eocene limestones, followed by Oligocene to lower Miocene limestones alternating with marls or coarser grained material. These sediments are intensely folded and overlain by (scarce outcrops of) early middle Miocene marls with sapropels and middle Miocene turbidites. The Plio-Pleistocene is absent on Lefkas. South of Lefkas, the Ionian Island of Kefallonia has a topographic high of Jurassic to Paleogene limestones in its centre. Around the core of the island, Plio-Pleistocene and some Miocene sediments were deposited, which can now be found along the coast. These young sediments closely resemble the Miocene to Pleistocene sediments of Zakynthos, the Ionian Island south of Kefallonia. However, on Kefallonia the Miocene sediments are coarser and more deformed and the Pliocene alternations of marine marls
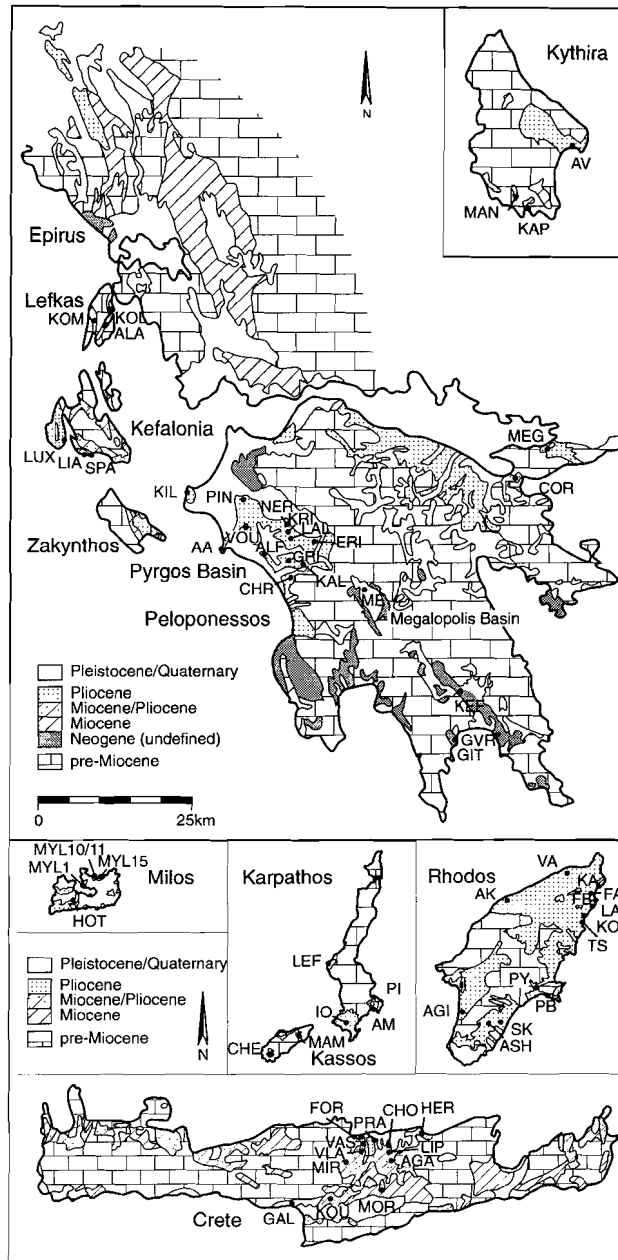
Fig 5.1 Simplified geological map of the outer Aegean arc with sample/site localities in codes (see also Appendix 5.1). For location of sites from Zakynthos, we refer to Duermeijer et al., 1999a.

and sapropels are much thicker, suggesting a similar but more proximal setting. The sediments on Zakynthos range in age from Cretaceous to Pleistocene and occur mostly in approximately parallel, linear zones running NW-SE. On the Peloponessos, several isopic zones (Pelagonian, Pindos, Gavrovo-Tripolitsa, Ionian) are recognised, but not many outcrops of Neogene sediments are exposed; most of the area is covered or contains Mesozoic limestones. Scattered upper Pliocene outcrops are located in the central-south (silty clay) and south (continental to shallow marine sand with occasional silt layers). In the Pyrgos basin of NW Peloponessos, extensive Plio-Pleistocene open bay to lagoonal sections are outcropping (Hageman, 1979). In the centre of the Peloponessos, the intramontane Megalopolis Basin is exposed, containing Pleistocene lacustrine sediments. In the NE of the Peloponessos, the Corinth and Megara basins are situated in the Pelagonian cover. The Megara basin contains Plio-Pleistocene lacustrine, deltaic to fluviatile deposits and is at present bounded by a NW active normal fault. Uplift in the footwall of this normal fault exposed the Neogene sediments of the Megara basin. Nearby, the actively extending Corinth basin can be found. The Corinth basin contains 4 Ma old andesites representing the initiation of the basin (Collier and Dart, 1991) and containing Plio-Pleistocene sandy deposits with a marine influx. We have sampled in the famous Corinth canal. Finally, the island of Kythira consists of Pre-neogene basement rocks, overlain by a terrigenous-clastic succession of presumably Tortonian age, overlain - with an angular unconformity- by an early Pliocene calcareous succession.

Paleomagnetic results

The detailed paleomagnetic results are listed in Appendix 5.1 and 5.2 (ages are indicated) and discussed in their context in the synthesis of the data.

Analysis of the natural remanent magnetisation (NRM)

The natural remanent magnetisation (NRM) was measured on a 2G Enterprise DC SQUID cryogenic magnetometer. At least one specimen per sampling level of a section, and at least 7 specimens from a site were analysed using stepwise thermal demagnetisation with temperature increments of 30 ° or 50 °C. As a rule, we took many widely-spaced samples to average out the effect of secular variation. In addition, most localities consist of fine-grained sediments (clays or marls) having a low sedimentation rate. We removed the weathered surface to reach fresh sediments, and care was taken to avoid sampling near major faults or otherwise clearly noted.

Demagnetisation diagrams usually show a very small and randomly oriented laboratory-induced component removed at ~100 °C; a present-day field component is sometimes present and removed at ~200 °C (Fig. 5.2). The characteristic remanent

Pliocene-Pleistocene
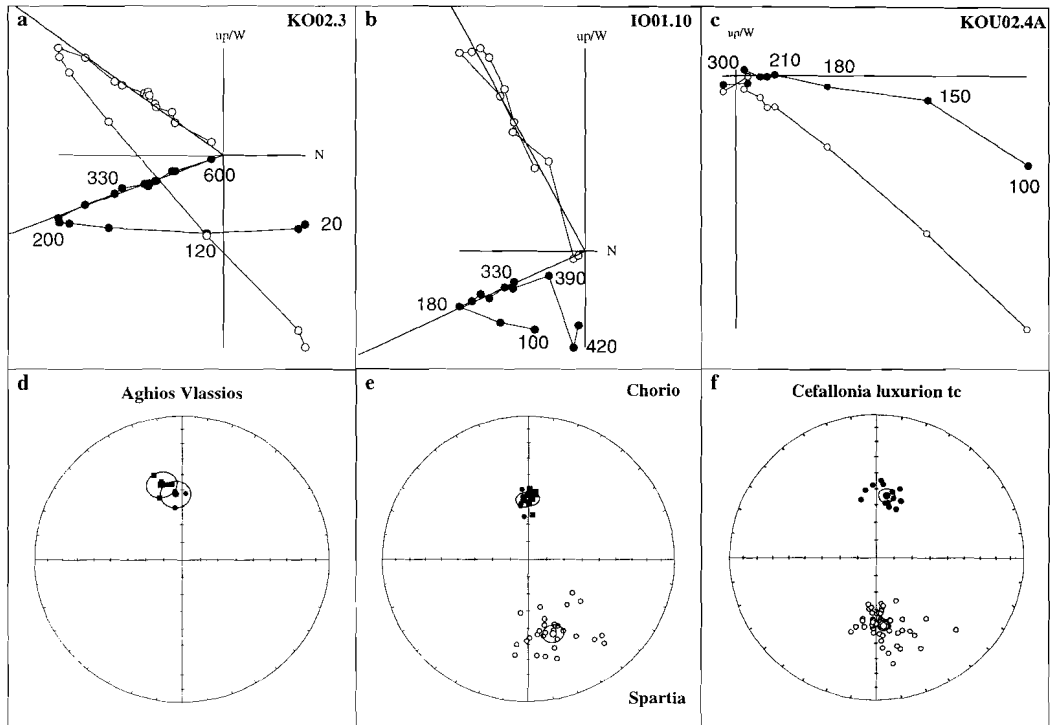
Fig. 5.2 *Orthogonal projections of stepwise thermal demagnetisation of selected samples are shown in (a,b and c) after bedding plane correction. Closed (open) circles represent the projection of the ChRM vector endpoint on the horizontal (vertical) plane. Values indicate temperatures in °C. Equal area projection of ChRM directions and their means are shown in (d, e and f); circles are 95% (α_{95}) confidence regions around the mean directions. In (d and e): closed squares (circles) denote ChRM directions after (before) bedding plane correction and open circles indicate ChRM from Spartia (Kefallonia) directions after bedding plane correction (e). In (f) closed (open) circles indicate normal (reversed) ChRM direction of Luxurion after bedding tilt correction.*

magnetisation component (ChRM) is removed at higher temperatures and shows both normal and reversed polarities. The paleomagnetic results of each region (Appendix 5.1) are characterised on the basis of several criteria and we distinguish three types of demagnetisation behaviour.

Type 1. The results show a linear decay towards the origin and the present-day field overprint is demonstrably removed (Fig. 5.2a,b). Some sediments, typically those from Rhodos and some from Kythira and the Peloponessos, contain ChRM components which are only entirely removed at 680°C indicating hematite as an important carrier, while other sediments have components mostly removed below 600°C (Fig. 5.2a), indicating magnetite. Ocasionally, the sediments (e.g. Luxurion on Kefallinia, some sites on the Peloponessos, on Milos and Aghios Ioannis on Karpathos) contain iron-sulphides as dominant carriers, since the ChRM components are mostly removed at lower

temperatures, below 350°C (Fig. 5.2b). These sediments show alteration starting at 390°C, resulting in scatter and random directions at higher temperatures (Fig. 5.2b). We regard type 1 as reliable and use the results to calculate rotations.

Type 2. Sometimes the individual directions per site/section are too dispersed for a statistically significant mean direction, like the results of Spartia Beach (Fig. 5.2e) and Cape Liakas (on Kefallonia), and the results must be considered with caution. In some sites/sections (on Milos, the Peloponessos, Kythira, Kassos and on Rhodos) not all individual results (of at least 7 cores) are reliable and therefore the means are hardly significant, but give merely an indication of the sense of rotation. Likewise, in rare occasions the inclination is anomalously large (> 60°; Avlemonas on Kythira) or small (< 30°; the basalt on Milos), and we regard the results as indicative only.

Type 3. "Spider-webs" in the demagnetisation diagrams are typically found on Lefkas and in the Miocene limestones on Kassos with low intensities. We also include in type 3 overprinted samples with a large present-day field overprint until 240°-270°C and containing a cluster or scatter above this temperature (Fig. 5.2c). In particular, results from Plio/Pleistocene sites on Crete and from some sites on Karpathos and Kassos show a present-day field before bedding tilt correction (Fig. 5.2d); these sites/sections are considered as overprinted, but we note that overprinted data is hard to distinguish from non-rotating if the bedding plane is sub-horizontal (Chorio in Fig. 5.2e). Type 3 is disregarded from any conclusion.

Anisotropy of the magnetic susceptibility

Analysis of the anisotropy of the magnetic susceptibility (AMS) can be used to establish the sedimentary and tectonic history in weakly deformed sediments, because there is a relationship between the AMS of rock samples and the regional stress field of the area. In undeformed sediments, the magnetic susceptibility is dominated by foliation coinciding with the bedding plane (i.e. the minimum axes of AMS, k_{min}, are perpendicular to the bedding plane) and a random orientation of the lineation (i.e. direction of the maximum axes of AMS, k_{max}). Upon deformation, the lineation quickly aligns along the direction of maximum extension or, equivalently, perpendicular to maximum compression.

The Miocene to Pleistocene sediments from the western Aegean arc and Crete, show NW-SE alignments of the k_{max} axes, indicating NW-SE extension or NE-SW compression (Appendix 5.2 and Fig. 5.3). In the eastern Aegean arc (Rhodos and Karpathos), the Plio/Pleistocene sediments reveal a roughly NE-SW aligment of the k_{max} axes, implying NE-SW extension or NW-SE compression (Fig. 5.3). The Miocene sediments on Kassos indicate an approximately E-W clustering of the k_{max} axes, but with a large error. The clustering of the k_{max} axes from Plio/Pleistocene sediments on the Peloponessos are not consistent over the peninsula, and therefore cannot be averaged. Likewise, the AMS of the sediments on Milos shows no clear indication of alignments.

Synthesis of data

Many paleomagnetic key investigations have been carried out by Kissel and Laj (1988 and references herein), aided by structural work from Le Pichon and Angelier (1979), Angelier et al. (1982), Mercier et al. (1979). They have extensively sampled the Neogene in Greece, visited most of the Aegean outer-arc islands and were the first to propose a kinematic time-constrained reconstruction of the Aegean area. As new techniques developed and more precise time-constraints can be given to Neogene marine sediments on the basis of cyclo/biostratigraphy, a new study of the sediments in the Aegean outer-arc is warranted. Our paleomagnetic results of Miocene to Pleistocene sediments are often compatible with the earlier results, but our new data contribute to a more detailed and significantly different picture of the geodynamics in the Aegean region (Fig. 5.3).

Ionian islands. Based on paleomagnetic data from Corfu (9 mean directions), Kefallonia (4) and Zakynthos (3), Laj et al. (1982) suggested that the western Aegean arc underwent a ~25° clockwise rotation, which started at 5 Ma with a rate of approximately 5°/Myr. Since a total 45-50° clockwise rotation was revealed from Paleocene to Eocene pelagic limestones (Horner and Freeman, 1983), which appeared to include the entire Oligocene (Kissel et al., 1985), it was concluded that two distinct clockwise rotations must have occurred in the western Aegean arc, one during the early to middle Miocene and one during the last 5 Myr. A recent and more detailed study of Zakynthos (Duermeijer et al., 1999a), however, has shown a different history of at least this part of the western Aegean arc. These data indicate no rotation between 8.11 and 0.77 Ma and a 22°± 5° clockwise rotation phase taking place between 0.77 Ma and Recent.

The Plio/Pleistocene section of Luxurion (Triantaphyllou, 1996) along the SW coast of Kefallonia reveals 4 polarity zones (N-R-N-R). The samples are mostly reversed and the section covers the Olduvai subchron and the late Matuyama Chron (~1.9 - ~1.0 Ma). The reversed samples (56 cores) give a mean declination indicating no rotation, while the mean of the normal samples (14 cores) shows a small clockwise rotation (Fig. 5.2f). Calculating the overall mean of the Luxurion section (Appendix 5.1) indicates no significant rotation since ~1.9 Ma. This is in contrast to the interpretation of Laj et al. (1982), who suggested a clockwise rotation based on their (three) normal sites. However, our mean directions of the reversed and normal samples are similar to those of Laj et al. (1982). The Miocene and Plio/Pleistocene sediments on SE Kefallonia indicate anticlockwise rotations, but the scatter in data-points is very large (Appendix 5.1). From Lefkas, no reliable data could be obtained, while data from Corfu indicates no significant rotation since ~3.5 Ma, according to earlier published data (Laj et al., 1982).

Peloponessos. In the southern Peloponessos, we found post Pliocene clockwise rotations (Kefalas, Cythion) in agreement with earlier results of Laj et al. (1982). The Pyrgos basin (Hageman, 1979) in the NW Peloponessos shows a post-Pliocene 16° clockwise rotation (Appendix 5.1). However, the youngest (probably Pleistocene) sediments in the NW

Peloponessos (Pineos) shows no rotation. The Megalopolis basin in the centre of the Peloponessos and the Megara/Corinth basin in the NE Peloponessos contain Pleistocene sediments covering the Brunhes-Matuyama boundary (0.9-0.4 Ma). The paleomagnetic results of the Brunhes indicate no rotation (Appendix 5.1). This reveals that the Peloponessos (at least the Pyrgos basin, Kefalas and Gythion) also underwent a young, late Pleistocene clockwise rotation phase, in agreement with the results derived from Zakynthos.

Central Aegean. Our paleomagnetic results from the late Tortonian to early Messinian sections show predominantly anticlockwise rotations on Crete, with amounts varying over the island (Duermeijer et al., 1998b). We concluded that the paleomagnetic rotations were of post-early Messinian age and governed by (local) rotations of fault-bounded blocks. To determine the actual age of the anticlockwise rotations on Crete, we sampled Plio/Pleistocene sediments in the Heraklion basin (central Crete). Unfortunately, almost all samples were either overprinted or the bedding plane was sub-horizontal and therefore no bedding correction could be applied, necessary for validating a stable characteristic component. Thus, the amount of rotation derived from the Plio/Pleistocene sediments seems to be zero, but this may equally be an artefact. One site (Chersonissos) shows a large anticlockwise rotation, but since the biostratigraphy revealed a Miocene age, rather than a Plio/Pleistocene age, this result agrees with the post early Messinian rotation. Overall, the results on Crete do not allow us to date the rotations other than post early Messinian (Duermeijer et al., 1998b). The Miocene and Pliocene results from Kythira reveal anticlockwise rotations, but the error is large and therefore this result may only be considered as indicative.

Our results from Milos indicate hardly any rotation. Recently, the inner arc of the Aegean region was paleomagnetically studied by Morris and Anderson (1996) and Avigad et al. (1998). These authors have shown that this area consists of two major blocks showing an opposite sense of rotation. The island of Mykonos and Tinos indicate post middle Miocene clockwise rotations, and Naxos and Milos (Kondopoulo and Pavlides, 1990) anticlockwise rotations. The clockwise rotations are consistent with rotations further to the northwest in Evia and Skyros (Kissel et al., 1986). Therefore, it was suggested that the clockwise domain extends as far as Mykonos (Morris and Anderson, 1996) and that the boundary between the two opposite rotating blocks lies north of Naxos.

South Eastern Aegean. Le Pichon and Angelier (1979) have suggested a model in which they expect the eastern Aegean arc to have been rotating anticlockwise. This idea was supported by a preliminary study of Laj et al. (1978), suggesting a ~23° anticlockwise rotation on Rhodos. However, a later study by the same group (Laj et al., 1982) of 5 sites from middle and upper Pliocene sediments from Rhodos indicated no significant rotation. Our new Plio/Pleistocene data of 13 sites from Rhodos confirm the earlier results since we find only anticlockwise rotations for all sites, having an average rotation of 18°±12. In addition, the paleomagnetic results from Karpathos and Kassos imply anticlockwise

rotations as well. Furthermore, results from Bey Daglari in southern Turkey (Kissel and Poisson, 1987) suggest a ~30° anticlockwise rotation since 15 Ma. This seems to denote an eastern arc area of anticlockwise rotations from Kassos to further east, including Rhodos and probably southern Turkey. The anticlockwise rotations are measured in the youngest (Plio/Pleistocene) sediments from Karpathos and Rhodos, implying that this rotation phase took place some time during the Pleistocene (Appendix 5.1). Unfortunately, the fossil content of the sediments does not allow a more precise age estimate.

On both sides of the Aegean arc, our new paleomagnetic results indicate a young rotation phase. In the western arc (Zakynthos and the Peloponessos), a rotation phase was clockwise and took place after ~0.8 Ma, and in the eastern arc (Kassos, Karpathos and Rhodos) anticlockwise occurring during the Pleistocene, i.e. younger than ~1.8 Ma.
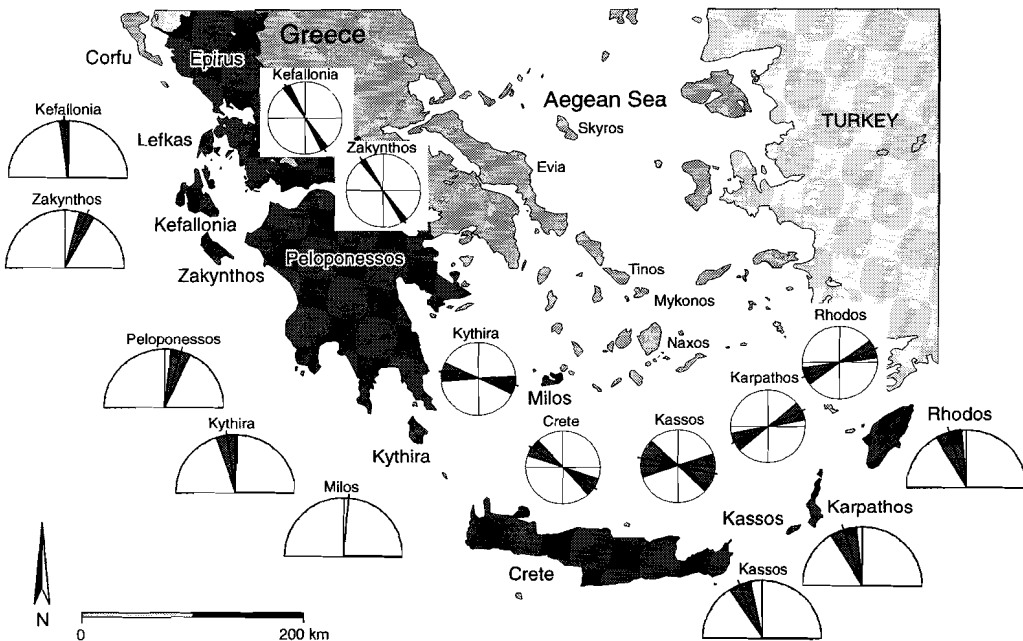
Fig 5.3 Distribution of ChRM and AMS data on the Aegean outer-arc, after bedding plane correction. Shaded segment in ChRM plots represent weighted α_{95} ($\alpha_{95}/ cosI$) with solid line as mean declination per area (see also Appendix 5.1). Shaded segment in AMS data indicates the δD in the AMS-analysis with solid line as mean lineation direction per area (see also Appendix 5.2).

Discussion

Coincident tectonic events during the early Pleistocene

The onset of the inferred young rotation phase shows a remarkable coincidence with other changes in the Aegean tectonics. It is generally believed that a change in stress regime between the Calabrian and the Milazzian (~0.8-0.3 Ma) affected the Aegean region (Angelier et al., 1982; Mercier et al., 1987). NE-SW tensional stress in central and northern Greece to N-S tension in Turkey prevailed in the early Pliocene - early Pleistocene. This changed in the middle Pleistocene - Recent to NNW-SSE tensional stress in central and northern Greece, changing towards NE-SW tension in western Turkey. Possibly, the two phases of extension were separated by a short period of dominant compression (Angelier et al., 1982; Mercier et al., 1987). Around the same time, a rapid phase of rifting started to affect the Corinth region and subsequently the Gulf of Corinth opened (Armijo et al., 1996). The major normal fault bounding the Megara basin (NE Peloponessos) was initiated at a similar age of 0.9 ± 0.2 Ma (unpublished data). The change of stress regime was accompanied by uplift of the entire Aegean outer-arc, which was confirmed by Westaway (1996), who demonstrated that much of the relief of southern Greece has developed during the last million years. These results imply that the tectonic regime of the Aegean outer-arc changed drastically around 1 Ma.

AMS results

The AMS data derived from the sediments of the Aegean arc clearly shows an extension direction parallel, or compression perpendicular to the Aegean arc (Fig. 5.3). Kissel et al. (1986) show similar AMS data from the Ionian islands. Geodetic data (Gilbert et al., 1994), earthquake focal mechanisms (Lyon-Caen et al., 1988), microseismics (Hatzfeld et al., 1993) and faults observed in the field by Armijo et al. (1992) suggest arc-parallel extension for the region between the volcanic arc and the outer-arc, in the southern Aegean. In the north-western Aegean, earthquake focal mechanisms (Baker et al., 1997) and field data (Mercier et al., 1987) imply a prevalence of arc-normal compression. Our AMS data is consistent with the other types of observations and provides independent support for the inferred pattern of strain. We consider our AMS data in the north-west, on the Ionian islands, to result from (NE-SW) thrusting, whereas in the south and south-east, along the outer-arc, the data is most likely caused by arc-parallel extension.

Translations versus rotations

Our new paleomagnetic data suggest a different tectonic evolution of the Aegean area and indicate a rapid, Pleistocene phase of rotation. We find no evidence for tectonic rotations prior to this young rotation phase, since the opening of the Aegean Sea (~13 Ma; Le Pichon and Angelier, 1979). It seems unlikely, however, that an entire arc can be formed in a period of less than 1 Myr. Indeed, given that the Aegean Sea was subject to extension, also its outer edge, the Hellenic arc, must have been deforming prior to the Pleistocene. It would follow that, prior to the Pleistocene, the Hellenic arc deformed in such a way that no significant paleomagnetic rotations were produced. There occurred no rotation about nearby poles but rather, on the scale of the Aegean, translation of crustal blocks dominated.

Comparison with active crustal rotation rates

The young age of the paleomagnetically observed rotations raises the question whether these rotations can also be observed in the present-day pattern of strain. Over the past years active crustal motion in the Aegean region has been extensively monitored by means of satellite geodesy. The results of more than 30 occupations of several local networks, performed by different groups between 1988 and 1998, and of the reoccupation by GPS in 1992 of a 100 year old triangulation network located at the centre of Greece (Davies et al., 1997) are now combined within one regional data set of about 240 velocity vectors. This is one of the subjects of the SING project (GPS Seismic hazard IN Greece), which has as its main goal the determination of overall GPS strain and assessment of seismic hazard in Greece. The processing of the main network, the Central Greece network, and its subsets is described by Clarke et al. (1998). They successfully removed the coseismic effects of the M_s=6.2, June 15, 1995 Egion earthquake in the Gulf of Corinth from the data set to derive a constant interseismic velocity field. Furthermore, they constrain the orientation of the 100 year triangulation-GPS velocity estimates using 14 sites common to both networks. The results show a high compatibility between short-term and 100 year deformation estimates. Kahle et al. (1998) describe the different local networks that build up the combined set, which covers the Aegean region and is especially dense in central Greece and the Peloponessos. We excluded from the main set those sites that had a large error or showed decimetre to metre displacements between two epochs. The remaining set is sufficiently dense to represent the regional velocity field (Fig. 5.4a); it now contains 209 velocity vectors.

For the interpretation of the velocity field we assume that crustal deformation encompasses slip along faults and continuous deformation in crustal blocks bounded by the faults. With the coseismic motions removed from the data, this fault slip represents a summation of aseismic motion and motion related to small earthquakes. Both seismic and aseismic motion contribute to the long term deformation of the crust. We assume

paleomagnetic data to represent the long term deformation. Therefore, by excluding the coseismic influences we expect the resulting crustal deformation field to be of lower amplitude than that predicted by the paleomagnetically observed rotations.

To calculate the deformation field we apply the inversion technique developed by Spakman and Nyst (1999). This method is purely kinematic, hence does not assume any particular rheology of the crust or faults, and inverts the velocity field into joint estimates of strain rates, rotation rates, and aseismic fault slip. The method is based on a model space parameterisation for fault motion and continuous deformation. We parameterise the major active faults as step functions on fault great-circle segments and the continuous deformation is parameterised as general linear strain and rotation rate behaviour between model nodes. The model nodes are defined by a triangulation of the crustal blocks. The inversion results are fault slip vectors on fault segments and the 4 elements of the velocity gradient tensor at each model node. We restricted the fault parameterisation to the largest and most active ones. This implies that in part the solution for continuous deformation can be due to slip on non-parameterised faults. We base the regional fault parameterisation on Jolivet et al. (1994), and apply a more detailed parameterisation of the Gulf of Corinth according to Armijo et al. (1996). The relative velocity differences between every pair of GPS stations constitute the basic data for the inverse problem.

The solution shows relatively small fault movements. However, the parameterisation of the faults is of significant influence on the results. The ability of the continuous deformation field to vary discontinuously over the fault traces avoids the presence of anomalously high deformation rates (especially in the Gulf of Corinth). In the present paper we are mainly concerned with the rotation rates (the antisymmetric part of the velocity gradient tensor). These results are presented as finite angles of rotation about vertical axes in Fig. 5.4b. In comparing Fig. 5.4b with the paleomagnetic results care should be taken for two reasons in particular. Of course the rotation rates obtained from inversion are at most representative for the kinematics that occurred during the period of observation (e.g. about 100 years). A comparison with paleomagnetic results can only be made if we assume that the present day pattern is also representative for the past 0.8 Myr. Furthermore, computed rotation rates refer to the motion of a small rigid equidimensional element entrained in the flow field, while in reality the rotating blocks may be of considerable size (England and Jackson, 1989). As shown in Fig. 5.4b, we indeed find large parts of the Aegean to rotate in the same manner. Here, we address only the general characteristics of the computed rotation pattern.

This bulk partitioning of crustal rotation is consistent with the paleomagnetic results presented earlier. The overall picture reveals rather high amplitude and predominantly clockwise rotations in the mainland of Greece and weaker anticlockwise rotations in the east and south-eastern Aegean. We find significant clockwise rotations in the region of the central Ionian islands (Lefkas, Kefallonia and Zakynthos), and of the western and central Peloponessos.
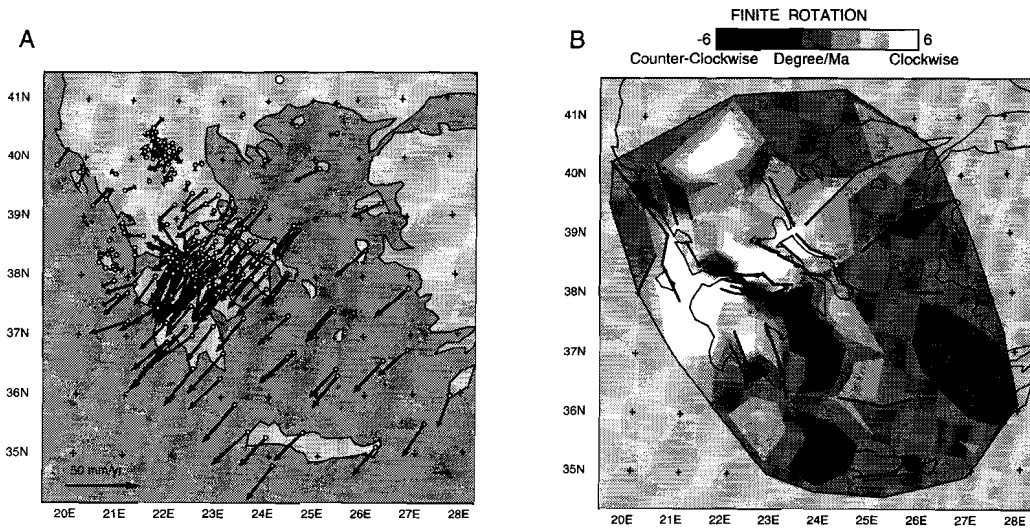
Fig. 5.4 A shows the velocity vectors from a combination of several GPS campaigns relative to the northernmost station (white dot). B indicates contoured finite angles of rotation in degrees per My.

Geodynamic models compared with paleomagnetic data

The occurrence of recent rotation of the eastern arc segment and the revised timing and rate of rotation of the western segment form new constraints on the mechanism of Aegean deformation. It would appear that at around 0.8 Ma an important change occurred in the distribution of forces acting on the region. The prevalence of arc-parallel extension in the southern Hellenic arc has been attributed to an increase in resistance at the central segment of the subduction zone, due, perhaps, to incipient collision with Africa (Lyon-Caen et al., 1988; Armijo et al., 1992; Le Pichon et al., 1995). From a geometrical point of view one can imagine such a blocking of southward motion to be associated with clockwise rotation of the western arc and anticlockwise rotation of the eastern arc segment (Fig. 5.5a). However, the arc-parallel extension is estimated to have started significantly earlier then 0.8 Ma. Its initiation is dated at about 2-4 Ma by Armijo et al. (1992) and between 3-6 Ma by Le Pichon et al. (1995). Perhaps, an essential role is played by the forces associated with the Arabia-Eurasia collision, transmitted to the Aegean through the westward motion of Anatolia. Armijo et al. (1996) argue that the onset of rapid extension across the Gulf of Corinth reflects the westward propagation of the North Anatolian fault system (Fig. 5.5b). Although the geometry of extension causes the Peloponessos to rotate clockwise relative to the area north of the Gulf (Armijo et al., 1996) it remains to be studied whether the changed configuration could fully explain our new observations. Temporal changes in the North Anatolian fault system have also been suggested to explain the Pleistocene change in the pattern of extension (Cianetti et al., 1997).

A third possibility is that the changes in deformation around 0.8 Ma reflect a change in the nature of the plate boundary of northwestern Greece (Fig. 5.5c). At present, subduction of African lithosphere below the southwestward moving Aegean overriding margin terminates in the region of the Ionian islands. West of Epirus the two plates are in collision and convergence is largely blocked (Fig 5.4). Geodesy indicates the transition to be localised in a narrow zone of which the Kefallonia fault (which runs just west of Kefallonia and Lefkas) is the most important discontinuity (Fig. 5.5). Geometrically, we expect the transition from subduction to collision to be associated with clockwise rotation of the region to the south (Fig. 5.5). This is confirmed by the rotation pattern computed from geodesy and by the results of numerical modelling (e.g. the modelled displacement field of Fig. 7b in Meijer and Wortel, 1997). If, prior to about 0.8 Ma, the margin west of Epirus was not yet blocked, the northwestern and western Aegean region may well have been deforming much more uniformly.
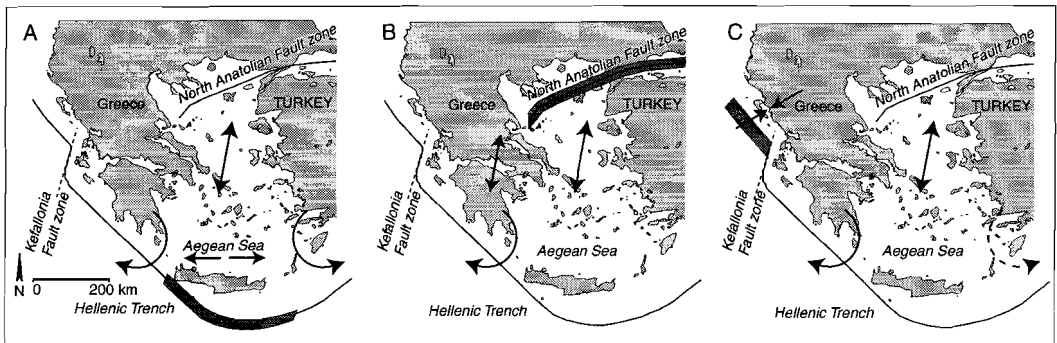
Fig. 5.5 Various models for the Aegean, for details see text. A represents a model based on increase in resistance at the central segment of the subduction zone (Lyon-Caen et al., 1988; Armijo et al., 1992; Le Pichon et al., 1995). B indicates a model involving a change of activity of the North Anatolian fault (Armijo et al., 1996) and C shows the lateral migration of slab detachment model of Wortel and Spakman (1992).

Numerical modelling has shown that a change in the nature of the margin of northwestern Greece as sketched in the above could also account for the Pleistocene change in the pattern of extension (Meijer and Wortel, 1996). The change of the northwestern margin to a collisional state was proposed by Meijer and Wortel (1996) to result from the southeastward propagation of a horizontal tear in the subducted African lithosphere, present below the margin. That such slab detachment took place is suggested by tomographic images of the Aegean upper mantle (Wortel and Spakman, 1992; Spakman et al., 1993). Thus, we may now speculate that also the rapid Pleistocene rotation of the western arc is caused by lateral migration of slab detachment. Although the hypothesis remains to be tested further it is interesting to note that detachment would also offer an explanation for the Pleistocene uplift of the Hellenic arc. When detachment

occurs, the weight of the detached slab is no longer felt by the overlying portion of downgoing lithosphere. Instead, this weight is transferred to places where the slab is still continuous. Immediately above the detachment, therefore, rebound and surface uplift are expected to occur (Van der Meulen et al., 1998). Moreover, increased slab pull at the segment of the subduction zone, where the downgoing part is still continuous, might cause increased roll back. Detachment would thereby affect the Hellenic arc along its full width and could also induce (anticlockwise) rotations on the eastern arc segment.

Conclusions

Our paleomagnetic data show that the western Aegean arc underwent a clockwise rotation phase, whereas the eastern arc experienced anticlockwise rotations. Furthermore, the results indicate that the clockwise rotation phase in the western arc took place between ~0.8 Ma and Recent on Zakynthos and in the central and eastern Peloponessos. The anticlockwise rotation phase in the south-eastern arc may be equally young (Pleistocene), although the sediments could not be accurately dated. The current pattern of rotations appears to match the interpreted geodetic data. The geodetic results also indicate mainly clockwise rotations in the western Aegean arc and anticlockwise rotations in the eastern Aegean arc. Because we find no evidence for tectonic rotations, since the opening of the Aegean basin, prior to the Pleistocene, we must conclude that the formation of the Aegean arc is caused by translations rather than by rotations.

Our AMS data indicate arc-parallel extension in the south and south-eastern Aegean arc and NE-SW compression in the north-west, which again is in agreement with geodetic data. At the time of our rotation phase the Aegean area was subjected to major uplift and to a major change in overall stress regime.

Acknowledgements

Appendix 5.1

Locality	Code	N	$D_{notc}(°)$	$I_{notc}(°)$	k	$a_{95}(°)$	Type	$D_{tc}(°)$	$I_{tc}(°)$	k	$a_{95}(°)$	polarity	rot		age(Ma)
Lefkas															
Komilio	KOM	4	-	-	-	-	3	-	-	-	-	N	-		Mid-Upper Pliocene
Alatron	ALA	6	-	-	-	-	3	-	-	-	-	N	-		Burdigalian-Langhian
Kolivata	KOL	4	-	-	-	-	3	-	-	-	-	N	-		Langhian
Kefallonia															
LUXmean[a]		70	159.0	-49.1	40.1	2.7	1	176.6	-51.2	45.1	2.6	N/R	3	ac	~1.9-1.0 Ma
Luxurion	LUX	14	346.4	57.7	52.2	5.6	1	9.2	53.9	88.6	4.2	N	9	c	Plio/Pleistocene
Luxurion	LUX	56	157.5	-46.9	44.8	2.9	1	173.7	-50.4	45.4	2.9	R	6	ac	Plio/Pleistocene
Spartia	SPA	28	129.8	-41.3	11.3	13.5	2	161.7	-44.0	26.0	5.5	R	-		Plio/Pleistocene
Liakas	LIA	12	153.9	-45.6	26.0	5.5	2	168.3	-38.2	17.0	10.8	N/R	-		Messinian
Zakynthos															
mean		8	-	-	-	-	1	21.6	48.8	128.0	4.9	N/R	22	c	8.11-0.77
Peloponessos															
mean		4	-	-	-	-	1	16.1	55.2	325.6	5.1	N/R	16	c	Plio
Pyrgos Basin:[b]															
Aghios Andreas	AA	5	25.2	51.7	35.8	13.0	2	14.0	55.5	36.4	12.8	N	-		Plio/Pleistocene
Killini*	KIL	11	183.50	-70.9	58.1	6.0	1	205.4	-57.0	53.7	6.3	N/R/N	25	c	Plio/Pleistocene
Pineos	PIN	7	356.1	57.2	43.0	9.3	2	357.4	65.2	43.0	9.3	N	-		Pleist
Erymanthos	ERI	6	194.4	-54.9	97.4	6.8	2	195.8	-43.3	96.4	6.9	R/N	-		Pliocene
Neraida	NER	5	211.9	-46.6	37.9	12.6	2	207.6	-48.6	37.9	12.6	R	-		Pliocene
Krionero*	KRI	14	14.8	55.2	87.0	4.3	1	10.7	53.5	87.0	4.3	N	11	c	Pliocene
Vounargon	VOU	5	201.9	-55.1	59.3	10.0	2	194.0	-50.5	54.7	10.4	R	-		Pliocene
Alfioussa	ALF	6	185.0	-27.0	14.2	18.4	2	184.7	-44.2	14.3	18.3	R	-		Pliocene
Lalas	LAL	6	2.6	48.7	147.2	5.5	2	358.7	51.4	197.1	4.8	N	-		Pliocene
Kalithea	KAL	4	161.8	-62.6	476.0	4.2	2	186.6	-52.4	475.9	4.2	R	-		Pliocene
Grillos	GRI	3	346.5	40.4	345.7	6.6	2	357.7	41.1	345.7	6.6	N	-		Upper Pliocene
Chrysophylli*	CHR	15	21.9	40.2	64.2	4.8	1	12.1	57.4	42.4	5.9	N	12	c	Pliocene

Locality	Code	N	D_{notc}(°)	I_{notc}(°)	k	a_{95}(°)	Type	D_{tc}(°)	I_{tc}(°)	k	a_{95}(°)	polarity	rot		age(Ma)
Peloponessos															
South:															
Kefalas*	KEF	11	13.0	52.3	89.1	4.9	1	16.5	52.4	154.0	3.7	N	17	c	Upper Pliocene
Gythion	GIT	2	7.7	41.6	0.0	99.9	2	8.0	48.6	-	-	N	-		Upper Pliocene
Glikovrisi	GVR	2	186.2	-48.0	0.0	99.9	2	180.0	-50.8	-	-	R	-		Upper Pliocene
East:															
Megara	MEG	12	3.1	48.9	20.5	9.8	1	2.7	46.7	35.5	7.4	/R/N/R/	3	c	Plio/Pleisto
Corinth	COR	5	177.4	-57.9	26.3	15.2	2	177.4	-57.9	26.3	15.2	R/N	-		Pleist
Centre:															
Megalopolis	ME	71	2.6	53.8	58.1	2.2	1	1.2	52.6	52.0	2.4	R/N	1	c	0.9-0.25
Milos															
mean		2	-	-	-	-	1	184.5	-51.8	-	-		5	c	
Basalt	MYL 1	7	171.6	-24.2	43.4	9.3	2	171.6	-24.2	43.4	9.3	R	-		Pliocene
Myl10	MYL 10	5	12.5	46.3	73.6	9.0	2	11.2	51.2	73.6	9.0	N	-		Plio/Pleistocene
Myl11	MYL 11	5	357.7	52.0	359.1	4.0	2	354.4	56.4	359.1	4.0	N	-		Plio/Pleistocene
Myl15*	MYL 15	7	347.2	54.3	66.8	7.4	1	348.9	57.1	66.8	7.4	N	11	ac	Plio/Pleistocene
Hot*	HOT	11	185.3	-48.9	114.7	4.3	1	192.0	-35.8	114.7	4.3	N/R/N/R	12	c	early Pliocene
Kythira															
Avlemonas	AV	8	345.9	56.6	39.2	9.0	2	341.1	63.7	43.5	8.5	N	-		Middle Pliocene
Kapsali	KAP	12	13.1	49.8	29.2	8.2	1	351.9	39.4	29.7	8.1	N	8	ac	Miocene
Manitochori	MAN	6	355.2	49.2	20.2	15.3	2	353.4	47.1	16.8	16.8	N	-		Miocene
Crete															
Fortetsa[c]	FOR	7	1.1	41.4	76.4	6.9	3	1.1	41.4	76.4	6.9	N	-		Pliocene
Vasileis	VAS	7	356.4	54.9	161.1	4.8	3	354.4	46.5	161.1	4.8	N	-		Pliocene
Prassas	PRA	8	358.5	51.2	87.6	6.0	3 [#]	3.0	45.7	153.8	4.5	N	-		Mio/Pliocene
Gallini	GAL	2	143.9	-80.4	0.0	99.9	2	162.7	-68.6	-	-	R	-		Pleistocene
Koutres	KOU	7	1.7	56.5	801.4	2.1	3 [#]	357.9	51.9	60.2	7.8	N	-		Pliocene
Moria	MOR	8	356.6	46.2	27.9	10.7	3 [#]	10.9	61.5	34.4	9.6	N/R	-		Plio/Pleistocene

Appendix 5.1

Locality	Code	N	D_{notc}(°)	I_{notc}(°)	k	a_{95}(°)	Type	D_{tc}(°)	I_{tc}(°)	k	a_{95}(°)	polarity	rot		age(Ma)
Crete															
Galipe	LIP	2	180.6	-52.4	0.0	99.9	2[#]	186.0	-57.8	-	-	R	-		Pliocene
Aghios Vlassios[d]	VLA	4	354.5	52.3	134.6	7.9	3	345.1	45.0	134.6	7.9	N/R	-		Pliocene
Moni Agarathou	AGA	6	356.1	36.2	345.1	3.6	3	358.4	38.9	345.2	3.6	N	-		Pliocene
Chorio	CHO	7	355.4	56.2	212.7	4.1	3[#]	2.9	55.2	212.7	4.1	N	-		Pliocene
Aghios Miron	MIR	5	356.0	42.9	418.2	3.7	3	344.7	40.2	418.2	3.7	N	-		Messinian
Chersonissos	HER	8	340.0	40.5	68.0	6.8	1	334.3	31.8	68.0	6.8	N	26	ac	Miocene
Kassos															
Aghios Mamas	MAM	7	-	-	-	-	3	-	-	-	-	R/?	-		Miocene
Chelatron 1	CHE 1	5	3.2	44.9	167.0	5.9	3	13.2	40.0	167.0	5.9	N	-		Miocene
Chelatron 2	CHE 2	5	336.7	47.3	99.5	7.7	2	337.3	48.1	99.5	7.7	N	23	ac	Miocene
Chelatron 3	CHE 3	5	2.5	51.8	582.7	5.1	3	350.2	46.2	582.7	5.1	N/R	-		Miocene
Karpathos															
Lefkos	LEF	17	354.9	55.2	102.9	3.5	3	356.2	60.9	83.7	3.9	N	-		Plio/Pleistocene
Amoopi[e]	AM	5	354.5	49.9	524.3	3.3	3	339.6	43.9	524.3	3.3	N	-		Pliocene
Aghios Ioannis	IO	9	166.1	-52.8	49.9	7.4	1	162.0	-55.9	48.4	7.5	R	18	ac	Pliocene
Pigadia[f]	PI	7	8.5	57.6	182.6	4.5	3	340.1	69.4	182.6	4.5	N	-		Pliocene
Rhodos															
mean		8	-	-	-	-	1	162.5	-46.8	45.3	8.3		18	ac	
Ancient Kameiros*	AK	19	356.9	19.7	9.5	11.5	1	352.8	45.8	9.4	11.6	N	7	ac	Pliocene
ASH*	ASH	12	115.1	-83.9	11.8	13.2	1	152.0	-36.8	8.8	15.5	R	28	ac	Oligocene?
Falliraki*	FA	8	340.2	49.4	70.0	6.7	1	348.7	48.6	70.0	6.7	N	11	ac	Upper Pliocene
Falliraki Beach*	FB	11	326.9	60.4	37.7	7.5	1	337.7	63.0	56.8	6.1	N	22	ac	Upper Pliocene
Kallithea	KA	4	149.9	-32.3	36.7	15.4	2	157.1	-36.9	36.7	15.4	R	-		Upper Pliocene
Kolimbia*[g]	KO	17	163.8	-42.2	18.2	8.6	1	165.8	-42.2	18.2	8.6	R	14	ac	Uppermost Pliocene
Ladiko*[h]	LA	9	332.2	30.2	44.8	7.8	1	335.1	29.6	44.8	7.8	N	25	ac	Pliocene
Pefki Beach*[i]	PB	12	184.9	-45.5	42.7	6.7	1	173.0	-49.8	42.6	6.7	R/N	7	ac	Upper Pliocene/Pleistocene
Pylonas[j]	PY	6	163.5	-37.5	21.4	14.8	2	160.2	-42.3	21.4	14.8	R/N	-		Uppermost Pliocene

Appendix 5.1

Locality	Code	N	$D_{notc}(°)$	$I_{notc}(°)$	k	$a_{95}(°)$	Type	$D_{tc}(°)$	$I_{tc}(°)$	k	$a_{95}(°)$	polarity	rot		age(Ma)
Rhodos															
Skaloniti	SK	5	176.8	-30.5	324.2	4.3	2	168.9	-51.0	324.2	4.3	R	-		Pliocene
Tsambika	TS	5	167.9	-41.1	11.7	23.4	2	168.7	-42.4	11.7	23.4	N/R	-		Pliocene
Vagies	VA	4	348.0	38.4	26.1	18.3	2	351.2	18.8	26.1	18.3	N	-		Upper Pliocene
Appolakkia*	AGI	17	35.7	58.1	35.3	6.1	1	335.8	56.1	35.3	6.1	N	24	ac	Pliocene

Appendix 5.1   Results from NRM analysis from the different sections/sites (Codes see Fig. 5.1) along the Aegean outer-arc.
Uncorrected (no tc) and corrected (tc) for bedding tilt, ages are indicated. N = number of specimens; D, I =
site mean ChRM declination and inclination; k = Fishers's precision parameter; $α_{95}$ = 95% cone of confidence.
Type 1 indicates reliable results, type 2 gives an indication of the sense of rotation, and type 3 is ureliable
(see also text for explanation; # = 3 or no rot). N (R) respresents normal (reversed) polarity, rot indicates amount
of tectonic rotation with a(c) indicating (anti)clockwise. For details on ChRM data from Zakynthos, we refer to
Duermeijer et al., 1999a. * marks the data-points used to calculate the mean of a certain area.
Biostratigraphy(ages after Rio et al., 1990, Langereis et al., 1997 and Lourens et al., 1996; 1998):
a= presence of lage Gephyrocapsa spp., H. balthica and H. selli, absence of C. Macintyrei
    and Gephyrocapsa sp.3= NN19d (Triantaphyllou 1996), 1.22-1.373 Ma
b= relative ages after Hageman (1979)
c= G. bononiensis (Jonkers, 1984)= 2.41-3.31 Ma
d= G. margaritae and D. assymetricus (Jonkers, 1984)= 3.81-4.12 Ma
e= H. selli and small Gephyrocapsa, no oceanica = until 1.71 Ma
f= P. lacunosa, R. pseudoumbulica, D. tamalis, H. selli, D. aymetricus, small Gephyrocapsa,
    D. Brouweri, no oceanica (this study)= 4.91-0.44 Ma
g= P. lacunosa (this study)= until 0.44 Ma
h= G. ruber and G. inflata (Broekman, 1974)= from 2.09 Ma
i= Gephyrocapsa oceanica, small Gephyrocapsa, P. lacunosa (this study) = until 0.44 Ma
j= Gephyrocapsa oceanica, small Gephyrocapsa, P. lacunosa, 12m Macintyrei (this study)= until 1.67 Ma
other ages are derived from Geological map of Greece

Appendix 5.2   Results from AMS analysis from the different sections/sites along the Aegean outer-arc; corrected for bedding tilt,
ages are indicated. N = number of specimens; D,I, = mean azimuth and dip of k_{max} axes; dD,dI = errors on mean k_{max}
L = magnetic lineation (k_{max}/k_{int}). For location of AMS data from Zakynthos, we refer to Duermeijer et al., 1999a. * marks
not enough data to perform a Hotelling T (anisotropy) test (Jelinek, 1977). Note that the means are unweighted due to program set-up.

Appendix 5.2

Locality	N	D(°)	I(°)	δD(°)	δI(°)	L	age(Ma)
Lefkas							
Komilio		-	-	-	-	-	Mid-Upper Pliocene
Alatron		-	-	-	-	-	Burdigalian-Langhian
Kolivata		-	-	-	-	-	Langhian
Kefallonia							
mean	149	149.3	0.6	5.7	1.3	1.0063	~1.9-1.0 Ma
Luxurion	95	158.9	1.3	4.7	1.4	1.0077	Plio/Pleistocene
Spartia	31	309.4	2.1	4.0	1.3	1.0062	Plio/Pleistocene
Liakas	23	125.7	2.4	14.5	4	1.0065	Messinian
Zakynthos							
mean	196	146.0	0.5	4.2	1.3	1.0082	
Porto Roma	25	173.1	2.3	4.8	3.2	1.0070	1.03-0.77
Bochali	18	195.9	1.9	6.6	2.1	1.0048	1.37-1.24
Zakynthos Town	40	24.8	1.6	7.0	2.1	1.0083	1.94-1.44
Gerakas	16	243.8	45.5	15.6	5.7	1.0033	1.94-1.61
Alikanes	18	164.1	3.7	15.8	2.6	1.0026	3.31-2.73
Kalamaki Beach	36	156.3	9.9	5.5	3.2	1.0064	5.95-5.21
Aghios Sostis	8	168.5	0.2	14.3	4.1	1.0071	Messinian
Limnou Keriou (N)	57	330.5	3.9	3.4	1.8	1.0103	7.24-6.60
Linmou Keriou (S)	4	160.5	6.0	20.7	7.5	1.0068	Tortonian
Ormos Alikon	33	300.4	3.0	3.8	1.4	1.0138	7.64-7.24
Vugiato	14	153.8	4.6	6.6	3.7	1.0160	8.11-7.70
Marathia	8	319.5	10.2	21.8	4.5	1.0124	Serravalian
Lagopodo	16	307.9	2.8	40.3	6.2	1.0023	early middle Miocene
Peloponessos							
Aghios Andreas	13	345.4	3.1	56.0	4.7	1.0010	Plio/Pleistocene
Killini	63	312.0	3.1	38.4	2.7	1.0006	Plio/Pleistocene
Pineos	24	316.1	6.3	48.6	5.9	1.0007	Pleistocene
Erymanthos	19	181.8	2.8	64.9	4.7	1.0004	Pliocene
Neraida	21	347.0	5.7	13.7	3.4	1.0017	Pliocene
Krionero	22	287.8	6.2	22.8	4.7	1.0009	Pliocene
Vounargon	9	304.6	4.2	14.7	3.6	1.0043	Pliocene
Lalas	10	344.9	7.5	26.9	15.7	1.0022	Pliocene
Kalithea	7	178.1	15.9	22.7	10.4	1.0066	Pliocene
Grillos	7	91.9	3.2	15.0	8.3	1.0021	Upper Pliocene
Chrysophylli	15	1.9	4.8	7.0	2.7	1.0060	Pliocene
Kefalas	17	53.9	0.7	18.0	2.3	1.0015	Upper Pliocene
Gythion	27	280.8	4.1	34.6	5.5	1.0018	Upper Pliocene
Glikovrisi	17	239.6	0.2	17.8	4.0	1.0015	Upper Pliocene
Megara	21	359.9	1.2	9.8	7.2	1.0052	Plio/Pleistocene
Corinth	11	34.0	7.5	24.5	8.1	1.0014	Pleistocene
Milos							
Basalt	7	293.1	4.4	21.9	5.8	1.0417	Pliocene
Myl10*	5	89.7	5.0	18.6	4.3	1.0053	Plio/Pleistocene
Myl11*	5	333.2	0.0	28.9	5.0	1.0073	Plio/Pleistocene
Myl15	7	139.1	22.4	30.8	9.9	1.0047	Plio/Pleistocene
Hot	98	240.5	15.0	40.2	12.1	1.0004	early Pliocene

Appendix 5.2

Locality	N	D(°)	I(°)	dD(°)	dI(°)	L	age(Ma)
Kythira							
mean	38	100.7	5.7	14.4	4	1.0033	
Avlemonas	12	347.9	38.3	31.2	17.4	1.0067	Middle Pliocene
Kapsali	26	89.4	1.7	7	2.2	1.0030	Miocene
Manitochori	13	114.7	6.9	29.9	6.3	1.0034	Miocene
Crete							
mean	93	303.2	0.9	14.3	2.9	1.0010	
Fortetsa	7	180.7	3.6	41.1	5.3	1.0015	Pliocene
Vasileis	7	127.8	3.6	35.4	5.5	1.0028	Pliocene
Prassas	6	24.7	3.2	26.1	14.6	1.0026	Mio/Pliocene
Chersonissos	8	326	0	24.3	4.7	1.0025	Miocene
Gallini	8	310.8	9.6	32.4	8	1.0018	Pleistocene
Koutres*	5	303.8	15.9	38.6	16.9	1.0008	Pliocene
Moira	12	273.5	16.1	38.6	7.3	1.0015	Plio/Pleistocene
Galipe	7	24.7	9.5	17.6	2.9	1.0014	Pliocene
Aghios Vlassios	7	106.8	12.4	9	3.9	1.0037	Pliocene
Moni Agarathou	7	275	4.2	18	3.9	1.0029	Pliocene
Aghios Miron	7	119.9	6	6.8	2.3	1.0039	Messinian
Chorio	8	60.9	4.1	10.5	5	1.0021	Pliocene
Kassos							
Chelatron all	16	102.4	1.7	30.9	2.6	1.0010	
Chelatron 1*	5	141.4	12.1	32.2	8.1	1.0009	Miocene
Chelatron 2*	5	237	1.8	29.6	7	1.0017	Miocene
Chelatron 3*	6	295.4	0.6	29.3	4.6	1.0023	Miocene
Aghios Mamas	8	267.8	44.6	17.8	8.7	1.2387	Miocene
Karpathos							
mean	73	64.4	0.9	14.3	1.9	1.0012	
Lefkos	21	73.9	9.1	24.7	3.9	1.0010	Plio/Pleistocene
Amoopi	7	63.5	9.1	60.2	6.2	1.0007	Pliocene
Aghios Ioannis	28	240.1	1.3	21.6	1.9	1.0018	Pliocene
Pigadia	7	159.1	1.3	46.8	8.3	1.0006	Pliocene
Rhodos							
mean	137	67.5	1.1	14.3	1.6	1.0019	
Ancient Kameiros	8	293.5	7.4	15.2	4.1	1.0026	Pliocene
ASH	21	69.6	1.6	17	3.6	1.0081	Oligocene?
Falliraki	8	293.9	1.4	83.1	4.2	1.0003	Upper Pliocene
Falliraki Beach*	5	267.7	0.3	51.2	9.3	1.0030	Upper Pliocene
Kallithea	6	294.4	1.9	58.6	15.5	1.0037	Upper Pliocene
Kolimbia	14	30.1	0	48.3	4.4	1.0018	Uppermost Pliocene
Ladiko	9	53.7	1.3	34.3	4.5	1.0031	Pliocene
Pefki Beach	13	92	12.5	19.1	2.8	1.0027	Upper Plio/Pleistocene
Pylonas	9	302.9	3	40.1	6.9	1.0014	Uppermost Pliocene
Skaloniti	7	88.7	15.9	60.5	11.7	1.0010	Pliocene
Tsambika	8	118.1	1.1	46.7	4	1.0013	Pliocene
Vagies*	4	41.8	2.7	48.9	9.3	1.0056	Upper Pliocene
Appolakkia	25	232.4	3.2	17.6	4	1.0022	Pliocene

6

The late Neogene to Recent geodynamic evolution of the central Mediterranean and the role of the African promontory: a paleomagnetic approach

Abstract

We present an up-to-date paleomagnetic overview of the central Mediterranean, with special emphasis on the Neogene. It appears that the Italian peninsula, west of the Apulian platform, underwent mostly anticlockwise rotations, whereas in the east the Dinarides/Albanides/western Hellenides experienced mostly clockwise rotations. In Italy, the area of no rotations is expanding through time from the north-east to the south-west. Furthermore, the paleomagnetic results from both Italy and the Hellenides indicate pulsed events instead of continuous rotations. Therefore, the current curvature of the Tyrrhenian and Aegean arc must have been formed by translations rather than by a continuous rotation process. We speculate that the tectonic rotations are related to lateral migration of slab detachment, which consequently also must have occurred in a pulsed manner. Finally, because we observe similar and time-equivalent features on both sides of the Apulian platform, we suggest a geodynamic link in the Pleistocene between southern Italy and north-western Greece.

Introduction

Geological and geophysical studies have shown that the Mediterranean region represents a complex puzzle of microcontinental and ophiolitic terranes, resulting from movements caused by closure between the African and Eurasian margins of the Tethyan Ocean. Paleomagnetic research has significantly contributed to the geodynamic evolution of the Mediterranean and has shown that many of these terranes underwent tectonic rotations and translations with respect to the major continents.
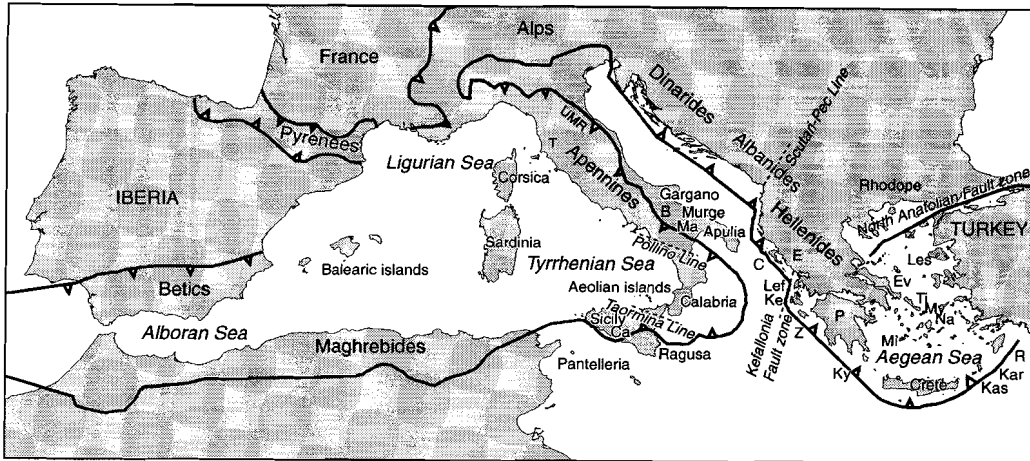

Fig. 6.1 Geographical locations of places in the Mediterranean mentioned in the text; UMR, Umbria-Marche-Romagna; T, Tuscany; B, Bradano; Ma, Matera; Ca, Caltanisetta basin; C, Corfu; E, Epirus, Lef, Lefkas; Ke, Kefallonia; Za, Zakynthos; P, Peloponessos; Les, Lesbos; Ev, Evvia; Ti, Tinos; My, Mykonos; Na, Naxos; Mi, Milos; Kas, Kassos; Kar, Karpathos and R, Rhodos. Solid lines with small open triangles roughly denote the outline of major thrusting.

After the opening of the northern Atlantic, Iberia containing present-day Spain and Portugal rotated anticlockwise between 120-80 Ma and subsequently collided with and/or slided along stable Europe, resulting in the formation of the Pyrenees (Van der Voo, 1993 and references therein). We consider this period as the initiation of the Mediterranean basin configuration (Fig. 6.1). At that time in the western Mediterranean, the Balearic islands and the Corsica-Sardinia microplate (with Calabria attached) were close to the coast of France and Spain. In early Miocene times, between 21 and 15 Ma, the Ligurian Sea opened and the Corsica-Sardinia microplate moved away from the French coast (Van der Voo, 1993 and references therein). At the same time, Africa with its promontory called the Apulian platform, was moving in a northeasternly direction, colliding with stable Europe at its northern edge resulting in the formation of the Alps (Van der Voo, 1993 and references therein). As the Corsica-Sardinia microplate moved eastward, it collided with the Apulian platform to form the Apennines. Subsequently, in late Miocene times (between 8.6-7.8 Ma; Duermeijer et al., 1998a) the Tyrrhenian basin opened, accompanied

by the movement of Calabria to the southeast, to its present-day location. On the eastern side of the Apulian platform, the Dinarides, Albanides and Hellenides are formed by amalgamating many different micro-continental blocks, again resulting from the Africa-Eurasia collision. Detailed sedimentological and structural studies led to a subdivision of the Dinarides, Albanides and Hellenides into elongated NW-SE trending isopic zones (Aubouin, 1959). The present-day Hellenic arc developed mainly during the Neogene, as the result of translations rather than through continuous rotations (Duermeijer et al., 1999a, b).

The central Mediterranean was shaped by various processes which have involved large tectonic rotations. In this paper, we focus on the Neogene paleomagnetic data from the central Mediterranean, on the east and west side of the Apulian platform. We first give a paleomagnetic overview. We discuss the observed tectonic rotations in terms of slab detachment and suggest a link in the Pleistocene between rotations and related features on both sides of the Apulian platform.

Paleomagnetic overview

We present an overview of paleomagnetic data published from 1992 onwards, as previous data was already compiled by Van der Voo (1993); using his selection criteria for the recently published paleomagnetic data. We concentrate on the Neogene development of the central Mediterranean and made a division in Pre-Miocene, Miocene, Pliocene and Pleistocene (absolute rotation) results (Appendix 6.1 and Fig. 6.1, 6.2). Previously unpublished results from southern Italy, referred to as this study, are also included.

Pre-Miocene

Many paleomagnetic results are available from pre-Miocene times (Fig. 6.2a). On the western side of the Apulian platform, the islands of Corsica and Sardinia indicate large (up to 47°) anticlockwise rotations since Permian times (Vigliotti et al., 1990; Van der Voo, 1993). The Oligocene/Miocene sediments from the Epiligurian units in the northern Apennines show large anticlockwise (47/51°) rotations (Muttoni et al., 1998; 1999). Likewise, in the central Apennines (Mattei et al., 1995) and in Murge, on the Apulian platform (Marton and Nardi, 1994), predominantly anticlockwise rotations are found.
On the eastern side of the Apulian platform, the northern/central Dinarides hardly indicate a rotation since the Eocene (Kissel et al., 1995). However, south of the Scutari-Pec line, clockwise rotations up to 49° since the Eocene/Oligocene are found in the Albanides and NW-Greece (Kissel et al., 1995; Mauritsch et al., 1995; Speranza et al., 1992; 1995; Peeters et al., 1998) and up to 22° in NE-Greece (Haubold et al., 1997). The Scutari-Pec line acted as a decoupling zone between the Dinarides and Albanides/Hellenides (Kissel et al., 1995). Thus, for the pre-Miocene period, the western central Mediterranean rotated anticlockwise, whereas the eastern central Mediterranean rotated clockwise.
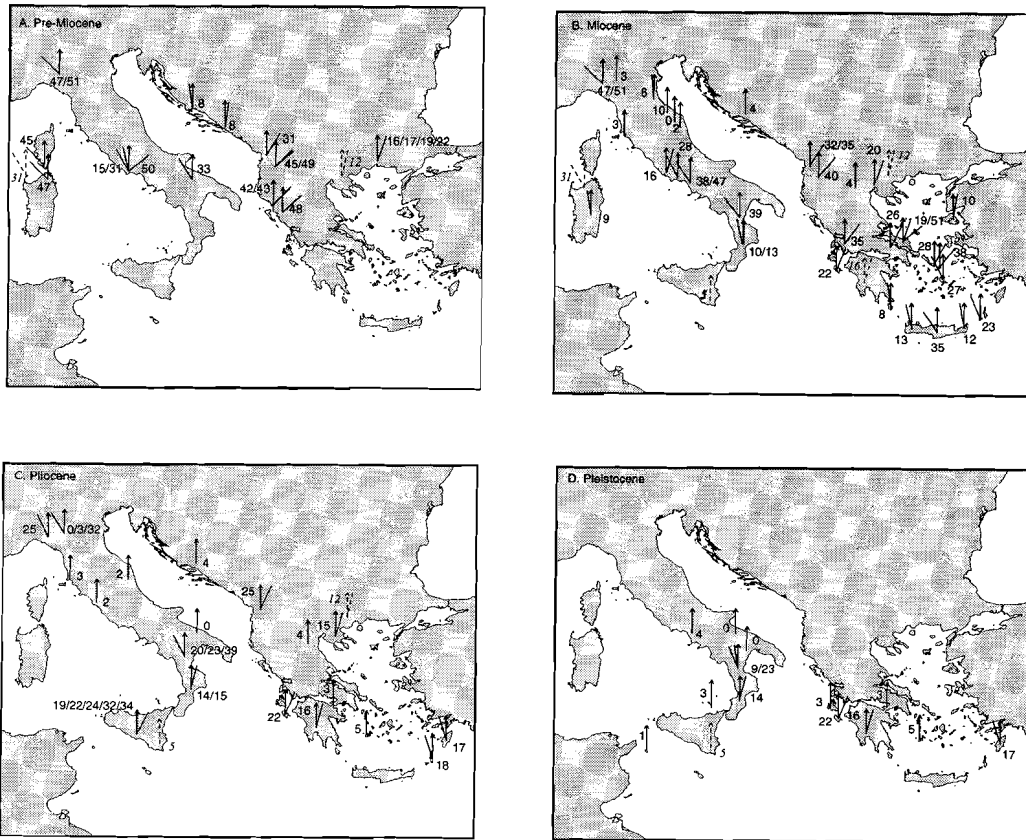
Fig. 6.2 Overview of paleomagnetic data from the central Mediterranean. The data denotes Pre-Miocene (a), Miocene (b), Pliocene (c) and Pleistocene (d). Arrow indicates present-day north, solid line represents the observed (anticlockwise or clockwise) tectonic rotations published since 1992 by various authors (see Appendix 6.1). Dashed lines (with italic numbers) are mean tectonic rotations per area, calculated from Van der Voo (1993).

Miocene

Sediments from Miocene age were abundantly sampled around the Apulian platform (Fig. 6.2b). The western part (Italy) shows a highly complex mixture of mostly anticlockwise rotations since the Miocene. The 47°/51° anticlockwise rotation of the Epiligurian units since the Middle Miocene was proposed by Muttoni et al. (1998) to have been caused by the movement of the Corsica/Sardinia block, where the anticlockwise rotation ended around anomaly 5A or 6 (Vigliotti and Langenheim, 1995). More, recently, however Muttoni et al. (1999) suggest that roughly half of this anticlockwise motion of the Epiligurian units in the northern Apennines is caused by the Oligocene-Miocene Corsica-Sardinia motion, the other half is of post-Miocene age. Some Messinian sediments from

the Stirone area (northern Apennines) show almost no rotation (Chanell et al., 1994). More to the south-east, small mainly anticlockwise tectonic rotations derived from the Umbria-Marche-Romagna arc are suggested to be a result of oroclinal bending (Dela Pierre et al., 1992; Speranza et al., 1997) as derived from tomography, or caused by the presence of an obstacle located in the Adriatic foreland against which the arc collided (Argnani and Frugoni, 1997). In the internal part of the arc, the Tuscan Tyrrhenian margin, containing normal fault basins, shows no significant regional rotations or compression since at least the late Messinian-early Pliocene (Sagnotti et al., 1994; Mattei et al., 1996). In the central Apennines, the results show both anti- and clockwise rotations which are related to thrust tectonics (Mattei et al., 1995; Iorio et al., 1996; Speranza et al., 1998). Large anticlockwise rotations are detected in Miocene sediments from the southern Apennines (Scheepers and Langereis, 1994b) and from northern Calabria (Duermeijer et al., 1998a). The northern Calabrian anticlockwise rotation phase took place between 8.6-7.6 Ma and coincides with the beginning of the opening of the Tyrrhenian basin. The Ragusa platform on Sicily, believed to be part of the African promontory, shows little evidence of rotations (Van der Voo, 1993).

On the eastern side of the Apulian platform, little or no rotation is found in the Dinarides (Kissel et al., 1995) but in Albania and Greece clockwise rotations are detected in the Miocene sediments, decreasing from ~40° in the north to ~16° in the south (Birch, 1990; Westphal et al., 1991; Van der Voo, 1993; Kondopoulou, 1994; Speranza et al., 1995; Morris, 1995; Mauritsch et al., 1995; Morris and Anderson, 1996; Avigad et al., 1998; Duermeijer et al., 1999a, b). Halfway the Aegean Sea, the sense of rotation turns to anticlockwise on Crete, Kassos and Naxos (Morris and Anderson, 1996; Duermeijer et al., 1998b; 1999b). On the basis of these paleomagnetic data, magnetic fabrics and structural lineation directions, Morris and Anderson (1996) suggest a major structural lineament dividing the central Aegean which is confirmed by low seismic reflection experiments (Mascle and Martin, 1990).

Pliocene

The sense of rotation is still approximately the same as the Miocene results (Fig. 6.2c). However, the area of virtually no rotation has expanded southwards in Italy, while also the magnitude of clockwise rotation in the Albanides is reduced (Speranza et al., 1995).

The remaining (~25° anticlockwise) rotation from the Epiligurian units took place after the Messinian (Muttoni et al., 1999). In the northern Apennines, the paleomagnetic data from the Salsomaggiore unit at the Apennine front reveals contradictory results, including both no and large anticlockwise rotations (Mary et al., 1993; Channell et al., 1994) possibly caused by a local, very complicated tectonic structure, referred to in the literature as the Salsomaggiore unit. In central Italy and in Apulia/Gargano, rotations have become negligible (Dela Pierre et al., 1992; Scheepers, 1992; Sagnotti et al., 1994; Mattei et al., 1996). In contrast, the southern Apennines experienced large anticlockwise rotations since the Pliocene (Sagnotti, 1992; Scheepers et al., 1993; Scheepers and Langereis, 1994b; this study).

Data from the southern Apennines indicates a Late Pliocene anticlockwise (from 39° to 23°) rotation phase (Scheepers and Langereis, 1994b), while Pliocene sediments show clockwise rotations in Calabria (Scheepers et al., 1994; this study). On Sicily, a clockwise rotation phase at 3.22 Ma was detected (Scheepers and Langereis, 1993; Duermeijer and Langereis, 1998). Since then (3.22 Ma), the Caltanisetta basin on Sicily must have experienced a significant (22°/24°) clockwise rotation. The Ragusa platform remains more or less stable (Van der Voo, 1993).

The Dinarides (Kissel et al., 1995) bear little evidence of rotations. Many sections and sites from the Albanides (Speranza et al., 1995), northern Greece (Van der Voo, 1993 and refs therein), Zakynthos (Duermeijer et al., 1999a) and the Peloponessos (Duermeijer et al., 1999b) however, show evidence for post-Pliocene clockwise rotations. This seems to indicate that the Scutari-Pec line was active as a decoupling zone at least until the end of the Pliocene (Kissel et al., 1995). In Eocene to Pliocene sediments from the Rhodope area, in north-eastern Greece, a systematic increase in magnitude of clockwise rotation from east to west was visualised by Dimitriadis et al. (1998). One exception was found in northern Greece (Ptolemais), where the sediments hardly show evidence of rotations (Westphal et al., 1991). In the south-eastern Aegean, on the islands of Karpathos and Rhodos, post Pliocene anticlockwise rotations were found (Duermeijer et al., 1999b).

Pleistocene

Paleomagnetic data derived from Pleistocene sediments is relatively scarce (Fig. 6.2d). In northern and central Italy no data is reported. Likewise, in the Dinarides and Albanides no information from Pleistocene sediments is available. In the central Apennines, Bradano and Matera, believed to be part of the Apulian platform, no rotation was detected (Scheepers 1992; Scheepers et al., 1993; Speranza et al., 1998). A very small (9°) anticlockwise rotation was found in the southern Apennines, in sediments younger than 0.5 Ma, which implies a middle Pleistocene (from 23° to 9°) rotation phase (Scheepers and Langereis, 1994b). The lower Pleistocene (0.7-0.2 Ma) sediments from Calabria show a 14° clockwise rotation (Scheepers et al., 1994). The volcanics from the Aeolian islands and Pantelleria indicate no detectable rotation (Lanza and Zanella, 1991; Zanella, 1998) since 0.15-0.13 Ma.

In the Aegean area, the Pleistocene sediments from Zakynthos (Duermeijer et al., 1999a) and the Peloponessos (Van der Voo, 1993) indicate young clockwise rotations. In contrast, the Pleistocene sediments on Rhodos (Duermeijer et al., 1999b) indicate young anticlockwise rotations, implying that the structural lineament in the central Aegean was still active. The clockwise rotation in the western Aegean arc was shown to take place between 0.8 Ma and Recent, whereas the anticlockwise rotation in the eastern Aegean arc occurred roughly between 2 Ma and Recent (op.cit.).

Discussion

In general, the pre-Miocene to Pleistocene paleomagnetic data from the Mediterranean implies a different sense of rotation on either side of the Apulian platform. We find predominantly anticlockwise rotations in Italy and clockwise rotations in the Dinarides/Albanides/Hellenides.

In Italy, the pre-Miocene data indicate large anticlockwise rotations expanding over a large geographic area. The results from Miocene sediments show hardly any rotations in northern Italy and anticlockwise rotations in central and southern Italy. The Pliocene results only reveal anticlockwise rotations in southern Italy, while central and northern Italy hardly bear evidence for rotations. In the Pleistocene, a tectonic phase was only detected in southern Italy; in northern and central Italy no rotations are found. Thus, it appears that in Italy, the area of no-rotation is expanding through time from the northwest to southeast (Fig. 6.2 and 6.3). Furthermore, it appears that tectonic rotations in Italy occur in discrete and short time-intervals (<1 Myr). A late Miocene rotation event is detected in Calabria between 7.6-8.6 Ma (Duermeijer et al., 1998a) and a Pliocene rotation phase at 3.21 Ma in Sicily which lasted for 80-100 kyr (Duermeijer and Langereis, 1998). Furthermore, the paleomagnetic data reveal a Pleistocene rotation event (around 0.8 Ma) in southern Italy and Calabria (Scheepers and Langereis, 1994b; Scheepers et al., 1994). Thus, tectonic rotations in Italy seem to occur in phases and not as a continuous process. Hence, this implies that the current curvature of the Tyrrhenian arc cannot have formed by a continuous rotation process.

East of the Apulian platform, the Dinarides indicate no rotational movements since the Eocene, i.e. after the termination of the subduction process in the northern Dinarides (Tari and Pamic, 1998). In the Albanides, the magnitude of (clockwise) rotation decreases during the Miocene to Pliocene. The western Hellenic arc indicates no rotation between the Tortonian and the Pleistocene, and a clockwise rotation between 0.8 Ma and Recent. The eastern Hellenic arc shows an anticlockwise rotation occurring between 2 Ma and Recent. Also, the paleomagnetic results from the Hellenic arc indicate young, pulsed rotations, clockwise in the west and anticlockwise in the east. This is in line with the present-day pattern of rotation as computed from the geodetic velocity field. There is thus no evidence for continuous rotations to shape the Hellenic arc and we must therefore conclude that the Hellenic arc is most likely formed by translation processes (Duermeijer et al., 1999b).

Paleomagnetic data compared with slab detachment

Many observations in Italy and Greece support the model of lateral migration of slab detachment (Wortel and Spakman, 1992). In this model, deeper parts of subducted lithosphere become/or have become detached from shallower parts of a downgoing slab. Furthermore, slab detachment is thought to be a self-perpetuating process of lateral migration of a tear in subducted lithosphere. For instance, Meijer and Wortel (1996) related the Pleistocene changes in the Aegean stress regime to this model, while Van der
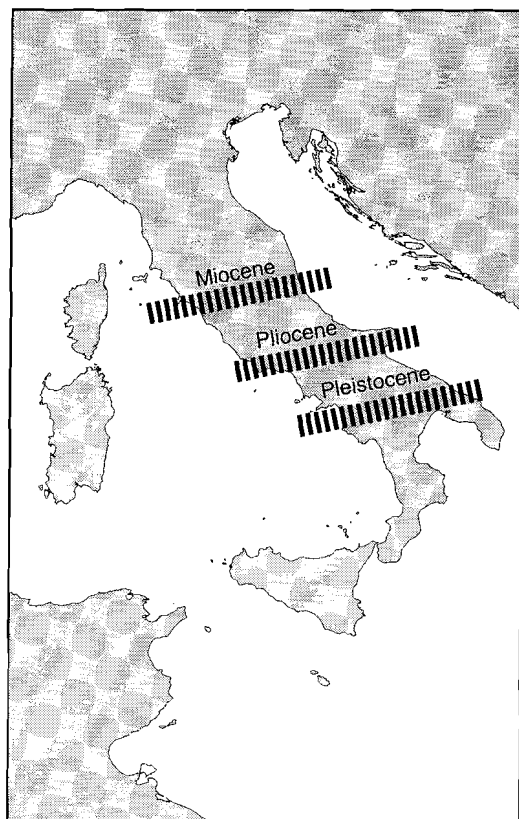
Fig. 6.3 Italy with bands indicating the approximate southern boundary of the non-rotating area at a specific time-interval, based on paleomagnetic data (see Fig. 6.2). Note the migration of this area from the northwest to the southeast.

Meulen et al. (1998) found that depocentres in Italy migrate from the northwest to the southeast through time. Therefore, we decided to test whether the observed tectonic rotations are likewise in accordance with this model. However, we realise that alternative models might appear that can explain our observations equally well.

The late Neogene geodynamic evolution of the central Mediterranean area is the result of northward movement of the African promontory, collision (at the location of the present-day Alps), subduction and subsequent slab roll-back. Tomography has shown that the Apulian platform is presently subducting in the west underneath Italy and in the east underneath former Yugoslavia and Greece (Spakman et al., 1993). In northern Greece and central Italy, the slab appears to be detached at a depth of 100-200 km, whereas in the south (at least in the Aegean region) it seems unruptured (Spakman et al., 1993). A likely explanation for this observation is lateral migration of slab detachment, which implies a migration from the north-west to the south-east (Wortel and Spakman, 1992). Increased slab pull at the segment of the subduction zone, where the downgoing part is still

continuous, might cause increased roll back. This can lead to a continued tendency for outward movement of the Apennines/Tyrrhenian and Dinarides/Albanides/Hellenides arcs respectively. In this scenario, we expect the area west of the Apulian platform to rotate anticlockwise and the area east of the Apulian platform clockwise (Fig 6.4). The expected sense of rotation is thus consistent with the paleomagnetic results.

When detachment occurs, the slab pull forces concentrate on the non-detached part of the slab, leading to a deepening of the foreland basin. Where the slab is just detached, the slab pull is reduced and the foreland basin shallows, resulting in a rebound effect. Furthermore, we expect that the area above the detached slab shows no evidence for further rotations. In Italy, the analysis of burial history data from the Oligocene to Recent Apenninic foredeeps (foreland sedimentary basins) reveals a lateral southeastward shift of the foredeep depocentres, in agreement with lateral migration of slab detachment (Van der Meulen et al., 1998). We can also expect the non-rotating area to expand laterally to the south over time, as slab detachment progresses. The paleomagnetic data from Italy indeed imply an expanding area of no rotation through time (Fig. 6.2 and 6.3). However, east of the Apulian platform, an expanding non-rotation area is not evident from presently existing data.

If the mechanism of lateral migration of slab detachment as described above is indeed valid, we expect this mechanism to be pulsed since the tectonic rotations occur as events. In Italy, we found a rapid tectonic phase around 8 Ma (Calabria), at 3.21 Ma (Sicily) and at 0.8 Ma (southern Italy and Calabria). The tectonic phase around 8 Ma is connected with the beginning of opening of the Tyrrhenian basin (Duermeijer et al., 1998a) and the phase around 3 Ma is related to an acceleration in opening of the Tyrrhenian basin (Duermeijer and Langereis, 1998). The migration of depocentres in Italy also happens in discrete time-intervals and turns out to be non-continuous (Van der Meulen et al., 1998). In Greece, a tectonic event took place between 0.8 Ma and Recent and no evidence for continuous rotations is found (Duermeijer et al., 1999a). This could imply that, if indeed lateral migration of slab detachment is present, also here it occurs pulsed.

Link between the Tyrrhenian and Aegean during the Pleistocene?

It appears that on both sides of the Apulian platform in southern Italy (southern Apennines and Calabria) and north-western Greece, young (Pleistocene) rotations are found. Concurrently in both regions, there is evidence for Pleistocene uplift (Sorel et al., 1988; Westaway, 1993; 1996) and a change in orientation of the stress regime. In southern Italy, the stress regime changed from ENE-WSW compression to NE-SW extension (Hippolyte et al., 1994). In the north-western external Hellenides compression started (at least on the Ionian islands) and in the Aegean Sea (internal Hellenides) the stress patterns changed from NE-SW compression to NNW-SSE extension (Mercier, 1976). Hence, on both sides of the Apulian platform, time-equivalent processes occur. The results imply that the tectonic regime in the central Mediterranean changed drastically after 1 Ma, which is concurrent with the observed rotations. Previous numerical modelling results (Meijer and

Wortel, 1996) indicated that the change in stress regime in Greece could have resulted from lateral migration of slab detachment in the eastern part of the Apulian platform. Furthermore, the uplift in southern Italy has also been related to slab detachment in the western part of the Apulian platform (Westaway, 1993). We have found similar features (uplift, change in stress and rotations) in southern Italy and northwestern Greece, which could both have been the result of lateral migration of slab detachment either in the west and/or in the east of the Apulian platform. As these features occur simultaneously on both sides, this might indicate a link between the two areas. The exact nature and mechanism of this link must await further, e.g. numerical modelling, studies.
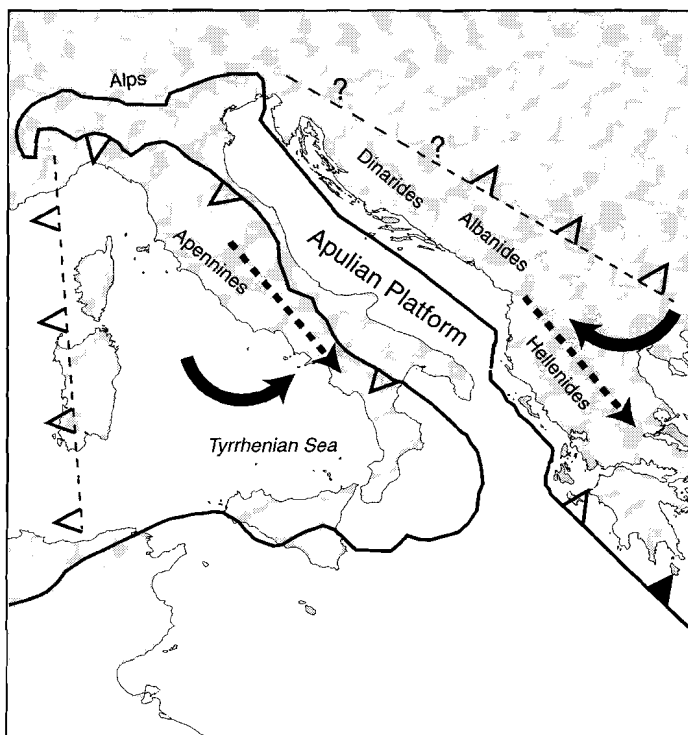
Fig. 6.4 Schematic overview of the geodynamics in the central Mediterranean, where increased slab roll-back causes the Tyrrhenian/Appenines to rotate anticlockwise, whereas the Dinarides/Albanides/Hellenides rotate clockwise (compiled after Wortel and Spakman, 1992). The dashed arrows indicate lateral migration of slab detachment from the north-west to the south-east. Solid arrows denote sense of rotation and solid lines with (closed/open) triangles indicate (active/ended) subduction, the dashed lines with open triangles shows the location of earlier subduction.

Conclusion

A review of existing and new paleomagnetic data reveals an opposite sense of rotations on both sides of the Apulian platform; anticlockwise rotations in Italy and clockwise rotations in the Dinarides/Albanides/western Hellenides. In Italy, the area of no rotations expands from the northwest to the southeast in time. These paleomagnetic results are in agreement with the process of lateral migration of slab detachment, both west and east of the African promontory. The tectonic rotations occur as rather rapid/pulsed events, and this may be taken as evidence of pulsed migration of slab detachment, although different processes may have played a role. It appears that the curvature of the Tyrrhenian and Aegean arc is formed by translations processes and not by continuous rotations. Finally, we find similar, time-equivalent (~0.8 Ma) observations in southern Italy and north-western Greece, which can each be related to lateral migration of slab detachment.

Acknowledgements

Appendix 6.1 Results from NRM analysis from the different sections/sites in the central Mediterranean; uncorrected (notc) and corrected (tc) for bedding tilt. Samples denote number of measured specimens with used Sites; D, I = site mean ChRM declination and inclination; k = Fisher's precision parameter; α_{95} = 95% cone of confidence, (a)c = (anti) clockwise rotation, authors and ages are indicated. Reliability, according to Van der Voo (1993) with a = well determined rock age; b = sufficient number of samples; c = adequate demagnetisation; d = field tests ;e = structural control; f = reversals present (g = no resemblance of paleopoles of younger age; but does not apply, because in general the ages of all localities are young). * indicates paleomagnetic results before oroclinal bending, + shows overprinted data according to the authors and # remagnetised results.

Appendix 6.1

Site/Section	Samples	Sites	D_{notc} (°)	I_{notc} (°)	k	a_{95} (°)	D_{tc} (°)	I_{tc} (°)	k	a_{95} (°)	rot (°)		reliability a b c d e f	authors	Age (Ma)
Corsica/Sardinia															
Sardinia	109	11	132.7	-1.6	41.0	7.3					47	ac	x x x x	Vigliotti et al., 1990	Permian
Corsica	111	11	134.7	-11.3	46.0	6.8					45	ac	x x x x	Vigliotti et al., 1990	Permian
Corsica/Sardinia	_	9					329.0	30.3	23.5	10.9	31	ac	x x x x x x	Van der Voo, 1993	37-11 Ma
Sardinia	84	7	348.5	47.4	213.0	6.3	351.0	45.3	82.0	10.2	9	ac	x x x x x	Vigliotti and Langenheim, 1995	Upp. Burdi-Langhian
Northern Italy															
Po valley (Stirone)	199	1	0.0	52.0	14.0	3.0					0		x x x x	Mary et al., 1993	Tvera-Bruhnes
Po valley (Stirone)	75	1	357.0	35.0	5.4	7.8					3	ac	x x x x	Channell et al., 1994	Messinian-U Pliocene
Po valley (Sant'Andrea)	13	1	328.0	61.0	18.5	9.9					32	ac	x x x x	Channell et al., 1994	Lower Pliocene
Epilugurian units	76	17	314.0	50.8	27.0	7.0	313.0	42.8	33.0	6.3	47	ac	x x x x x	Muttoni et al., 1998	late Oligo/MidMio
Epilugurian units	_	19	148.2	-56.6	6.5	14.3	154.6	-51.8	23.0	7.1	25	ac	x x x x x	Muttoni et al., in press	Tortonian/Messinian
Epilugurian units	_	19	310.7	48.2	17.5	8.3	309.4	42.5	23.0	7.2	51	ac	x x x x x	Muttoni et al., in press	early Oligo/MidMio
Central Italy															
Umbria/Marche	73	7					2.0	43.0	60.5	8.7	2	c	x x x x	Dela Pierre et al., 1992	Messinian/Low Plio
Tyrrhenian margin	92	7	351.4	50.5	34.3	10.5	357.8	52.0	147.9	5.0	2	ac	x x x x x	Sagnotti et al., 1994	4.2-1.8
Tiburtini Mountains	32	4	8.0	-55.0	1.0	69.0	50.0	29.0	16.0	17.5	50	c	x x x	Mattei et al., 1995	late Cretaceous-Oligo
Sabina	170	21	346.0	45.0	7.0	12.8	329.0	44.0	52.0	4.0	31	ac	x x x x x x	Mattei et al., 1995	Paleocene-Oligocene
Montagna dei Fiori	22	3	10.0	67.0	2.0	54.2	345.0	39.0	18.0	18.6	15	ac	x x	Mattei et al., 1995	Eocene-Oligocene
Marsica[+]	32	4	329.0	39.0	8.0	24.4	4.0	48.0	9.0	22.9	4	c	x x x x x	Mattei et al., 1995	late Miocene
Latium-Abruzzi (Roveto)	54	8	332.0	42.0	10.0	18.0	332.0	42.0	28.0	10.5	28	ac	x x x x x	Mattei et al., 1995	late Miocene
Prenestini	53	7	9.0	48.0	10.0	19.5	16.0	43.0	28.0	11.5	16	c	x x x x x	Mattei et al., 1995	early Miocene
Tuscany	314	29	356.9	57.6	35.0	4.6	357.3	56.9	76.7	3.1	3	ac	x x x x x	Mattei et al., 1996	Mio/Plio
Matese	26	8	304.5	36.1	_	_	313.0	57.0	172.0	4.0	47	ac	x x	Iorio et al., 1996	Early/Mid Miocene
Umbria-Marche-Romagna arc	_	38					173.6	-49.4	14.0	6.4	6	ac	x x x x x x	Speranza et al., 1997	Messinian
Acquasanta	_	9	342.3	45.7	12.7	15.0	0.1	41.4	44.6	7.8	0		x x x x x x	Speranza et al., 1997	Messinian
Sibillini/Marche-Romagna[*]	_	26					169.7	-48.8	13.7	8.0	10	ac	x x x x x x	Speranza et al., 1997	Messinian
Molise	55	5	321.5	30.1	5.4	36.1	321.9	56.4	25.0	15.6	38	ac	x x x x	Speranza et al., 1998	Late Miocene
Molise	7	1	3.6	60.8	_	_	3.6	60.8	38.5	9.8	4	c	x x x x	Speranza et al., 1998	Pleistocene
Southern Italy															
Bradano	_	3					359.1	56.3	218.0	8.4	0		x x x x	Scheepers et al., 1993	Pleistocene
southern Appenines	135	13	168.3	-56.1	17.8	9.2	157.8	-56.1	111.2	3.7	23	ac	x x x x x	Sagnotti, 1992	Plio/Pleisto
southern Appenines	_	3					336.6	57.2	254.0	7.8	23	ac	x x x x	Scheepers et al., 1993	Plio/Pleisto
southern Appenines	_	8					320.8	52.4	159.0	4.4	39	ac	x x x x	Scheepers and Langereis, 1994	Late Mio/mid Plio
southern Appenines	_	4					351.3	56.1	144.0	7.7	9	ac	x x x x	Scheepers and Langereis, 1994	<0.5 Ma
southern Appenines	72	3					340.0	53.4	214.1	8.4	20	ac	x x x x	this study	Middle/Upper Plio

Appendix 6.1

Site/Section	Samples	Sites	D_{note} (°)	I_{note} (°)	k	a_{95} (°)	D_{tc} (°)	I_{tc} (°)	k	a_{95} (°)	rot (°)		a b c d e f	authors	Age (Ma)
Calabria															
Ionian/Tyrrhenian coast	--	8					13.7	46.7	108.0	5.4	14	c	x x x x	Scheepers et al, 1994	Lower Pliocene
Ionian/Tyrrhenian coast	--	12					13.7	47.3	140.0	3.7	14	c	x x x x	Scheepers et al, 1994	LPlio/LPleisto
Calabria (Basilicoi)	35	1					347.2	48.0	21.6	5.1	13	ac	x x x x	Duermeijer et al., 1998a	Miocene
Calabria (Lese)	59	1					349.6	45.3	12.1	5.6	10	ac	x x x x	Duermeijer et al., 1998a	Miocene
Calabria	250	8					15.0	48.8	191.5	4.0	15	c	x x x x	this study	Upper Pliocene
Sicily															
Aeolian islands	287	37					356.6	54.9	28.0	4.5	3	ac	x x x	Lanza and Zanella, 1991	0.15-0.13 Ma
Caltanisetta basin	27	1					203.9	-36.7	154.0	2.2	24	c	x x x x x	Scheepers and Langereis, 1993	2.8-2.5 Ma
Caltanisetta basin	10	1					34.2	46.4	1212	1.4	34	c	x x x x x	Scheepers and Langereis, 1993	4.9-2.9Ma
Caltanisetta basin	92	1					22.4	49.7	103.0	1.5	22	c	x x x x x x	Duermeijer and Langereis, 1998	kaena-normal
Caltanisetta basin	35	1					211.8	-48.2	166.9	1.9	32	c	x x x x x x	Duermeijer and Langereis, 1998	mammoth
Pantelleria	150	27					358.5	46.9	30.0	5.2	1	ac	x x x	Zanella, 1998	last 150 ka
Sicily	34	2					19.2	52.2	0.0	99.9	19	c	x x x x	this study	Pliocene
Iblei/Gargano/Apulia															
Apulia/Gargano	178	5					359.8	56.3	491.0	3.5	0		x x x x	Scheepers, 1992	Late Plio/early Pleis
Gargano[#]	114	14	355.0	56.0	27.0	7.8	352.0	47.0	57.6	5.3	8	ac	x x x	Speranza and Kissel, 1993	Middle Eocene
Apulia (Murge)	56	12	327.0	44.0	55.0	17.0	327.0	38.0	76.0	15.0	33	ac	x x x x	Marton and Nardi, 1994	Cenomanian/Turonian
Ragusa	--	4					354.5	38.6	172.4	7.0	5	ac	x x x x x x	Voo, 1993	14-3 Ma
Dinarides															
Central Dinarides[*]	171	14	325.0	71.0	5.0	20.0	352.0	46.0	49.0	5.7	8	ac	x x x x	Kissel et al., 1995	mid-up Eocene
Central Dinarides	50	4	185.0	-65.0	11.0	29.0	184.0	-51.0	98.0	9.3	4	c	x x x x	Kissel et al., 1995	Mio/Plio
Southern Dinarides	61	6	141.0	-70.0	24.0	14.0	188.0	-41.0	334.0	3.7	8	c	x x x x	Kissel et al., 1995	Eocene
Albanides															
Southern Albania	27	3					42.0	28.0	_	_	42	c	x x x	Speranza et al., 1992	Oligocene
Southern Albania	124	11					43.0	39.0	131.3	4.0	43	c	x x x	Speranza et al., 1992	Eocene
Outer Albanides	--	7					32.0	40.0	62.4	7.7	32	c	x x	Mauritsch et al., 1995	Tortonian
Inner Albanides	--	3					40.0	38.0	129.0	10.9	40	c	x x	Mauritsch et al., 1995	Tortonian
external Albanides	142	13	182.0	-38.0	3.4	26.0	205.0	-48.0	33.5	7.2	25	c	x x x x x	Speranza et al., 1995	Lower-Mid Pliocene
external Albanides	289	24	35.0	46.5	4.0	18.2	35.0	44.0	35.0	5.0	35	c	x x x x x	Speranza et al., 1995	Upper Miocene
external Albanides	172	12	224.0	-65.0	9.2	15.1	225.0	-41.0	57.0	5.8	45	c	x x x x x	Speranza et al., 1995	Oligocene
external Albanides	64	6	77.5	-78.0	115.0	6.3	229.0	-40.0	114.0	6.3	49	c	x x x x x	Speranza et al., 1995	upper Eocene
Northern Albanides	33	4	238.0	56.0	2.5	74.0	31.0	46.0	41.0	14.0	31	c	x x x x	Kissel et al., 1995	Eocene

Table header: NRM-Analysis (Samples, Sites, D_{note}, I_{note}, k, a_{95}, D_{tc}, I_{tc}, k, a_{95}, rot); reliability (a b c d e f, authors, Age)

Appendix 6.1

Site/Section	Samples	Sites	D_{notc} (°)	I_{notc} (°)	k	a_{95} (°)	D_{tc} (°)	I_{tc} (°)	k	a_{95} (°)	rot (°)	reliability a b c d e f	authors	Age (Ma)
Greece														
Western outer arc	–	4					16.0	33.9	188.6	6.7	16	c	x x x x	Van der Voo, 1993	11-1 Ma
Western inner arc	–	6					11.8	37.8	9.8	22.5	12	c	x x x x	Van der Voo, 1993	28-2 Ma
Akarnia (Paleros)	32	3	22.4	55.2	31.8	22.2	34.5	49.0	30.0	22.9	35	c	x x x x x x x	Birch, 1990	Miocene
Ptolemais (Epirus)	–	6					4.0	50.0	21.0	15.0	4	c	x x	Westphal et al., 1991	Upper Mio/Pliocene
Riza	–	1					195.0	-45.0	_	8.0	15	c	x x	Westphal et al., 1991	early Pliocene
Axios	–	4					20.0	46.0	30.0	17.0	20	c	x x	Kondopoulou, 1994	Late Miocene
Medousa (NE Greece)	–	6	350.0	60.0	144.1	5.6	17.0	46.0	152.8	5.4	17	c	x x x	Haubold et al., 1997	30-31 Ma
Zagradenia (NE Greece)	–	6	199.0	-49.0	221.6	4.5					19	c	x x x	Haubold et al., 1997	30-31 Ma
Elatia (NE Greece)	–	6	202.0	-39.0	36.5	11.2					22	c	x x x	Haubold et al., 1997	39-47 Ma
Pithion (NE Greece)	–	3					16.0	51.0	197.1	8.8	16	c	x x x	Haubold et al., 1997	mid Oligocene
Epirus	17	1					228.0	-37.6	18.1	8.6	48	c	x x x x	Peeters et al.,1998	Eocene/Oligocene
Kefallonia	70	1	159.0	-49.1	40.1	2.7	176.6	-51.2	45.1	2.6	3	ac	x x x x	Duermeijer et al., 1999b	1.9-1.0 Ma
Zakynthos	153	8					21.6	48.8	128.0	4.9	22	c	x x x x	Duermeijer et al., 1999a	8.11-0.77 Ma
Megara	12	1	3.1	48.9	20.5	9.8	2.7	46.7	35.5	7.4	3	c	x x x x	Duermeijer et al., 1999b	Plio/Pleistocene
Corinth	5	1	177.4	-57.9	26.3	15.2	177.4	-57.9	26.3	15.2	3	ac	x x x x	Duermeijer et al., 1999b	Pleistocene
Peloponessos	51	4					16.1	55.2	325.6	5.1	16	c	x x x x	Duermeijer et al., 1999b	Plio/Pleistocene
Kimi (Evia)	31	4	198.4	-13.2	12.0	27.9	199.0	-42.1	62.0	11.7	19	c	x x x x	Morris, 1995	Miocene
Kimi (Evia)	33	4	222.5	-31.4	55.0	12.5	230.8	-40.3	55.0	12.5	51	c	x x x x x	Morris, 1995	Upper Mio-Plio
northern Attica (Kalamos)	5	1	358.9	62.4	331.0	4.2	26.1	51.8	331.0	4.2	26	c	x x	Morris, 1995	14.8-13.2 Ma
Kythira	12	1	13.1	49.8	29.2	8.2	351.9	39.4	29.7	8.1	8	ac	x x x	Duermeijer et al., 1999b	Miocene
Milos	18	2					184.5	-51.8	0.0	99.9	5	c	x x x x	Duermeijer et al., 1999b	Plio/Pleistocene
Tinos	57	13					27.8	41.9	15.3	9.9	28	c	x x x x	Avigad et al., 1998	11.5±0.4 Ma
Mykonos	64	5	63.7	12.1	31.0	14.0	38.4	23.0	111.0	7.3	38	c	x x x	Morris and Anderson, 1996	11 Ma
Naxos	87	5	350.7	32.5	27.0	15.0	333.4	37.6	81.0	8.6	27	ac	x x x	Morris and Anderson, 1996	13-11 Ma
Crete-west	217	5					346.5	45.9	108.4	7.4	13	ac	x x x x	Duermeijer et al., 1998b	Tort/Messinian
Crete-central	105	3					325.3	45.9	207.2	8.6	35	ac	x x x x	Duermeijer et al., 1998b	Tort/Messinian
Crete-east	68	1					347.9	48.7	37.4	2.9	12	ac	x x x x	Duermeijer et al., 1998b	Tort/Messinian
Crete (Heraklion basin)[+]	63	11											x x x	Duermeijer et al., 1999b	Plio/Pleistocene
Lesbos	~	2					10.0	31.0	0.0	99.9	10	c	x x x x	Van der Voo, 1993	19-15 Ma
Kassos	5	1	336.7	47.3	99.5	7.7	337.3	48.1	99.5	7.7	23	ac	x x x	Duermeijer et al., 1999b	Miocene
Karpathos	9	1	166.1	-52.8	49.9	7.4	162.0	-55.9	48.4	7.5	18	ac	x x x x	Duermeijer et al., 1999b	Pliocene
Rhodos	86	8					162.5	-46.8	45.3	8.3	17	ac	x x x x	Duermeijer et al., 1999b	Plio/Pleistocene

References

Alvarez, W., Cocozza T. and F.C. Wezel, 1974. Fragmentation of the Alpine orogenic belt by microplate dispersal. *Nature* 248, 309-314.

Angelier, J., Lybéris, N., Le Pinchon, X, Barrier, E. and Ph. Huchon, 1982. The tectonic development of the Hellenic arc and the Sea of Crete: a synthesis. *Tectonophysics* 86, 159-196.

Argnani, A., 1990. The Strait of Sicily rift zone: Foreland deformation related to the evolution of a back-arc basin. *J. Geodyn.* 12, 311-331.

Argnani, A. and F. Frugoni, 1997. Foreland deformation in the central Adriatic and its bearing on the evolution of the Northern Apennine, *Annali Geofisica 15*, 771-780.

Armijo, R, Lyon-Caen, H. and D. Papanastassiou, 1992. East-west extension and Holocene normal-fault scarps in the Hellenic arc. *Geology* 20, 491-494.

Armijo, R., Meyer, B., King, G.C.P., Rigo, A. and D. Papanastassiou, 1996. Quaternary evolution of the Corinth Rift and its implications for the Late Cenozoic evolution of the Aegean. *Geophys. J. Int.* 126, 11-53.

Aubouin, J., 1959. Contribution à l'étude de la Grèce septrionale; les confins de l'Epire et de la Thessalie. *Ann. Géol. Pays Hellén.* 10, 1-483.

Aubouin, J., Bonneau, M., Davidson, J., Leboulenger, P., Matesco, S. and A. Zambetakis, 1976. Esquissse structurale de l'arc égéen externe: des Dinarides aux Taurides. *Bull. Soc.géol. Fr.* 18, 327-336.

Avigad, D., Baer, G. and A. Heimann, 1998. Block rotations and continental extension in the central Aegean Sea: paleomagnetic and structural evidence from Tinos and Mykonos (Cyclades, Greece). *Earth and Planetary Science Letters* 157, 23-40.

Baker, C., Hatzfeld, D., Lyon-Caen, H., Papadimitriou, E. and A. Rigo, 1997. Earthquake mecahnisms of the Adriatic Sea and Western Greece: implications for the oceanic subduction-continental collision transition. *Geophysical Journal International* 131, 559-594.

Berggren, W.A., Hilgen, F.J., Langereis, C.G., Kent, D.V., Obradovich, J.D., Raffi, I, Raymo, M.E., and N.J. Shackleton, 1995a. Late Neogene chronology: New perspectives in high-resolution stratigraphy. *GSA Bulletin* 107, 1272-1287.

Berggren, W.A., Kent, D., Swisher III, C.C. and M.-P. Aubry, 1995b. A revised Cenozoic geochronology and chronostratigraphy, Geochronology Time-scales and Global Stratigraphic Correlation. *SEPM Special Publication* No. 54, 129-212.

Besse, J. and V. Courtillot, 1991. Revised and Synthetic Apparent Polar Wander Paths of the African, Eurasian, North American and Indian Plates, and true polar wander since 200 Ma. *Journal of Geophys. Res.*, Vol. 96, 4029-4050.

Birch, W.G., 1990. Paleomagnetic studies in western and central Greece: tectonic evolution of the Aegean domain since the Triassic. *Thesis Liverpool University*, 321 pp.

Bizon, G. and C. Muller, 1977. La limite Pliocène-Pleistocène dans l'ile de Zante. La coupe de la Citadelle. *C.R. Soc. Géol. France* 4, 212-216.

Blake, M.C., Bonneau, M., Greyssant, J., Kienast, J.P., Lepvrier, C., Maluski, H. and D. Papanikolaou, 1981. A geological reconnaissance of the Cycladic blueschist belt. Greece. *Bull. Geol. Am.* 92, 247-254.

Bonneau, M., 1982. Evolution geodynamique de l'arc égéen depuis la Jurassique supérieur jusqu'au Miocène. *Bull. Soc. Géol. Fr.* 7 (24), 229-242.

Bonneau, M. and J.R. Kienast, 1982. Subduction, collision et schistes bleu: exemple de l'Égée, Grèce. *Bull. Soc. Géol. Fr.* 7, 785-791.

Broekman, J.A., 1974. Sedimentation and paleoecology of Pliocene lagoonal-shallow marine deposits on the island of Rhodos (Greece). *Utr. Micropal. Bull.* 8, 148 pp.

Brolsma, M.J., 1978. Quantitative foraminiferal analysis and environmental interpretation of the Pliocene and topmost Miocene on the south coast of Sicily. *Utrecht Micropal. Bull.* 18, 1-159.

Buiter, S.J.H., Wortel, M.J.R. and R. Govers, 1998. The role of subduction in the evolution of the Apennines foreland basin. *Tectonophysics* 296, 249-268.

Busby, C. J. and R.V. Ingersoll, 1995. Tectonics of Sedimentary basins, Blackwell, Oxford, 580 pp.

Butler, R.F., 1992. Paleomagnetism: Magnetic Domains to Geologic Terranes. Blackwell, Boston, MA, 319 pp.

Butler, R.W.H., Lickorish, W.H., Grasso, M, Pedley, H.M. and L. Ramberti, 1995. Tectonics and sequence stratigraphy in Messinian basins, Sicily: Constraints on the initiation and termination of the Mediterranean salinity crisis. *Geol. Soc. Am. Bull.* 107, 425-439.

Cande, S.C., and D.V. Kent, 1995. revised calibration of the geomagnetic polarity time scale for the late Cretaceous and Cenozoic. *J. Geoph. Res.* 100, 6093-6095.

Catalano, R., Channell, J.E.T., D'Argenio, B. and G. Napoleone, 1976. Mesozoic Paleogeography of the southern Apennines and Sicily. Problems of paleotectonics and paleomagnetism. *Mem. Soc. Geol. It.* 15, 95-118.

Catalano, R., Infuso, S. and A. Sulli, 1993. The Pelagian foreland and its northward foredeep. Plio-Pleistocene structural evolution. In: M.D. Max and P. Colantoni (Eds.), Geological development of the Sicilian-Tunesian Platform. *Unesco Reports in marine science* 58, 37-42.

Catalano, R., Infuso, S. and A. Sulli, 1995. Tectonic history of the submerged Maghrebian Chain from the southern Tyrrhenian Sea to the Pelagian foreland. *Terra Nova* 7 (2), 179-188.

Catalano, R., Di Stefano, P., Sulli, A. and F.P. Vitale, 1996. Paleogeography and structure of the central Mediterranean: Sicily and its offshore area. *Tectonophysics* 260, 291-323.

Channell, J.E.T. and D.H. Tarling, 1975. Paleomagnetism and the rotation of Italy. *Earth and Planetary Science Letters* 25, 177-188.

Channell, J.E.T., Poli, M.S., Rio, D., Sprovieri, R. and G. Villa, 1994. Magnetic stratigraphy and biostratigraphy of Pliocene "argille azzurre" (Northern Apennines, Italy). *Palaeogeography, Palaeoclimatology, Palaeoecology,* 110(1-2): 83-102.

Cianetti, S, Gasparini, P, M. Boccaletti and C. Giunchi, 1997. Reproducing the velocity and stress fields in the Aegean region. *Geophysical Research Letters* 24, No. 16, 2087-2090.

Clarke, P.J., Davies, R.R., England, P.C., Parsons, B., Billiris, H., Paradissis, D., Veis, G., Cross, P.A., Denys, P.H., Ashkenazi, V., Bingley, R., Kahle, H.-G., Müller, M.-V. and P. Briole, 1998. Crustal strain in central Greece from repeated GPS measurements in the interval 1988-1997. *Geophysical Journal International* 135, 195-214.

Collier, R.E.Ll and C. Dart, 1991. Neogene to Quaternary rifting, sedimentation and uplift in the Corinth Basin, Greece. *Journal Geol. Soc. London* 148, 1049-1065.

Dankers, P.H., 1978. Magnetic properties of dispersed natural iron oxides of known grain size. *Ph.D. Thesis, Univ. Utrecht, 143 pp.*

Davies, R., England, P., Parsons, B., Billiris, H., Paradissis, D. and G. Veis, 1997. Geodetic strain of Greece in the interval 1892-1992. *Journal of Geophysical Research* 102 (11), 24,571-24,588.

De Boer, C.B. and M.J. Dekkers, 1996. Grain-size dependence of the rock magnetic properties for a natural maghemite. *Geophys. Res. Lett.* 23, 2815-1818.

Dela Pierre, F., Ghisetti, F., Lanza, R. and L. Vezzani, 1992. Paleomagnetic and structural evidence of Neogene tectonic rotation of the Gran Sasso range (central Apennines, Italy). *Tectonophysics 215*, 335-348.

Dercourt, J., Zonenshain, L.P., Ricou, L.-E., Kazmin, V.G., Le Pinchon, X., Knipper, A.L., Grandjacquet, C., Sbortshikov, I.M., Geyssant, J., Lepvrier, C., Pechersky, D.H., Boulin, J., Sibuet, J.-C., Savostin, L.A., Sorokhtin, O., Westphal, M., Bazhenov, M.L. Lauer, J.P. and B. Biju-Duval, 1986. Geological evolution of the Tethys belt from the Atlantic to the Pamirs since the Lias. *Tectonophysics 123*, 241-315.

Dermitzakis, M.D., Papanikolaou, D. and Z. Karotsieris, 1979. The marine Quaternary formations of SE Zakynthos island and their Paleogeographic implications. *Proc. 6*[th] *Geol. Aegean Region*, Athens 1977, I, 407-415.

Dewey, J.F., Helman, M.L., Turco, E., Hutton, D.H.W. and D. Knott, 1989. Kinematics of the western Mediterranean. *Alpine tectonics*, Geol.Soc.London, Spec.Publ.45, 265-283.

Dimitriadis, S., Kondopoulo, D. and A. Atzemoglou, 1998. Dextral rotations and tectonomagmatic evolution of the southern Rhodope and adjacent regions (Greece). *Tectonophysics 299*, 159-173.

Duermeijer, C.E. and C.G. Langereis, 1998. Astronomical dating of a tectonic rotation on Sicily and consequences for the timing and extent of a middle Pliocene deformation phase. *Tectonophysics 298*, 243-258.

Duermeijer, C.E., Van Vugt, N., Langereis, C.G., Meulenkamp, J.E. and W.J. Zachariasse, 1998a. A major late Tortonian rotation phase of the Crotone Basin; implications using AMS as tectonic tilt correction and first indication of timing in opening of the Tyrrhenian Basin. *Tectonophysics 287* (1-4), 233-249.

Duermeijer, C.E., Krijgsman, W., Langereis, C.G. and J.H. Ten Veen, 1998b. Post early Messinian counter-clockwise rotations on Crete: implications for the Late Miocene to Recent kinematics of the southern Hellenic Arc. *Tectonophysics 298*, 177-189.

Duermeijer, C.E., Krijgsman, W., Langereis, C.G., Meulenkamp, J.E., Triantaphyllou, M.V. and W.J. Zachariasse, 1999a. A middle Pleistocene clockwise rotation phase of Zakynthos (Greece) and implications for the evolution of the western Aegean arc. *Earth and Planetary Science Letters*, submitted.

Duermeijer, C.E., Nyst, M., Meijer, P.Th. and C.G. Langereis, 1999b. The Neogene evolution of the Aegean arc: indications for a Pleistocene tectonic rotation phase. *Earth and Planetary Science Letters*, submitted.

Duermeijer, C.E. and C.G. Langereis, 1999. The late Neogene to Recent geodynamic evolution of the central Mediterranean and the role of the African promontory: a paleomagnetic approach. *Tectonics*, submitted.

England, P. and J. Jackson, 1989. Active deformation of the continents, *Ann. Rev. Earth Planet. Sci.*, 17, 197-226.

Fisher, R.A., 1953. Dispersion on a sphere. *Proc. R. Soc. Lond.* A 217, 295-305.

Flores, J.A., Sierro, F.J. and G. Glaçon, 1992. Calcareous plankton analysis in the pre-evaporitic sediments of ODP Site 654 (Tyrrhenian Sea, Western Mediterranean). *Micropaleontology 38* (3), 279-288.

Gilbert, L., Kastens, K., Hurst, K., Paradissis, D., Veis, G., Billiris, H., Höppe, W. and W. Schlüter, 1994. Strain results and tectonics from the Aegean GPS experiment. *EOS*, Suppl. April 19, 116 p.

Grasso, M. and R.W.H. Butler, 1991. Tectonic controls on the deposition of lateTortonian sediments in the Caltanisetta Basin of Central Sicily. *Mem. Soc. Geol. It.* 47, 313-324.

Hageman, J., 1979. Benthic foraminiferal assemblages from Plio-Pleistocene open bay to lagoonal sediments of the western Peloponessus (Greece). *Utr. Micropal. Bull.*, vol. 20, 171 pp.

Hatzfeld, D., Besnard, M., Makropoulos, K. and P. Hatzidimitriou, 1993. Microearthquake seismicity and fault-plane solutions in the southern Aegean and its geodynamic implications. *Geophysical Journal International* 115, 799-818.

Haubold, H., Scholger, R., Kondopoulou, D. and H.J. Mauritsch, 1997. New paleomagnetic results from the Aegean extensional province. *Geologie en Mijnbouw 76*, 45-55.

Hilgen, F.J., 1987. Sedimentary cycles and high-resolution chronostratigraphic correlations in the Mediterranean Pliocene. *Newsletters on Stratigraphy 17*, 109-127.

Hilgen, F.J., 1991a. Extension of the astronomically calibrated (polarity) time scale to the Miocene/Pliocene boundary. *Earth and Planetary Science Letters 107*, 349-368.

Hilgen, F.J., 1991b. Astronomical calibration of Gauss to Matuyama sapropels in the Mediterranean and implication for the Geomagnetic Polarity Time Scale. *Earth and Planetary Science Letters 104*, 226-244.

Hilgen, F.J., Krijgsman, W., Langereis, C.G., Lourens, L.J., Santarelli, A. and W.J. Zachariasse, 1995. Extending the astronomical (polarity) time scale into the Miocene. *Earth and Planetary Science Letters 136*, 495-510.

Hippolyte, J.-C., Angelier, J. and F. Roure, 1994. A major geodynamic change revealed by Quarternary stress patterns in the Southern Apennines (Italy). *Tectonophysics 230*, 199-210.

Horner, F. and R. Freeman, 1985. Paleomagnetic evidence from pelagic limestones for clockwise rotation of the Ionian zone, western Greece. *Tectonophysics 98*, 11-27.

Hsü, K.J., 1977. Tectonic evolution of the Mediterranean Sea basins. *In:* Nairn, A.E.M., Kanes, W.H. & Stehli, F.G. (eds). *The Ocean Basins and Margins, 4a, The eastern Mediterranean*, Plenum Press, New York, pp. 29-75.

Iorio, M., Nardi, G., Pierattini and D.H. Tarling, 1996. Paleomagnetic evidence of block rotations in the Matese mountains, southern Apennines. Italy, In: Morris, A and D.H. Tarling (Eds.), *Geological Society Special Publication 105*, 133-139.

Jelinek, V. 1977. The statistical theory of measuring anisotropy of magnetic susceptibility of some igneous and metamorphic rocks. Geofyzika Brno.

Jelinek, V., 1978. Statistical processing of anisotropy of magnetic susceptibility on groups of specimens. *Studia Geophys. Geod. 22*, 50-62.

Jolivet, L., Brun, J.-P., Gautier, P., Lallemant, S. and M. Patriat, 1994. 3D-kinematics of extension in the Aegean region from the early Miocene to the Present, insights from the ductile crust. *Bull. Soc. Géol. France*, t. 165, No. 3, 195-209.

Jonkers, H.A., 1984. Pliocene benthonic foraminifera from homogeneous and laminated marls on Crete. *Utr. Micropal. Bull.*, vol. 31, 179 pp.

Kahle, H-G., Müller, M.V. and G. Veis, 1996. Trajectories of crustal deformation of western Greece from GPS observations 1989-1994. *Geophysical Research Letters 23*, No. 6, 677-680.

Kahle, H-G., Straub, C., Reilinger, R, McClusky, S, King, R., Hurst, K, Veis, G., Kastens, K and P. Cross, 1998. The strain rate field in the eastern Mediterranean region, estimated by repeated GPS measurements. *Tectonophysics 294* (3-4), 237-252.

Kastens, K.A.. Mascle, J. Auroux, C. et al., 1987. *Proc. ODP, Init. Repts. (Pt A)*, 107, College Station, TX (Ocean Drilling Program).

Kirschvink, J.L., 1980. The least-square line and plane and the analysis of paleomagnetic data. *Geophys. J. R. Astron. Soc. 62*, 699-718.

Kissel, C., Laj, C. and C. Müller, 1985. Tertiary geodynamical evolution of northwestern Greece: paleomagnetic results. *Earth and Planetary Science Letters 72*, 190-204.

Kissel, C. and A. Poisson, 1986. Etude paléomagnétique préliminaire des formations néogène du bassin d'Antalya (Taurides occidentale, Turquie). *C.R. Acad. Sc. Paris* 302, II, No. 10, 711-716.

Kissel, C., Laj, C. and A. Malzaud, 1986. First paleomagnetic results from Neogene formations on Evvia, Skyros and the Volos region and the deformation of Central Aegea. *Geophysical Research Letters* 13, No. 13, 1446-1449.

Kissel, C., Barrier, E., Laj, C. and T-Q Lee, 1986. Magnetic fabric in "undeformed" marine clays from compressional zones. *Tectonics* 5, No. 5, 769-781.

Kissel, C. and A. Poisson, 1987. Etude paléomagnétique préliminaire des formations cénozoïques des Bey Daglari (Taurides occidentale, Turquie). *C.R. Acad. Sc. Paris*, 304, II, No. 8, 343-348.

Kissel, C. and C. Laj, 1988. The Tertiary geodynamical evolution of the Aegean arc: a paleomagnetic reconstruction. *Tectonophysics* 146, 183-201.

Kissel, C. and F. Speranza, 1995. Paleomagnetism of external southern and central Dinarides and northern Albanides: Implications for the Cenozoic activity of the Scutari-Pec transverse zone. *Journal of Geophysical Research* 100, No. B8, 14999-15007.

Kissel, C., Speranza, F and V. Milicevic, 1995. Paleomagnetism of external southern and central Dinarides and northern Albanides: Implications for the Cenozoic activity of the Scutari-Pec transverse zone, *Journal of Geophysical Research 100*, B8, 14999-15007.

Kondopoulo, D.P. and S.B. Pavlides, 1990. Paleomagnetic and neotectonic evidence for different deformation patterns in the south Aegean volcanic arc: the case of Melos island. Intern. Earth Sci. Congress on Aegean Regions, Proceedings 1, 210-223.

Kondopoulou, D., 1994. Some constraints on the origin and timing of the magnetization for Mio-Pliocene sediments from northern Greece. *Bull. Geol. Soc. Greece 30* (5), 53-66.

Krijgsman, W., Hilgen, F.J., Langereis, C.G. and W.J. Zachariasse, 1994. The age of the Tortonian/Messinian boundary. *Earth and Planetary Science Letters* 121, 533-547.

Krijgsman, W., Hilgen, F.J., Langereis, C.G., Santarelli, A. and W.J. Zachariasse, 1995. Late Miocene magnetostratigraphy, biostratigraphy and cyclostratigraphy in the Mediterranean. *Earth and Planetary Science Letters* 136, 475-494.

Krijgsman, W., Hilgen, F.J., Raffi, I., Sierro, F.J. and D.S. Wilson, 1999. Chronology, causes and progression of the Messinian salinity crisis. *Nature*, in press.

Kroon, D., Alexander, I., Little, M., Lourens, L.J., Matthewson, A., Robertson, A.H.F. and T. Sakamoto, 1998. Oxygen isotope and sapropel stratigraphy in the eastern Mediterranean during the last 3.2 million years. *In* Emeis, K.-C., Robertson, A.H.F., Richter, C., et al., *Proc. ODP, Sci. Results*, 160: College Station, TX (Ocean Drilling Program), 191-197.

Laj, C., Gauthier, A.J. and B. Keraudren, 1978. Mise en évidence d'une rotation plio-quaternaire de l'île de Rhodes (Grèce): résultats préliminaires. *Réun. Ann. Sci. Terre*, 6e, Orsay, p.224.

Laj, C., Jamet, M., Sorel, D. and J.P. Valente, 1982. First paleomagnetic results from Mio-Pliocene series of the Hellenic sedimentary arc. *Tectonophysics* 86, 45-67.

Langereis, C.G., 1984. Late Miocene magnetostratigraphy in the Mediterranean. PhD thesis, Utrecht University, *Geologica Ultraiectina* 34, 178 pp.

Langereis, C.G. and F.J. Hilgen, 1991. The Rossello Composite: a Mediterranean and global reference section for the Early to early Late Pliocene. *Earth and Planetary Science Letters* 104, 211-225.

Langereis, C.G., van Hoof, A.A.M. and P. Rochette, 1992. Longitudinal confinement of geomagnetic reversal paths as a possible sedimentary artefact. *Nature* 358, 226-230.

Langereis, C.G., Dekkers, M.J., de Lange, G.J., Paterne, M. and P.J.M. van Santvoort, 1997. Magnetostratigraphy and astronomical calibration of the last 1.1 Myr from an eastern Mediterranean piston core and dating short events in the Bruhnes. *Geophys.J.Int.* 129, 75-94.

Lanza, R. and E. Zanella, 1991. Paleomagnetic directions (223-1.4 ka) recorded in the volcanites of Lipari, Aeolian islands. *Geophys. Res. Lett* 107, 191-196.

Lee, T., Kissel, C., Laj, C., Horng, and Y. Lue, 1990. Magnetic fabric analysis of the Plio-Pleistocene sedimentary formations of the Coastal Range of Taiwan. *Earth and Planetary Science Letters* 98, 23-32.

Le Pichon, X. and J. Angelier, 1979. The Hellenic arc and trench system: a key to the neotectonic evolution of the eastern Mediterranean area. *Tectonophysics* 60, 1-42.

Le Pichon, X. and J. Angelier, 1981. The Aegean Sea. *Phil. Trans. R. Soc. London* A 300, 357-372.

Le Pichon, X., 1982. Landlocked oceanic basins and continental collision: the Eastern Mediterranean as a case example. In: K. Hsü (Editor), Mountain Building Processes, Academic Press, London, pp. 201-211.

Le Pichon, X, Chamot-Rooke, N., Lallemant, S., Noomen, R. and G. Veis, 1995. Geodetic determination of the kinematics of central Greece with respect to Europe: Implications for eastern Mediterranean tectonics. *Journal of Geophys. Res.* 100, B7, 12675-12690.

Lourens, L.J., Antonarakou, A., Hilgen, F.J., Van Hoof, A.A.M., Vergnaud-Grazzini C. and W.J. Zachariasse, 1996. Evaluation of the Plio-Pleistocene astronomical timescale. *Paleoceanography* 11 (4), 391-413.

Lourens, L.J., Hilgen, F.J. and I. Raffi, 1998. Base of large Gephyrocapsa and astronomical calibration of early Pleistocene sapropels in site 967 and Hole 969D: solving the chronology of the Vrica section (Calabria, Italy). in: Robertson, A.H.F, K.C.Emeis, C.Richter, and A.Camerlenghi (Eds.), *Proc. ODP Sc. Results* 160, 191-197.

Lowrie, W, 1990. Identification of ferromagnetic minerals in a rock by coercivity and unblocking temperature properties. *Geophys. Res. Letters* 17 (2), 159-162.

Lybéris, N. , Angelier, J., Barrier, E. and S. Lallemant, 1982. Active deformation of a segment of arc: the strait of Kythira, Hellenic arc, Greece. *Journal of Structural Geology* 4 (3), 299-311.

Lyon-Caen, H., Armijo, R., Drakopoulos, J., Baskoutass, J., Delibassis, N., Gaulon, R., Kouskouna, V., Latoussakis, J., Makropoulos, K., Papadimitriou, P., Papanastasiou, D. and G. Pedotti, 1988. The 1986 Kalamata (South Peloponessos) earthquake: detailed study of a normal fault, evidences for east-west extension in the Hellenic arc. *Journal of Geophysical Research* 93, no. B12, 14967-15000.

Malinvero, A. and W.B.F. Ryan, 1986. Extension in the Tyrrhenian Sea and shortening in the Apennines as result of arc migration driven by sinking of the lithosphere. *Tectonics* 5, 227-245.

Marton, E. and G. Nardi, 1994. Cretaceous paleomagnetic results from Murge (Apulia, southern Italy): tectonic implications. *Geophys.J.Int.* 119, 842-856.

Mary, C., Iaccarino, S., Courtillot, V., Besse, J. and M. Aissaoui, 1993. Magnetostratigraphy of Pliocene sediments from the Stirone River (Po Valley). *Geophy. J.Int* 112, 359-380.

Mascle, J. and L. Martin, 1990. Shallow structure and recent evolution of the Aegean Sea: a synthesis based on continuous reflection profiles. *Mar. Geol.* 94, 271-299.

Mattei, M., Funiciello, R. and C. Kissel, 1995. Paleomagnetic and structural evidence for Neogene block rotations in the central Apennines, Italy. *Journal of Geophysical Research* 100, B9, 17863-17883.

Mattei, M., Kissel, C. and R. Funiciello, 1996. No tectonic rotation of the Tuscan Tyrrhenian margin (Italy) since the late Messinian. *Journal of Geophysical Research 101*, B2, 2835-2845.

Mauritsch, H.J., Scholger, R., Bushati, S.L. and H. Ramiz, 1995. Paleomagnetic results from southern Albania and their significance for the geodynamic evolution of the Dinarides, Albanides and Hellenides. *Tectonophysics 242*, 5-18.

McFadden, P.L. and F.J. Lowes, 1981. The discrimination of mean directions drawn from Fisher distributions. *Geophys. J. R. Astron. Soc. 67*, 19-33.

Meijer, P.Th, and M.J.R. Wortel, 1996. Temporal variations in the stress field of the Aegean region. *Geophys. Res. Lett.* 23, 439-442.

Meijer, P.Th, and M.J.R. Wortel, 1997. Present-day dynamics of the Aegean region: A model analysis of the horizontal pattern of stress and deformation. *Tectonics*, Vol. 16, 879-895.

Mele, G., 1998. High-frequency wave propagation from mantle earthquakes in the Tyrrhenian Sea: New constraints for the geometry of the south Tyrrhenian subduction zone. *Geophys. Res. Lett.* Vol. 25 (15), 2877-2880.

Mercier, J-L, 1976. La néotectonique. Ses méthodes et ses buts. Un exemple: l'arc égéen (Méditerranée orientale). *Revue de géographie physique et de géologie dynamique* (2), vol. XVIII, fasc. 4, 323-346.

Mercier, J, Carey, E., Phillip, H. and D. Sorel, 1976. La néotectonique Plio-Quaternaire de l'arc égéen externe et de la mer Egée et ses relations avec la seismicité. Vème Coll. Géol. Régions Egéennes, Orsay février 1975. *Bull. Soc. Géol. Fr.* (7), 19, 355-372.

Mercier, J-L, Delibassis, N., Gauthier, A., Jarrige, J-J., Lemeille, F., Philip, H., Sébrier and D. Sorel, 1979. La néotectonique de l'Arc égéen. *Revue de géologie dynamique et de géographie physique* 21, fasc. 1, 67-92.

Mercier, J. L., Sorel, D. and K. Simeakis, 1987. Changes in the state of stress in the overriding plate of a subduction zone; the Aegean arc from the Pliocene to the present. *Annales Tectonicae* 1, 20-39.

Meulenkamp, J.E., Hilgen F. and E. Voogt, 1986. Late Cenozoic sedimentary-tectonic history of the Calabrian arc. *Giornale di Geologia* Ser. III 48 (1-2), 345-359.

Meulenkamp, J.E., Wortel, M.J.R., van Wamel, W.A., Spakman, W. and E. Hoogerduyn Strating, 1988. On the Helllenic subduction zone and the geodynamic evolution of Crete since the late Middle Miocene. *Tectonophysics* 146, 203-215.

Meulenkamp, J.E., Van der Zwaan, G.J. and W.A. van Wamel, 1994. On Late Miocene to Recent vertical motions in the Cretan segment of the Hellenic arc. *Tectonophysics* 234, 53-72.

Montigny, R., Edel, J.B. and R. Thuizat, 1981. Oligo-Miocene rotation of Sardinia: K-Ar ages and paleomagnetic data of Tertiary volcanics. *Earth and Planetary Science Letters* 54, 261-271.

Morris, A., 1995. Rotational deformation during Palaeogene thrusting and basin closure in eastern central Greece: palaeomagnetic evidence from Mesozoic carbonates. *Geophys.J.Int.* 121, 827-847.

Morris, A. and M. Anderson, 1996. First paleomagnetic results from the Cycladic Massif, Greece, and their implications for Miocene extension directions and tectonic models in the Aegean. *Earth and Planetary Science Letters* 142, 397-408.

Mullender, T.A.T., A.J. Van Velzen and M.J. Dekkers, 1993. Continuous drift correction and separate identification of ferrimagnetic and paramagnetic contributions in thermomagnetic runs. *Geophys. J. Int.* 114, 663-672.

Muttoni, G., Argnani, A., Kent, D.V., Abrahamsen, N. and U. Cibin, 1998. Paleomagnetic evidence for Neogene tectonic rotations in the northern Apennines. Italy, *Earth and Planetary Science Letters 154*, 25-40.

Muttoni, G., Lanci, L., Argnani, A., Hirt, A.M., Cibin, U., Abrahamsen, N. and W. Lowrie, 1999. Paleomagnetic evidence for a Neogene two-phase counterclockwise rotation in the northern Apennines (Italy). *Tectonophysics*, submitted.

Oldow, J.S., Channel, J.E.T., Catalano, R. and B. D'Argenio, 1990. Contemporaneous thrusting and large-scale rotations in the western Sicilian fold and thrust belt. *Tectonics* 9 (4), 661-681.

Özdemir, Ö., 1990. High-temperature synthesis and thermoremanence of SD maghemite, *Phys. Earth Planet. Inter.* 65, 125-136.

Peeters, F.J.C., Hoek, R.P., Brinkhuis, H., Wilpshaar, M., De Boer, P.L., Krijgsman, W. and J.E. Meulenkamp, 1998. Differentiating glacio-eustacy and tectonics; a case study involving dinoflagellate cysts from the Eocene-Oligocene transition of the Pindos Foreland Basin (NW Greece). *Terra Nova* 10, 245-249.

Rio, D., Raffi, I. And Villa, C., 1990. Pliocene-Pleistocene calcareous nannofossil distribution patterns in the Western Mediterranean. *Proc. ODP Sci. Results* 107, 513-533.

Robertson, A.H.F. and M. Grasso, 1995. Overview of the Late Tertiary-Recent tectonic and palaeo-environmental development of the Mediterranean region. *Terra Nova* 7(2), 114-127.

Sagnotti, L., 1992. Paleomagnetic evidence for a Pleistocene counter-clockwise rotation of the Sant'Arcangelo Basin, southern Italy. *Geoph. Res. Lett.* 19 (2), 135-138.

Sagnotti, L., Mattei, M., Faccenna, C. and R. Funiciello, 1994. Paleomagnetic evidence for no tectonic rotation of the central Italy Tyrrhenian margin since upper Pliocene. *Geophysical Research Letters 21*, no. 6, 481-484.

Scandone, P., 1979. Origin of the Tyrrhenian Sea and Calabrian arc. *Boll. Soc. Geol. It.* 98, 27-34.

Scheepers, P.J.J., 1992. No tectonic rotation for the Apulia-Gargano foreland in the Pleistocene. *Geophysical research Letters 19*, 2275-2278.

Scheepers, P.J.J. and C.G. Langereis, 1993. Analysis of NRM directions from the Rossello Composite: implications for tectonic rotations of the Caltanisetta basin (Sicily). *Earth and Planetary Science Letters* 119, 243-258.

Scheepers, P.J.J., Langereis, C.G. and F.J. Hilgen, 1993. Counter-clockwise rotations in the southern Apennines during the Pleistocene: paleomagnetic evidence from the Matera area. *Tectonophysics* 225 (4), 379-410.

Scheepers, P.J.J., 1994a. Tectonic rotations in the Tyrrhenian arc system during Quaternary and Late Tertiary. (PhD-thesis, Utrecht University) *Geol. Utraiectina* 112, 352 pp.

Scheepers, P.J.J., 1994b. Paleomagnetic evidence for a mjaor counterclockwise rotation in the middle Miocene for the Calabro-Peloritan block. (PhD-thesis, Utrecht University) *Geol. Utraiectina* 112, Chapter 5C 209-227.

Scheepers, P.J.J., 1994c. Some paleomagnetic evidence for clockwise rotations in the Sicilian fold-and-thrust belt during the late Pliocene and the middle Pleistocene. (PhD-thesis, Utrecht University) *Geologica Utraiectina* 112, Chapter 6B 251-265.

Scheepers, P.J.J. and C.G. Langereis, 1994a. Magnetic fabric of clays from the Tyrrhenian arc: a magnetic lineation induced in the final stage of the middle Pleistocene compressive event. *Tectonics* 13 (5), 1190-1200.

Scheepers, P.J.J. and C.G. Langereis, 1994b. Paleomagnetic evidence for counter-clockwise rotations in the southern Apennines fold-and-thrust belt during the Late Pliocene and middle Pleistocene. *Tectonophysics* 239, 43-59.

Scheepers, P.J.J., Langereis, C.G., Zijderveld, J.D.A. and F.J. Hilgen, 1994. Paleomagnetic evidence for a Pleistocene clockwise rotation of the Calabro-Peloritan block (southern Italy). *Tectonophysics* 230, 19-48.

Selvaggi, G. and C. Chiarabba, 1995. Seismicity and P-wave velocity image of the Southern Tyrrhenian subduction zone. *Geophys. J. Int.* 121, 818-826.

Sen, S., Valet, J-P. and C. Ioakim, 1986. Magnetostratigraphy and biostratigraphy of the Neogene deposits of Kastellios Hill (Central Crete, Greece). *Palaeogeography, Palaeoclimatology, Palaeoecology* 53, 321-334.

Smith, A.G. and E.M. Moores, 1974. Hellenides, in: Spencer, A.M. (ed.) Mesozoic and Cenozoic orogenic belts. *Geological Society of London Special Publication* 4, 159-185.

Sorel, D., 1976. Etude néotectonique des îles ioniennes de Cephalonie et Zante et de l'Elide occidentale (Greece). *Thèse du 3ᵉ cycle*, Univ. Paris-Sud, Faculté Sciences Orsay.

Sorel , D., Mercier, J-L., Keraudren, B. and M. Cushing, 1988. The role of slab-pull force in the Plio-Pleistocene geodynamic evolution of the Aegean arc: subsidence and uplift of the external arc and changes in the tectonic regime. *C. R. Acad. Sci. Paris*, t. 307, 1981-1986.

Spakman, W., 1986. Subduction beneath Eurasia in connection with the Mesozoic Tethys. *Geologie en Mijnbouw* 65, 145-153.

Spakman, W., Wortel, M.J.R. and N.J. Vlaar, 1988. The Hellenic subduction zone: a tomographic image and its geodynamic implications. *Geophysical Research Letters* 15, 60-63.

Spakman, W., 1990. Tomographic images of the upper mantle below central Europe and the Mediterranean. *Terra Nova* 2, 542-553.

Spakman, W., Van der Lee, S and R. van der Hilst, 1993. Travel-time tomography of the European-Mediterranean mantle down to 1400 km. *Physics of the Earth and Planetary Interiors* 79, 3-74.

Spakman. W and M. Nyst, 1999. A new approach to the inversion of relative displacement data. *Geophysical Research abstracts* 1, no 1, p 203.

Speranza, F., Kissel, C., Islami, I., Hyseni, A. and C. Laj, 1992. First paleomagnetic evidence for rotation of the Ionian zone of Albania. *Geophysical Research Letters, vol 19*, No 7, 697-700.

Speranza, F. and C. Kissel, 1993. First paleomagnetism of Eocene rocks from Gargano: widespread overprint or non-rotation? *Geophys. Res. Lett. 20*, No. 23, 2627-2630.

Speranza, F., Islami, I., Kissel, C. and A. Hyseni, 1995. Paleomagnetic evidence for Cenozoic clockwise rotation of the external Albanides. *Earth and Planetary Science Letters* 129, 121-134.

Speranza, F., Sagnotti, S. and M. Mattei, 1997. Tectonics of the Umbria-Marche-Romagna Arc (central northern Apennines, Italy): New paleomagnetic constraints. *Journal of Geophysical Research 102*, No. B2, 3153-3166.

Speranza, F., Mattei, M., Naso, G., Di Bucci, D. and S. Corrado, 1998. Neogene-Quarternary evolution of the central Apennine orogenic system (Italy): a structural and paleomagnetic approach in the Molise region. *Tectonophysics 299*, 143-157.

Tari, V. and J. Pamic, 1998. Geodynamic evolution of the northern Dinarides and the southern part of the Pannonian Basin. *Tectonophysics 297*, 269-281.

Tarling, D.H. and F. Hrouda, 1993. The magnetic anisotropy of rocks. Chapman and Hall, London, 217 pp.

Tauxe, L., Besse, J. and J.L. LaBreque, 1983. Palaeolatitudes from DSDP Leg 73 sediment cores implications for the apparent polar wander path for Africa during the late Mesozoic and Cenozoic. *Geophys. J.R.Astron.Soc.* 73, 315-324.

Taymaz, T., Jackson, J. and D. McKEnzie, 1991. Active tectonics of the north and central Aegean Sea. *Geophys. J. Int.* 106, 433-490.

Ten Veen, J.H., 1998. Neogene outer-arc evolution in the Cretan segment of the Hellenic Arc: tectonic, sedimentary and geodynamic reconstructions. (PhD-thesis, Utrecht University) *Geologica Ultraiectina* 160, 192 pp.

Ten Veen, J.H. and P.Th. Meijer, 1998. Late Miocene to Recent tectonic evolution of Crete (Greece): geological observations and model analysis. *Tectonophysics* 298, 191-208.

Triantaphyllou, M.V., 1996. Biostratigraphical and ecostratigraphical observations based on calcareous nannofossils, of the eastern Mediterranean Plio-Pleistocene deposits. (PhD-thesis, Athens University) *Gaia* No. 1, 229 pp.

Triantaphyllou, M.V., Drinia, H. and M.D. Dermitzakis, 1997. The Plio-Pleistocene boundary in the Gerakas section, Zakynthos (Ionian Islands). Biostratigraphical and paleoecological observations. *N.Jb.Geol.Paläont.Mh.*1, 12-30.

Underhill, J.H., 1988. Triassic evaporites and Plio-Quaternary diapirism, western Greece. London, England, *Geological Society Journal* 145, 269-282.

Underhill, J.H., 1989. Late Cenozoic deformation of the Hellenide foreland, western Greece. *G.S.A. Bull* 101, 613-634.

Valente, J-P., Laj, C., Sorel, D., Roy, S. and J.-P. Valet, 1982. Paleomagnetic results from Mio-Pliocene marine sedimentary series in Crete. *Earth and Planetary Science Letters* 57, 159-172.

VandenBerg, J., Klootwijk, C.T. and A.A.H. Wonders, 1978. Late Mesozoic and Cenozoic movements of the Italian Peninsula: Further paleomagnetic data from the Umbrian sequence. *Geological Society of America Bulletin* 89, 133-150.

Van der Meulen, M.J., Meulenkamp, J.H. and M.J.R. Wortel, 1998. Lateral shifts of Apenninic foredeep depocentres reflecting detachment of subducted lithosphere. *Earth and Planetary Science Letters* 154, 203-219.

Van der Voo, R., 1993. Paleomagnetism of the Atlantic, Tethys and Iapetus oceans. *Cambridge University Press*, 411 pp.

Van Dijk, J.P. and P.J.J. Scheepers, 1995. Neotectonic rotations in the Calabrian arc; implications for a Pliocene-Recent geodynamic scenario for the central Mediterranean. *Earth-Science Reviews* 39, 207-246.

Van Hoof, A.A.M. and C.G. Langereis, 1991. Reversal records in marine marls and delayed acquisition of remanent magnetization. *Nature* 351, 223-225.

Van Hoof, A.A.M., Van Os, B.J.H., Rademakers, J.G., Langereis, C.G. and G.J. De Lange, 1993. A paleomagentic and geochemical record of the upper Cochiti reversal and two subsequent precessional cycles from southern Sicily (Italy). *Earth and Planetary Science Letters* 117, 235-250.

Van Velzen, A. and J.D.A. Zijderveld, 1990. Rock magnetism of the Early Pliocene Trubi formation (Sicily). *Geophys. Res. Lett.* 17, 791-794.

Van Velzen, A.J. and J.D.A. Zijderveld, 1992. A method to study alterations of magnetic minerals during thermal demagnetisation applied to a fine-grained marine marl (Trubi formation, Sicily). *Geophys.J.Int.* 110, 79-90.

Van Velzen, A.J., Dekkers, M.J. and J.D.A. Zijderveld, 1993. Magnetic iron-nickel sulphides in Plio-Pleistocene marine sediments from the Vrica section (Calabria, Italy). *Earth and Planetary Science Letters* 115, 43-56.

Vigliotti, L., Alvarez, W. and M. McWilliams, 1990. No relative rotation between Corsica and Sardinia. *Earth and Planetary Science Letters 98*, 313-318.

Vigliotti, L. and V.E. Langenheim, 1995. When did Sardinia stop rotating? New paleomagnetic results. *Terra Nova 7*, 424-435.

Wegener, A., 1912. Die Enstehung der Kontinente. *GRZAG 3*, 276-292.

Westaway, R., 1991. Continental extension on sets of parallel faults: observational evidence and theoretical models, In: A.M. Roberts, G. Yielding and B. Freeman (eds.), The Geometry of Normal Faults, *Geol. Soc. London Spec. Publ. 56*, 143-169.

Westaway, R., 1993. Quaternary uplift of southern Italy. *Journal of Geophysical Research*, vol. 98, no. B12, 21741-21772.

Westaway, R., 1996. Quaternary elevation change of the Gulf of Corinth in central Greece. *Phil. Trans. R. Soc. London. A 354*, 1125-1164.

Westphal, M., Kondopoulou, D., Edel, J. and S. Pavlides, 1991. Paleomagnetism of Tertiary and Plio-Pleistocene formations from N. Greece. *Bulletin of the Geological Society of Greece 25*, 239-250.

Wortel, M.J.R. and W. Spakman, 1992. Structure and dynamics of subducted lithosphere in the Mediterranean region. *Proc. K. Ned. Akad. Wet. 95* (3), 325-347.

Zachariasse, W.J. and M.P. Aubry, 1994. Origin and early dispersal of *Neogloboquadrina*. *Paleobios* 16, 68 pp.

Zanella, E., 1998. Paleomagnetism of Pleistocene volcanic rocks from Pantelleria Island (Sicily Channel), Italy. *Physics of the Earth and Planetary Interiors 108*, 291-303.

Zijderveld, J.D.A., 1967. Demagnetisation of rock: analysis of results. Collinson, D.W., Creer, K.M. and Runcorn, S.K. (Eds.), *Methods in paleomagnetism*. Elsevier, Amsterdam, pp. 254-386.

Zijderveld, J.D.A., Zachariasse, W.J., Verhallen, P.J.J.M. and F.J. Hilgen, 1986. The age of the Miocene-Pliocene boundary. *Newslett. Stratigr.* 16, 169-181.

Zijderveld, J.D.A., Hilgen, F.J., Langereis, C.G., Verhallen, P.J.J.M. and W.J. Zachariasse, 1991. Integrated magnetostratigraphy and biostratigraphy of the upper Pliocene-lower Pleistocene from the Monte Singa and Crotone areas in Calabria, Italy. *Earth and Planetary Science Letters* 107, 697-714.

Epilogue

Paleomagnetism has played a crucial role in one of the major scientific discoveries in the Earth Sciences: continental drift and plate tectonics. Looking back after roughly 40 years, it seems almost unbelievable that the rocks used in the earlier studies gave the appropriate results. We now know that the quality of much of the old paleomagnetic data was not according to modern standards. Indeed, technology has evolved. Still the elegant hypothesis of plate tectonics remains: where two plates are moving apart new oceanic crust is formed, and where two plates converge one plate usually descends. This process is monitored by the Earth's magnetic field, acting both as a chronometer and as a recording medium of plate movements.

Earth scientists make use of paleomagnetism in establishing accurate time scales. On the basis of these time scales detailed tectonic reconstructions can be made. Recently, environmental studies utilise these time scales. Many disciplines, like (bio)stratigraphy, structural geology, geochemistry, geodesy can greatly benefit from combining their results with paleomagnetism, and vice versa. Moreover, the early hypotheses on the geodynamic evolution of the Mediterranean arose from paleomagnetic data. Often, various disciplines propose geodynamic evolutions for the Mediterranean which do not agree with the paleomagnetic observations. This is easily overcome if one argues that paleomagnetic data at best reflect local or crustal movements. Of course, if paleomagnetic observations agree with certain models, they are considered a confirmation of the hypothesis.

More than 10 years ago, Kissel and Laj (1988) provided the earth scientists working in Greece with a tectonic reconstruction based on paleomagnetic data. By integrating geodesy and bio- and cyclostratigraphy we have been able to add value to the research previously done in the same area, using the same sediments. Although expertise and technology has developed and has led to more reliable results, time has proven to be crucial in understanding the evolution of the Mediterranean. Hence, this integration involves a first but essential step in our efforts to comprehend timing and relations of tectonic processes in the Mediterranean. In this case, it has led to a better understanding of the Neogene tectonic evolution of the Tyrrhenian and Aegean arc. By incorporating accurate timing, we obtained information on tectonic events encompassing large geographic areas, which otherwise could not have been discovered. Furthermore, we combined our paleomagnetic results with geodesy. The onset of this combination already led to important new findings. This tells us that an integrating approach works and is the only way to go.

A thesis can never be complete. Perhaps in the next 10 years, new developments may lead to yet another and even more detailed tectonic reconstruction for the central Mediterranean. Although not all late Neogene sediments in the central Mediterranean have been sampled (yet), there seems little advantage in simply increasing the number of sampling localities. Still lacking is a reliable reconstruction of the Mediterranean for the early Neogene. Long stratigraphic sections of this period are notoriously hard to find, and far from suitable to establish an accurate tectonic reconstruction. It would be more fruitful to expand the combination with other disciplines, for instance geodesy, modelling, tomography and dating tools. Geodesy and paleomagnetism both shed light on upper

crustal movements, but on a different time scale. In addition, it is useful to further develop the connection with structural geology, by investigating the anisotropy of the magnetic susceptibility (AMS) and of the anhysteretic suseptibilty (AAS) in terms of the local versus regional strain.

I am confident in saying that this paleomagnetic research has solved yet another important part of the complicated Mediterranean puzzle, but, perhaps more importantly, it forms a firm basis for future integrated research.

Samenvatting

Summary in Dutch

Het Middellandse Zeegebied is waarschijnlijk, geologisch gezien, een van de meest onderzochte gebieden. Mijns inziens niet verwonderlijk, aangezien dit gebied naast een heerlijk klimaat, lekker eten en prachtig natuurschoon, ook een rijke geologische historie herbergt. Het ontstaan van de Middellandse Zee is zeer gecompliceerd vanwege diverse grote en kleine plaat interacties, die uiteindelijk geleid hebben tot de huidige configuratie. Om een deel van deze gecompliceerde puzzel op te lossen, hebben wij ons beperkt tot het verzamelen van materiaal uit Griekenland and Italië. De onderzochte gesteenten/ sedimenten uit deze gebieden hebben een ouderdom van 10 miljoen jaar en jonger. Het belangrijkste deel van dit onderzoek betrof het paleomagnetisch analyseren van de gesteente monsters. Deze analyses geven onder andere informatie over het (horizontaal) bewegen van platen (of delen daarvan) over onze aarde door de tijd. Vervolgens zijn onze paleomagnetische gegevens gecombineerd met andere gegevens die ook verborgen zitten in de sedimenten; bijvoorbeeld ouderdomsbepalingen (o.a. m.b.v. fossielen) en verticale bewegingen van vroeger en nu.

Italië

In de zeventiger jaren hebben een aantal onderzoekers met behulp van paleomagnetisme (Channel and Tarling, 1975; Vandenberg et al., 1978) bewegingen van Italië waar genomen. Bovendien, ontdekten zij dat het Italiaanse schiereiland aan Afrika had vast gezeten vanaf het vroeg Jura tot het vroeg Tertiair (dus van ongeveer 200 tot 65 miljoen jaar geleden). Vervolgens is het Italiaanse schiereiland onafhankelijk van Afrika gaan bewegen vanaf ongeveer 50 miljoen jaar geleden. Na deze belangrijke ontdekkingen, hebben de (paleomagnetische) onderzoekers zich vooral gericht op het gedetailleerder beschrijven van deze bewegingen door de tijd. Hierdoor is bijvoorbeeld ontdekt dat Italië bestaat uit diverse blokken die soms wel, en soms niet samen bewegen.

Recentelijk werk, beschreven in het proefschrift van Scheepers (1994), heeft verschillende tektonische rotatie fasen (= draaiingen in het horizontale vlak) opgeleverd. De resultaten laten zien dat de zuidelijke Appenijnen in het Pleistoceen (laatste 1.81 miljoen jaar) een rotatie tegen de klok in hebben doorgemaakt, waarbij Calabrië gelijktijdig met de klok mee bewoog. Oudere sedimenten uit Calabrië suggereren eveneens een rotatie fase die plaats vond in het laat Mioceen (om en nabij de 7 à 8 miljoen jaar). Bovendien lijkt Sicilië een midden Pliocene (3 miljoen jaar) rotatie te hebben ondergaan. Het Apulische platform, of wel het uitsteeksel van Afrika wat momenteel voor een groot deel onder de Adriatische zee ligt, heeft geen rotatie meer ondervonden sinds het laat Plioceen (2 miljoen jaar). Het werk van Scheepers heeft een aantal onbeantwoorde vragen opgeroepen, aangaande de exacte timing van de Miocene rotatie in Calabrië en de Pliocene rotatie in Sicilië; dit vormde de basis van het nu voor u liggende proefschrift.

In **Hoofdstuk 1** is de datering van de (Miocene) rotatie van Calabrië beschreven, die gerelateerd kan worden aan de opening van de Tyrrheense zee. Bovendien voorziet dit hoofdstuk in een methode om bruikbare paleomagnetische resultaten uit gedeformeerde sedimenten te verkrijgen.

Calabrië blijkt een belangrijke rotatie fase te hebben ondergaan die nu exact gedateerd is tussen 8.6 en 7.6 miljoen jaar. Uit de literatuur is bekend dat Calabrië aan Sardinië heeft vastgelegen en vervolgens naar het zuidoosten is bewogen tot haar huidige positie. Dit proces is gepaard gegaan met het openen van de Tyrrheense zee. Wanneer de opening exact heeft plaatsgevonden is reeds lang een discussiepunt. Er is bekend vanuit boringen dat de oudste zeeafzettingen ten oosten van Sardinië gelegen zijn en deze hebben een ouderdom van ongeveer 7.8 miljoen jaar. Derhalve, denken wij dat de opening van de Tyrrheense zee tussen de 8.6 en 7.8 miljoen jaar begonnen is.

In **Hoofdstuk 2** wordt de Pliocene rotatie van (het Caltanisetta bekken in) Sicilië belicht, die waarschijnlijk te maken heeft met een Mediterrane verandering. De rotatie is nu precies gedateerd op 3.21 miljoen jaar en duurde 80 tot 100 duizend jaar, wat geologische gezien erg kort is. Deze rotatie vindt plaats op een moment dat het Caltanisetta bekken een stuk ondieper wordt. Gelijktijdig versneld de opening van de Tyrrheense zee en treedt er een paleoceanografische verandering op in de oostelijke Middellandse zee. Derhalve beschouwen wij deze Pliocene rotatie als een regionaal verschijnsel van een groter proces wat wellicht de gehele (centraal-oostelijke) Middellandse zee omvatte.

Griekenland

Vanwege de combinatie paleomagnetisme en gedetailleerde biostratigrafie, zijn we in staat geweest om tektonische processen in Italië zeer nauwkeurig te bepalen. Daarom is vervolgens besloten om naar Griekenland te gaan en dezelfde aanpak te proberen. We wilden zien of rotaties in Griekenland gelijktijdig en even snel plaatsgevonden hebben en daarvoor hebben we de gehele Griekse eilanden boog en een deel van het vaste land bezocht en bemonstert.

Allereerst hebben we oude Miocene data van Kreta ge-herinterpreteerd, wat beschreven is in **Hoofdstuk 3**. Het blijkt dat de sedimenten van Kreta voornamelijk een tegen de klok in beweging hebben ondergaan. Dit in tegenstelling tot wat bekend is uit de literatuur (Valente et al., 1982; Laj et al., 1982). Eerder studies suggereren geen enkele beweging voor Kreta in de afgelopen 7 miljoen jaar.

Vervolgens hebben we het Ionische eiland Zakynthos bezocht, omdat dit eiland vele zeeafzettingen kent van diverse ouderdommen. Zeeafzettingen zijn zeer goed te dateren aan de hand van hun fossiel-inhoud. **Hoofdstuk 4** beschrijft de resultaten, die aangeven dat Zakynthos een kloksgewijze rotatie heeft ondergaan tussen 0.77 miljoen jaar en nu.

Eerder werd gedacht (Kissel en Laj, 1988) dat een continue rotatie sinds 5 miljoen jaar heeft plaatsgevonden. Maar, mede doordat we meer en jongere sedimenten hebben bemonsterd met een zeer goede tijdscontrole, hebben we andere conclusies moeten trekken.

Aangezien onze aanpak vruchten leek af te werpen, hebben we besloten om de rest van de Egeïsche boog te bezoeken (**Hoofdstuk 5**). De resultaten geven aan dat de gehele boog zeer jonge rotaties heeft ondergaan. De westelijke boog is met de klok meegedraaid vanaf ongeveer 0.77 miljoen jaar en de oostelijke tegen de klok in vanaf ongeveer 2 miljoen jaar.

Dit staat lijnrecht tegen over de alom bekende resultaten van Kissel en Laj (1988). Zij concludeerden op basis van hun paleomagnetische data dat de Egeïsche boog ontstaan is in twee fasen. De eerste fase, tijdens het laat Mioceen, resulteerde in kloksgewijze draaiing van Epirus en een tegen de klok in beweging van westelijk Anatolië. De tweede, continue deformatie, fase zou plaats gevonden moeten hebben in de laatste 5 miljoen jaar. Deze fase zorgde ervoor dat slechts het westelijk deel van de Egeïsche boog een verdere draaiing ondervonden heeft. Bovendien, zouden Kreta en Rhodos geen beweging hebben ondergaan sinds 7 respectievelijk 5 miljoen jaar. Dit alles zou geleid moeten hebben tot het ontstaan van de Egeïsche boog.

Onze resultaten laten zien dat er geen sprake is van een continue formatie van de Egeïsche boog sinds de laatste 5 miljoen jaar, maar dat er rotaties hebben plaatsgevonden in de laatste 1 à 2 miljoen jaar. Aangezien het onwaarschijnlijk is dat een gehele boog in 1 miljoen jaar kan ontstaan, zal er een ander proces een dominante rol gespeeld hebben in de vorming van de boog. We suggereren dat de boog voornamelijk door grootschalige translaties is ontstaan, hetgeen een belangrijk gegeven is voor modelstudies die de evolutie van de Egeïsche boog beschrijven. Aangezien de gevonden rotaties erg jong blijken te zijn, hebben we vervolgens gekeken naar de huidige bewegingen van Griekenland. Deze blijken zeer goed overeen te komen, met onze bevindingen; voornamelijk kloksgewijze draaiingen in de westelijk boog en in de oostelijke boog draaiingen tegen in de klok in. De jonge rotaties vinden plaats in een tijd (ongeveer 1 miljoen jaar geleden) waar het tektonische regime in het Egeïsche gebied drastisch verandert.

Overzicht

In **Hoofdstuk 6** geven we een overzicht van alle paleomagnetische data uit het centrale Middellandse zeegebied. Het blijkt dat het westelijke Middellandse zeegebied voornamelijk tegen de klok in bewegingen heeft ondergaan, terwijl het oostelijke Middellandse zeegebied een kloksgewijze beweging heeft ondervonden. In Italië, zijn er ook gebieden die geen rotatie hebben ondergaan. Deze gebieden hebben zich door de tijd heen, geografisch naar het zuiden uitgebreid. In het algemeen, passen de paleomagnetische data goed in het geodynamische model wat veronderstelt dat inscheuren van de Afrikaanse plaat door de tijd heen lateraal (van het noordwesten naar het zuidoosten) migreert. Tenslotte vinden we zowel in Italië als in Griekenland even

jonge Pleistocene rotaties, die in beide gevallen gepaard gaan met grote tektonische veranderingen. Deze veranderingen zorgen onder andere voor grote opheffing van zuid Italië en noordwest Griekenland. Het lijkt erop dat zowel onder zuid Italië als onder noordwest Griekenland de Afrikaanse plaat tegelijkertijd inscheurt, of dit met elkaar in verband gebracht kan worden moet toekomstig onderzoek uitwijzen.

Nabeschouwing

Met het paleomagnetisch onderzoek wat beschreven is in dit proefschrift, zijn we weer een stap verder gekomen in onze kennis over de vorming van de Middellandse zee. Vanwege de integratie met diverse disciplines (bio- en cyclostratigrafie en geodesie) zijn we in staat geweest om uit stenen, die reeds eerder door andere teams onderzocht zijn, belangrijke nieuwe informatie te verkrijgen, voornamelijk wat betreft de tijdscontrole van diverse tektonische gebeurtenissen. Dit heeft ertoe geleid dat bepaalde gebeurtenissen over grote geografische gebieden herkend konden worden.

Ondanks vele nieuwe gegevens, is een proefschrift nooit helemaal gereed. Misschien dat in de komende jaren nieuwe ontwikkelingen ertoe zullen leiden dat er nog meer informatie uit de stenen gehaald kan worden, zodat er een weer een gedetailleerde reconstructie van de Middellandse zee gemaakt kan worden. We missen nog een vergelijkbare detailstudie van voor 10 miljoen jaar geleden. Helaas zal dat moeilijk op te lossen zijn, aangezien er niet veel goede sedimenten van die ouderdom in de Middellandse zee te vinden zijn. Naar alle waarschijnlijkheid, zal (verdere) integratie met bijvoorbeeld geodesie, numeriek modelleren, gedetailleerde dateringsmethoden en stukturele geologie meer vruchten af werpen. Ik denk dat we met dit proefschrift een goede basis hebben gelegd voor toekomstig geïntegreerd onderzoek.

Site locations and descriptions

Sections and sites from Italy

Location of sites/sections is based on route maps of Atlante stradale d'Italia; Touring Club Italiano, scale 1:200.00

BOG, Borgato Gannano, South Basilicata, 1 site with 17 levels (Sud/blz.17/B4)
This section was previously described by *Lentini* in *1969*, as middle Pliocene to lower Pleistocene.
The section can be found along the road from Borgato Gannano to Stigliano, after Borgato Gannano (~2.8 Km) first track left.

CAN, Canolo Nuovo, South Calabria, 1 site with 10 cores. (Sud/blz.25/A6)
This roadoutcrop contains Oligo-Miocene clays and can be found along the road of Canolo to Canolo Nuovo, after the hairpin on the right just below the top (opposite two houses and barns).

CAR, Cariati, Middle Calabria, 1 site with 9 cores (Sud/blz.21/E6)
The Pliocene clay can be found just outside Cariati, direction Campana; Take the track at Ponte Varco to a soccer playground.

EPI, Episcopia, South Basilicata, 1 site with 9 cores (Sud/blz.17/E2)
These highly fractured Tortonian clays can be found along the national road of Episcopia to Latronico. Before the road crosses the autostrada, take the track left to the pastures near the riverbed, at the exit Agromente.

GOR, Gorgolione, South Basilicata, 1 site with 9 cores (Sud/blz.17/A2)
This ?Pliocene? site (one of my favourites) can be found at the Fiumarella Gorgolione, under the bridge.

LES, Lese, Middle Calabria, 1 site with 81 cores (Sud/blz.23/A6)
This section, containing cyclic Tortonian clays, is named after the Lese river, which runs in front of the section. To reach the section: follow a road (unknown number) from the SS107 direction Verzino and walk through the pastures in the valley of the Lese. Take care of the snakes.

MAR, Monte Arancio, Sicily, 2 sites with 17 cores (Sud /blz.30/C7,D7)
The sites are found in a quarry on the SS188B at the base of the Monte Arancio. The outcrop contains clays overlain by a regressive Pliocene sequence.

MART, Martone South, Calabria, 1 site with 9 cores (Sud/blz.25/A7)
The outcrop is formed by a small piece of Miocene clay just outside Martone. To reach
the outcrop: Entering the village (from the "main" road), keep right at all crossings,
opposite a little well from 1955.

MAS, Masella, South Calabria, 1 site with 8 cores (Sud/blz.25/F3)
These middle Miocene clays are found on the right side along the road direction
Montebello Ionico, before the village of Masella, under conglomerates, near a bridge.

MOT, Motta San Giovanni, South Calabria, 1 site with 7 cores (Sud/blz.25/E3)
This roadoutcrop, containing Miocene clay, can be reached from the village of Motta
San Giovanni direction graveyard (cimetrio) in the valley.

MUR, le Murgie, Middle Calabria, 1 site with 9 cores (Sud/blz.23/A7)
These Tortonian clays are found on the right along the road of San Nicola dell'Alto to
Strongoli, after descending in a left-turning curve.

PER, Perticaro, Middle Calabria, 1 site with 9 cores (Sud/blz.23/A6)
This outcrop is situated outside Perticaro, on the road from Verzino to Umbriatico, just
after the Strongoli exit, turn right before the bustop. The Tortonian clays are found
below a little sandy hill.

PRL, Poggioreale, Sicily, 3 sites with 29 cores (Sud/blz.26/F6,7)
Two sites can be found along the main road, behind the "old" village of Poggioreale.
These Trubi sediments are found in a small quarry-like exposure with a fault, dividing
the outcrop into two sites.
The third site is found along the SS 624 between km 53-54.

PRU, Prunella, South Calabria, 1 site with 11 cores (Sud/blz.25/F4)
These middle Miocene clays are found in a little quarry, outside Prunella, along the
riverbed.

PUS, Punta Secca, Sicily, 1 site with 93 levels. (Sud/blz.31/E2)
This coast section can be reached from Siculiana direction Punta Secca, and contains
the Trubi-Narbone transition.

RI, Ribera, Sicily, 166 cores.
Ribera is the detail set of the Secca Grande section, covering the Trubi-Narbone
transition.

SGR, Secca Grande, Sicily, 1 site met 92 cores (Sud/blz.30/F8)
The outcrop is found behind the village of Secca Grande, is formerly known as the *Ribera* section and contains the Trubi-Narbone transition. The type locality of an olisostrome was defined here. The section was extended on the other side of the valley, stratigraphically above the olisostrome.

SI, Siculiana, Sicily, 73 cores.
Siculiana is the detail set of the Punta Secca section, covering the Trubi-Narbone transition.

SNI, San Nicola dell'Alto, Middle Calabria, 7 sites (Sud/blz.23/A6)
These sites contain Tortonian clays and can be found below the village of San Nicola dell' Alto in the valley.

Sections and sites from Greece

Location of sites/sections are mostly based on touristic route maps.

AA, Aghios Andreas, NW Peloponessos, 1 site with 12 levels.
The outcrop consists of very soft Plio-Pleistocene clay along the coast near Katakolon direction Aghios Andreas.

AGA, Moni Agarathou on Crete (SE of Iraklion), 1 site with 9 cores.
This Pliocene outcrop is found along the road from Sambus to Moni and consists of alternating laminated (clayey) sands with homogeneous sands.

AK, Ancient Kameiros, NW Rhodos, 1 site with 5 levels and 32 cores.
The extensive Pliocene outcrop can be found on the main west coast road, towards Rhodos town, as enormous sandbodies intercalated with clays, containing Theodoxus shells.

ALA, Alatron, on (Ionian zone) Lefkas, 6 sites with 44 cores.
The Burdigalian to Langhian marls and turbidites are located on the road from Nidri to Katachorion, then direction Kharadiatika and finally, just before the village, towards Alatron on a steep track, up hill.

ALE, Alikanes, Zakynthos, 2 sites with 20 cores.
Middle Pliocene clay alternating with sandlayers are situated along the north coast, below a small garbage belt under a cliff.

ALF, Alfioussa, NW Peloponessos, 6 sites with 42 cores.
Four sites are located on the road, outside Alfioussa direction coast. Two other sites are on the coast-road from Kiparissia to Pyrgos, outside Epitalion, in a small cliff. All sites are probably Pliocene.

ALI, Aliphera, NW Peloponessos, 1 handsample.
Eocene (Tripolitsa) flysch is found on the road from Krestena to Andritsena, before the Aliphera exit.

ALO, Ormos Alikon, Zakynthos, 6 sites with 48 cores.
Tortonian clays with sapropels can be found along the north coast, on the NW-side of the bay, opposite Alikanes.

AM, Amoopi, Karpathos, 1 site with 15 cores.
Some Pliocene? clays between sands can be found, south of Karpathos/Pigadia near the village of Amoopi.

AMA, Ayia Marina, Zakynthos, 1 handsample.
Upper Cretaceous massive laminated limestones are situated outside the village, direction bar.

AMO, Ammoa, Kassos, 1 core.
Pleistocene? red (loose) clayey sands in between conglomerates are located near the little church of Ammoa, on the beach.

ASH, ash layer near Skaloniti, SE Rhodos, 17 cores.
The outcrop contains a thick Oligo-Miocene ash layer, follow the riverbed for about an hour by foot.

AV, Avlemonas, Kythira, 2 sites with 14 cores.
Shallow middle Pliocene sediments are found in a ditch, along the road Paleopoli-Avlemonas.

BOC, Bochali, Zakynthos, 4 sites with 43 cores.
The Pleistocene sites (blue clays between sands) are all situated in NE Zakynthos. One site was found along the Akrotiri road (follow the sign "best view in town") in a pit. The second one is located on the left along the road of Akrotiri to Zakynthos, just before the "best view in town" sign. The last two sites are found along the cliffs near the coast, NE of Zakynthos Town.

CHE, Chelatros, Kassos, 3 sites with 24 cores.
Miocene clay and thin laminated limestones are found on the road to Aghios Georgos/Chelatros and towards the bay.

CHO, Kenouri Chorio, on Crete (SE of Iraklion), 1 site with 8 cores.
The outcrop consists of Pliocene Trubi-like sediments on the road near Kenouri Chorio.

CHR, Chrysophyli, NW Peloponessos, 5 sites met 15 monsters.
?Older than middle Pliocene clay alternating with lignite is found in a small open pit mine, on the road from Zacharo to Arini and finally to Tripiti.

COR, Corinth Canal, NE Peloponessos, 1 site met 43 cores.
The Corinth Canal contains mostly sands but also some sandy Plio/Pleistocene clays.

ERI, Erimanthos, NW Peloponessos, 23 sites with 90 cores.
The Pliocene red coloured sites are located on a dirt road and can be reached from Olympia direction Lala, towards Nemouta and finally take the track to Chora into the valley.

FA, Faliraki, Rhodos, 1 site with 13 cores.
The small upper Pliocene? Faliraki outcrop is situated in the NE corner of the island, in the village.

FB, Faliraki Beach, Rhodos, 3 sites with 19 cores.
The upper Pliocene? Faliraki Beach outcrop is formed by a little cliff containing several clay layers, just outside Faliraki and before Ladiko bay.

FIG, Kato Figalia, W Peloponessos, 1 handsample.
The steeply dipping limestone outcrop of Kato Figalia can be found taking the exit Kato Figalia from the mainroad Kiparissia to Zacharo, continuing along this road through forests.

FOR, Fortetsa on Crete, 1 site with 10 cores.
The Pliocene thin laminated Fortetsa diatomites are located south of Iraklion, into the valley (see thesis Jonkers, 1984).

GAL, Aghios Gallini, south central Crete, 2 sites with 16 cores.
Pleistocene? red conglomerates with some clay layers are found along the road from Aghia Gallini towards Festos.

GER, Gerakas, Zakynthos, 2 sites with 30 cores.
Plio/Pleistocene clays can be found along Cape Gerakas in the so-called moonvalley.

GIT, Gythion, South Peloponessos, 7 sites with 22 cores.
These upper Pliocene sites are situated along the coast-road from Gythion to Skala and represent a transition from a continental to marine environment.

GRI, Grillos, NW Peloponessos, 2 sites with 14 cores.
Upper Pliocene clays are found on the road from Krestena, direction Andritsena just outside Grillos.

GVR, Glikovrisi, South Peloponessos, 2 sites with 17 cores.
Upper Pliocene can be found in ditches along the coast-road from Kato Glikovrisi to Elaea.

HER, Chersonissos, on Crete (west of Iraklion), 1 site with 8 cores.
The laminated Miocene clays alternating with homogeneous intervals are situated west (just before) of Chersonissos.

HOT, hot section is situated on Milos, 98 levels with 292 cores.
The Pliocene hot section contains a rhythmic alternation of clays and sapropels and is situated in the NW corner of Milos, near the Tsondola hill.

IO, Aghios Ioannis, South Karpathos, 3 sites with 29 cores.
The Pliocene small clay hills of Aghios Ioannis are located on the plains near the airport, near windmills and Aghios Ioannis. These hills have many different bright colours, alternating with diatomites and manganese/sand layers.

KA, Kallithea, on Rhodos, 2 sites with 15 cores.
Upper Pliocene? coarse grained sediments are found along the main coast-road in the NE corner of Rhodos.

KAL, Kalithea, W Peloponessos, 1 site met 12 cores.
The Pliocene clays of Kalithea were located in a garden (now covered with concrete) along the road Krestena - Andritsena, near Kalithea, next to a petrol station (KMOIL).

KAP, Kapsali, S Kythira, 6 sites with 32 cores.
The terrigeneous clastic Miocene? outcrop is situated along the road, with a beautiful view on Chori and Kapsali.

KAT, Katakolo, NW Peloponessos, 2 sites with 15 cores.
Highly fractured uppermost Pliocene to lowermost Pleistocene clay is found in Katakolo, behind the harbour.

KE, Keri, Zakynthos, <u>3 sites</u> with 9 cores.
The Keri outcrop is formed by <u>Eocene</u> limestones alternating with marls, along the road to Keri in the forest.

KEF, Kefalas, central Peloponessos, <u>3 sites</u> with 26 cores.
These upper Pliocene sites are situated in the vicinity of Sparta, on the road to Kefalas, near Skoura. One of the sites is located in Skoura, opposite the graveyard, along a small stream near a garbage dump.

KIL, Kilini, NW Peloponessos, <u>35 levels</u> with 122 cores.
Kilini is a <u>Pleistocene</u> sections along the beach containing clays and some sand intercalations. The top is formed by thick sandy deposits.

KLB, Kalamaki beach, Zakynthos, <u>35 levels</u> with 63 cores.
At Kalamaki beach thick evaporite layers are alternating with fresh blue clays. This <u>Messinian</u> part is overlain by some meters of <u>Pliocene</u> "Trubi" sediments.

KO, Kolimbia beach, E Rhodos, <u>7 levels</u> with 35 cores.
The <u>uppermost Pliocene</u> sandy clay layers of Kolimbia can be found in small cliff at the beach.

KOL, Kolivata, Lefkas, <u>4 levels</u> with 20 cores.
This wonderful <u>Langhian</u> outcrop (in the Ionian zone) is situated near the village of Kolivata. It can be reached from the only square in town, direction valley, crossing (a mostly dry) stream. Beware of big spiders.

KOM, Komilio, Lefkas, <u>2 sites</u> with 16 cores.
The <u>Mid-upper Miocene</u> steep cliff (in the Pre-Apulian zone) is found along the road of Aghios Petros (SW) to Khortata (NW), just after the Komilio exit on the right-hand side.

KOR, Koroni, W Peloponessos, <u>4 sites</u> met 28 monsters.
The <u>Pliocene</u> clay of Koroni is found in an old lignite quarry (partly under water), on the road from Koroni to Falanti, behind the village.

KOU, Koutres, central Crete, <u>2 sites</u> with 16 cores.
The <u>Pliocene</u> hill, containing homogeneous and laminated marl/clay intervals, is situated in the deserted village of Koutres, near Zaros.

KRI, Krionero, NW Peloponessos, <u>8 sites</u> met 25 monsters.
The sites containing <u>Pliocene</u> clays can be reached after taking the road from Olympia to Lalas, turn left before the village of Lalas, immediately left again, keep left and after

4 km the village of Krioneri is reached. The sites are situated along the road to Chelidoni just outside Krioneri.

LA, Ladiko, Rhodos, 1 site with 13 cores.
Pliocene blue clays are found in the NE corner of the island, at the S-side of Ladiko beach, behind a restaurant.

LAG, Lagopodo, Zakynthos, 5 sites with 39 cores.
The Aquitanian, Burdigalian, Late Burdigalian, Langhian-Serrevalian, Serrevallian outcrops are located on the road of Kiliomeno to Lagopodo, after the limestone quarry.

LAL, Lalas, NW Peloponessos, 12 sites with 87 cores.
The sandy coarse grained Pliocene Lalas section is found on the road from Olympia to Lalas.

LAZ, Lazarata, Lefkas, 1 handsample.
Middle Miocene, late Burdigalian marls are found on the road from Lefkada to Lazarata.

LEF, Lefko, Karpathos, 10 sites with 30 cores.
Plio-Pleistocene sandy clays and conglomerates are found along the beach at Lefko.

LIA, Cape Liakas, Kefallonia, 27 levels with 112 cores.
This Messinian section ("heroic section") can be reached (difficult!) along the beach and rocks at Cape Liakas.

LIP, Galipe, Crete SE of Iraklion, 1 site with 8 cores.
Pliocene yellow homogeneous and laminated marls are found along the road outside Galipe village.

LIT, Lithakia, Zakynthos, 3 sites with 26 cores.
Miocene?/Oligocene? laminated blue limestones (weathering colour is blue/grey) can be reached from Lithakia, take the road to the Cretaceous limestone belt, turn right before a small quarry onto a gravel road.

LMN, Limnou Keriou north, Zakynthos, 31 levels with 97 cores.
Along the beach, Messinian sand and clay alternations are found, which can be reached only with a (small) boot.

LMS, Limnou Keriou south, Zakynthos, 4 sites with 12 cores.
A small Tortonian outcrop of marls and sapropels is found at the bay of Limnou Keriou.

LUX, Luxurion, Kefallonia, 46 levels with 158 cores.
South of Luxurion, Plio/Pleistocene clays and sapropels can be found along the coast.

MA, Marathia, Zakynthos, 4 sites with 32 cores.
Blue marine Langhian marls can be found in a small bay, on a track from Keri to Marathia, near a restaurant down at the beach.

MAN, Manitochori, Kythira, 2 sites with 14 cores.
Miocene clay is found along the road from Kythira to Mantochori, just outside the village on the left side.

MAM, Aghios Mama, Kassos, 2 sites with 14 cores.
Miocene limestones and conglomerates are situated along a track from Fry to Aghios Mama. The sites are taken on top of the mountain.

MEG, Megara, NE Peloponessos, 4 areas with 119 cores.
The Plio/Pleistocene basin of Megara contains many different sediments and is situated along the Gulf of Alkonides.

MIR, Aghios Miron, Crete SW of Iraklion, 1 site with 8 cores.
Just outside Aghios Miron, Messinian clays, sapropels and ash-layers are found.

MOR, Moria, Crete, 4 sites with 28 cores.
Three clayey sites, north of Moria, are of Pliocene age and contain laminated and homogeneous intervals. The fourth sandy (Pleistocene) marl site is located south of Moria.

MYL, Milos, 20 sites with 83 cores.
The Plio/Pleistocene sites are distributed over the island:
MYL 1 is a basalt and located on a track to Skinapi direction Adamas with an age of 1.47-.005 Ma.
MYL 2-9 is formed by beautiful white tuffites/marls and located at Sarakino beach
MYL 10-12 are shallow marls and diatomites and are located, on the mainroad, in the vicinity of the Sarakino beach exit.
MYL13-15 are bright white tuffs on the road to Pollinia near Sarakino beach and a small chapel.
MYL 16-20 are marine marls on the SW part of the island, after the "Golden Beach".

NER, Neraida, NW Peloponessos, 6 sites with 24 cores.
Pliocene clay is found on the road from the village of Neraida, direction Lantzi, along the river.

PB, Pefki Beach, Rhodos, <u>4 sites</u> with 34 cores.
<u>Upper Pliocene/Pleistocene</u> clay is found on the beach of Pefki.

PI, Pigadia, Karpathos, <u>1 site</u> with 9 cores.
<u>Pliocene?</u> sand and clay alternations are found in the bay of Karpathos town, underneath apartments, near the bar/disco "FILAGRI".

PIN, Pineos river, NW Peloponessos, <u>5 sites</u> with 33 cores.
Small <u>Pleistocene</u> cliffs can be found if you take the exit Kendro, from the Pyrgos-Patras road.

PR, Porto Roma, Zakynthos, <u>5 sites</u> with 51 cores.
<u>Plio/Pleistocene</u> clays intercalated with sandlayers are found at the Cape Gerakas cliffs and along the rocky beach until the bay of Porto Roma

PRA, Prassas, on Crete (SE of Iraklion), <u>4 sites</u> with 35 cores.
These <u>Pliocene</u> sites are found on the road, descending from Prassas. The first site contains a white laminated unit. The second site is formed by yellow marls with laminated intervals (third site). The fourth site contains Trubi sediments with sapropels.

PSK, Kythira, <u>1 site</u> with 7 cores.
<u>Pliocene</u> limestones are found along the road, NE of Mitata.

PY, Pylonas, Rhodos, <u>2 sites</u> with 15 cores.
<u>Uppermost Pliocene</u> clay underneath laminated limestones are located along the (non-coastal) road to Lindos, direction Lardos, opposite the "Lardos" sign.

RIZ, Riza, Epirus, <u>10 sites</u> with 34 cores.
<u>Lowermost Pliocene</u> clay and sapropel alternations are situated along the road of Preveza-Mezopotama, at the Riza exit. Further along the road, <u>upper Pliocene?</u> channels are found with occasional clay layers.

TS, Tsambkia, Rhodos, <u>2 sites</u> with 14 cores.
<u>Pliocene</u> channels with some clays are found on the road to Tsambika (of the main coastal road).

SK, Skaloniti, Rhodos, <u>2 sites</u> with 14 cores.
To reach a <u>Pliocene</u> rhythmically alternating clay-hill in the SE part of Rhodos, take the old national dirt road just before Genadi, turn right and follow the river; preferably without car.

SKI, Skiloundia, NW Peloponessos, 1 handsample.
Highly fractured Pliocene limestone layers are found along the road from Krestena to Andritsena, exit Skiloundia.

SOS, Ayios Sostis, Zakynthos, 10 sites with 38 cores.
The outcrop consists of Messinian clay and sand alternations at Laganas bay, near the disco-island.

SPA, Spartia, Kefallonia, 15 sites with 45 cores.
Plio/Pleistocene sandy clays and sapropels are located at Spartia Beach.

VA, Vagies, Rhodos, 1 site with 7 cores.
Upper Pliocene greenish fractured clays are found along the new highway near the coast/airport.

VAS, Vasileis, on Crete (SE of Iraklion), 1 site with 9 cores.
Pliocene Trubi-like sediments are located at a crossing just outside Vasileis.

VLA, Aghios Vlassios, on Crete (SE of Iraklion), 1 site with 9 cores.
Pliocene Trubi-like sediments are found just outside Aghios Vlassios, underneath the house of Chrisoula and Socrates.

VOU, Vounargon, NW Peloponessos, 10 sites with 54 cores.
The Pliocene clays are located around the village of Vounargon; on the main coastal road, in some small quarries and outside the village.

VUG, Vugiato, Zakynthos, 15 sites with 38 cores.
Tortonian clays alternating with sapropels can be found near the village of Macherado in the backyard of the NOTIS family.

ZT, Zakynthos Town, Zakynthos, 21 sites with 64 cores.
A long Plio/Pleistocene section is located behind Zakynthos town.

Curriculum Vitae

Charon Estelle Duermeijer werd geboren op 7 december 1970 in Utrecht. In 1983 begon zij haar middelbare schoolopleiding aan het zelfstandige christelijke gymnasium te Utrecht. Na het behalen van het gymnasium diploma in 1989, begon zij datzelfde jaar met de studie geologie aan de Universiteit Utrecht. In 1995 legde zij het doctoraal examen (Geologie/Geofysica, Endogene processen en Petrogenese) af aan de Universiteit Utrecht. Vanaf juni 1995 tot juni 1999 werkte zij als Assistent in Opleiding bij de Vening Meinesz Research School of Geodynamics op het Paleomagnetisch Laboratorium "Fort Hoofddijk" te Utrecht. Vanaf september 1999 werkt zij als publishing editor bij Kluwer Academic Publishers.

Acknowledgements